

Melanie Kienzl, BSc

**Evaluating the immunogenicity of measles virus T cell epitopes in  
a cancer immunogene therapy approach for aggressive  
squamous cell carcinoma**

**MASTER'S THESIS**

to achieve the university degree of

Master of Science

Master's degree programme: Molecular Microbiology

submitted to

**GRAZ UNIVERSITY OF TECHNOLOGY**

Supervisor

Ao. Univ.-Prof. Dipl.-Ing. Dr.techn. tit.Univ.-Prof. Günther Daum

Institute of Biochemistry

Dr. Josefina Piñon Hofbauer and Dr. Christina Gruber  
Laboratory for Molecular Therapy, EB-House Austria

## AFFIDAVIT

I declare that I have authored this thesis independently, that I have not used other than the declared sources/resources, and that I have explicitly indicated all material which has been quoted either literally or by content from the sources used. The text document uploaded to TUGRAZonline is identical to the present master's thesis.

---

Date

---

Signature

## **ACKNOWLEDGEMENTS**

First of all, I would like to thank Univ.-Prof. Dr. Günther Daum for accepting this master thesis and for his supervision.

I am grateful to Prim. Univ.-Prof. Dr. Johann Bauer and Dr. habil. Julia Reichelt for giving me the opportunity to perform my master thesis in the EB-House Austria in Salzburg.

Special thanks to my co-supervisors Dr. Josefina Piñon Hofbauer and Dr. Christina Gruber for their outstanding supervision, excellent guidance, intellectual input, help, support and encouragement throughout my time in the Cancer and Wound Healing Group, as well as for the proof-reading of my master thesis.

I would like to thank Dr. Victoria Reichl for her scientific advice, beneficial discussions, support and patience, especially when working nights together under the cell culture hood.

Thanks a lot to my colleagues of the Cancer and Wound Healing Group as well as the whole EB-House team for excellent teamwork, a friendly working atmosphere and mental support.

Furthermore, I would like to thank Dr. Angelika Stöcklinger, Dr. Gabriele Brachtl und Sophie Kitzmüller for their scientific expertise and technical support.

I am deeply grateful to my whole family, especially my parents, for supporting my studies and always being there for me. In addition, I especially want to thank my companion Markus for his patience and for having a strong shoulder to lean on.

I would like to thank my friends Melanie Kos and Anna Neumayer for their support and for always having an open ear.

Finally, I would like to thank the Paracelsus Medical University (PMU) for funding this project (E-14/20/105-PIN) and DEBRA-Austria for the financial support of my master thesis.

## TABLE OF CONTENTS

<b>Summary</b> .....	<b>1</b>
<b>Zusammenfassung</b> .....	<b>2</b>
<b>1 Introduction</b> .....	<b>3</b>
<b>1.1 The immune system – security control of the human body</b> .....	<b>3</b>
1.1.1 Adaptive immune response.....	4
1.1.2 The interaction of cells of the immune system and cancer.....	8
<b>1.2 Cancer immunotherapy</b> .....	<b>11</b>
1.2.1 Checkpoint blockers .....	12
1.2.2 Adoptive T cell therapy.....	13
1.2.3 Cancer Vaccination .....	13
<b>1.3 Morphology and function of human skin</b> .....	<b>14</b>
1.3.1 Immunological functions of the skin .....	16
<b>1.4 Epidermolysis bullosa</b> .....	<b>18</b>
1.4.1 Recessive dystrophic epidermolysis bullosa.....	21
<b>1.5 Hypothesis</b> .....	<b>25</b>
<b>2 Specific aims and scope of this thesis</b> .....	<b>26</b>
<b>3 Materials and methods</b> .....	<b>27</b>
<b>3.1 Reagents</b> .....	<b>27</b>
3.1.1 Measles virus peptides .....	27
3.1.2 Dextramer .....	27
<b>3.2 DNA plasmids</b> .....	<b>27</b>
3.2.1 Plasmid constructs for DNA immunization.....	27
3.2.2 Retroviral constructs for integration of MV-epitopes in cell lines.....	28
3.2.3 Sequence analysis.....	30
<b>3.3 Cell culture</b> .....	<b>30</b>
3.3.1 Primary cells and cell lines.....	30
<b>3.4 Generation of cell lines</b> .....	<b>31</b>
3.4.1 Viral transduction .....	31
3.4.2 Transient transfection .....	31
<b>3.5 Characterization of cell lines</b> .....	<b>32</b>
3.5.1 Integration PCR.....	32
3.5.2 Reverse transcriptase PCR (RT-PCR) .....	33
3.5.3 FACS analysis .....	33
<b>3.6 Animals</b> .....	<b>34</b>
3.6.1 Immunization protocol.....	34
3.6.2 Preparation of bullets for the gene gun system and <i>in vivo</i> gene gun transfection.....	34

<b>3.7</b>	<b>Blood sampling</b> .....	<b>35</b>
3.7.1	Blood sampling from the vena saphena .....	35
3.7.2	Collection of serum .....	35
<b>3.8</b>	<b>IFN<math>\gamma</math> ELISA</b> .....	<b>36</b>
<b>3.9</b>	<b>Antibody ELISA</b> .....	<b>36</b>
<b>3.10</b>	<b>Preparation of murine lymphoid organs and cell isolation</b> .....	<b>37</b>
<b>3.11</b>	<b>IFN<math>\gamma</math> ELISpot</b> .....	<b>37</b>
<b>3.12</b>	<b>Identification of MV specific CTLs</b> .....	<b>38</b>
<b>3.13</b>	<b>T cell proliferation assay</b> .....	<b>38</b>
<b>3.14</b>	<b><i>In vivo</i> CTL killing assay</b> .....	<b>38</b>
<b>3.15</b>	<b><i>In vivo</i> CTL blocking assay</b> .....	<b>39</b>
<b>3.16</b>	<b><i>In vivo</i> tumor challenge</b> .....	<b>39</b>
<b>3.17</b>	<b>Fluorescence microscopy</b> .....	<b>40</b>
<b>3.18</b>	<b>H/E staining of skin sections</b> .....	<b>40</b>
<b>3.19</b>	<b>Statistical analysis</b> .....	<b>41</b>
<b>4</b>	<b>Results</b> .....	<b>42</b>
<b>4.1</b>	<b>Preliminary considerations</b> .....	<b>42</b>
<b>4.2</b>	<b>Gene gun immunization is successful in the generation of functional MV-specific CD8<sup>+</sup> T lymphocytes in C3H mice</b> .....	<b>44</b>
4.2.1	Monitoring of the developing MV specific immune response .....	44
4.2.2	Identification of functional N81 specific CD8 <sup>+</sup> T cells in immunized mice .....	47
4.2.3	Gene gun vaccination with MV CTL epitopes evokes cellular adaptive immunity only .....	48
<b>4.3</b>	<b>The generated MV specific immune response is capable of specific target cell killing <i>in vivo</i></b> .....	<b>49</b>
4.3.1	CD8 <sup>+</sup> T cells are responsible for MV specific target cell killing <i>in vivo</i> .....	50
<b>4.4</b>	<b>Generation of a MV epitope-expressing SCCVII cell line</b> .....	<b>51</b>
4.4.1	SCCVII cells offer an immunological relevant phenotype.....	53
<b>4.5</b>	<b>Previously generated immunity protects mice from tumor development</b> .....	<b>55</b>
<b>5</b>	<b>Discussion</b> .....	<b>58</b>
<b>6</b>	<b>Bibliography</b> .....	<b>63</b>
<b>7</b>	<b>List of figures</b> .....	<b>71</b>
<b>8</b>	<b>List of tables</b> .....	<b>72</b>
<b>9</b>	<b>List of abbreviations</b> .....	<b>73</b>
<b>10</b>	<b>Appendix</b> .....	<b>74</b>
10.1	Primer list.....	74
10.2	Solutions .....	74

## SUMMARY

Recessive dystrophic epidermolysis bullosa (RDEB) is a rare genetic disorder caused by mutations in the *COL7A1* gene. Patients suffer from excessive blister formation in skin and mucous membranes upon minor mechanical trauma and have an increased risk to develop aggressive cutaneous squamous cell carcinoma (cSCC), which constitutes the primary cause of premature death. Surgery over a wide area represents the favored treatment option, but recurrence and metastasizing rates are high. Therefore, less invasive and more comprehensive therapies are needed. In this context, cancer immunotherapy already demonstrated to be a promising tool for treatment of different solid tumors, highlighting the potential of the strategy to activate the immune system to fight cancer.

We therefore hypothesize that it is possible to harness the pre-existing immunity against measles virus (MV), against which the majority of the population is vaccinated, and redirect this cellular immune response toward tumor cells that are modified to express MV epitopes. To provide proof-of-principle and as a first step we developed an immunocompetent mouse model with a cellular adaptive immune response against MV epitopes. DNA vaccination using the Helios gene gun system (Bio-Rad) was applied for the immunization of C3H mice (H-2K<sup>k</sup>) with DNA plasmids encoding an Interleukin 2 signal sequence, MV cytotoxic T lymphocyte (CTL) epitopes and a T helper epitope. The quality of the MV specific immunity was investigated both *in vivo* and *in vitro* by CTL killing and blocking, cytokine-ELISA, ELISPOT and T cell proliferation assays. Using a customized dextramer, consisting of MV-epitopes complexed with H-2K<sup>k</sup> molecules on a dextran backbone, we confirmed the generation of MV-specific CD8<sup>+</sup> T cells *in vitro*. Those CTLs were further identified as effector cells that are responsible for *in vivo* lysis of up to 90 % of donor splenocytes that were pre-loaded with the MV-peptide. This effect was abolished when CD8<sup>+</sup> T cells were blocked with a specific anti CD8-blocking antibody resulting in reduced killing of peptide-pulsed syngeneic donor splenocytes *in vivo*. As a second aim we engineered a syngeneic SCC cell line stably expressing a MV-specific epitope and presenting it on MHC class I. These tumor cells were further used in an *in vivo* tumor experiment, where they were injected intradermally into the flank of vaccinated mice and tumor development was monitored over a period of approximately one month. Mice that had a pre-existing immune response against the MV-epitope, showed significantly less tumor development compared to control mice.

In conclusion we successfully induced a MV specific CTL response in mice using the Helios gene gun system and could show that a pre-existing immunity against MV is enough to prevent the tumor growth of a syngeneic SCC cell line that was modified to express MV epitopes. These data highlight that the immune system can be harnessed to fight cancer and serve as basis for translating our findings into the human system, particularly for the therapy of RDEB-SCC and developing new delivery systems for future *in vivo* applications.

## ZUSAMMENFASSUNG

Rezessiv dystrophe Epidermolysis bullosa ist eine seltene, genetische Erkrankung verursacht durch Mutationen im Gen *COL7A1*. Patienten leiden an exzessiver Blasenbildung in der Haut und Schleimhäuten, verursacht durch geringe mechanische Einwirkung und weisen ein erhöhtes Risiko für die Entwicklung von aggressiven Plattenepithelkarzinomen auf, welche auch den primären Grund für frühzeitigen Tod darstellen. Großflächige Operationen sind die bevorzugte Behandlungsweise, jedoch ist die Rückkehr- als auch die Metastasenbildungsrate sehr hoch. Aufgrund dessen ist es dringend notwendig weniger invasive und umfassendere Therapiemöglichkeiten zu entwickeln. Krebs-Immuntherapien haben sich in der Behandlung einiger solider Tumore als vielversprechend herausgestellt. Das zeigt das Potential der Aktivierung des Immunsystems im Kampf gegen Krebs auf. Daher vermuten wir, dass das bestehende Immungedächtnis gegen Masernviren (MV) – gegen welche die Mehrheit der Bevölkerung geimpft ist – genutzt werden kann um Tumorzellen zu zerstören, die zuvor so verändert worden sind, dass sie MV-Epitope präsentieren. Um diese Hypothese zu bestätigen, wurde ein immunkompetentes Mausmodell mit zellulärer, adaptiver Immunantwort gegen MV entwickelt. Die C3H-Mäuse (H-2K<sup>k</sup>) wurden mit DNA Plasmiden, welche eine IL-2 Signalsequenz, MV-CTL Epitope sowie ein T Helfer-Epitop exprimieren mittels der Helios Gen-Gun von Bio-Rad immunisiert. Die Qualität der hervorgerufenen Immunantwort wurde *in vitro* und *in vivo* mit CTL Tötungs- und Blockierungsexperimenten, Cytokin-ELISA, ELISpot und T Zell Proliferationsexperimenten überprüft. Ein maßgeschneidertes Dextramer, bestehend aus einem Dextran-Gerüst und H-2K<sup>k</sup> komplexierten MV-Epitopen, wurde verwendet um die MV-spezifischen CD8<sup>+</sup> T Zellen zu identifizieren. Diese CTLs waren verantwortlich für bis zu 90 % spezifische Lyse von MV-Peptid beladenen Donormilzzellen. Dieser Effekt konnte durch die Verwendung eines CD8 spezifischen Blockierungsantikörpers aufgehoben werden und führte zu verminderter Lyse von MV-Peptid beladenen Donorzellen. Das zweite Ziel war die Veränderung einer Plattenepithelkarzinomzelllinie dahingehend, dass diese MV-Epitope exprimiert und auf MHC I präsentiert. Diese Tumorzellen konnten anschließend in einem *in vivo* Tumorexperiment verwendet werden. Hierfür wurden sie intradermal in die Flanke von immunisierten Mäusen injiziert und das Tumorwachstum wurde für einen Monat beobachtet. Mäuse welche eine Immunantwort gegen MV aufwiesen, zeigten eine signifikant geringere Tumorbildung im Vergleich zu Kontrollmäusen. Das Hervorrufen einer MV spezifischen CTL-Immunantwort mit Hilfe der Helios Gene Gun war erfolgreich und es konnte gezeigt werden, dass diese ausreicht um das Wachstum eines MV-Epitop präsentierenden Tumors zu vermeiden. Diese Daten betonen die Möglichkeit das Immunsystems zu nutzen um Krebs zu bekämpfen und dienen als Basis für die Umwandlung der Erkenntnisse in ein humanes System. Insbesondere um eine Therapie von Plattenepithelkarzinomen in RDEB Patienten und um neue Methoden für Verabreichungsverfahren für zukünftige *in vivo* Anwendungen zu entwickeln.

# 1 INTRODUCTION

## 1.1 THE IMMUNE SYSTEM – SECURITY CONTROL OF THE HUMAN BODY

The immune system is tasked with the defense of the body against unwanted pathogens and components from the environment. The two major branches of immune responses are called innate and adaptive immunity. Innate immune responses constitute the initial defense network and consist of biochemical (complement system, acute phase proteins) as well as cellular (macrophages, dendritic cells, amongst others) mechanisms that recognize broad characteristics of related microbes via pattern recognition receptors. As such, fine distinctions between various pathogens are not recognized. The major role of innate immune cells is the eradication of pathogens. The intensity and kinetics of the innate immune response stay similar upon repeated exposure. Additional to its role in direct defense particularly at barrier tissues, cells of the innate immune response play an important role in activation and stimulation of cells of the adaptive immune response [1], [2]. The adaptive immunity represents the second line of defense. It is very specific in its recognition of antigens and this response is more rapid and more intense with each exposure to the same antigen. This phenomenon is known as immune memory. T and B lymphocytes constitute the major players in the cellular and humoral responses of the adaptive immunity, respectively [1]. Figure 1 depicts the different branches of the immune system together with cells associated with each branch.

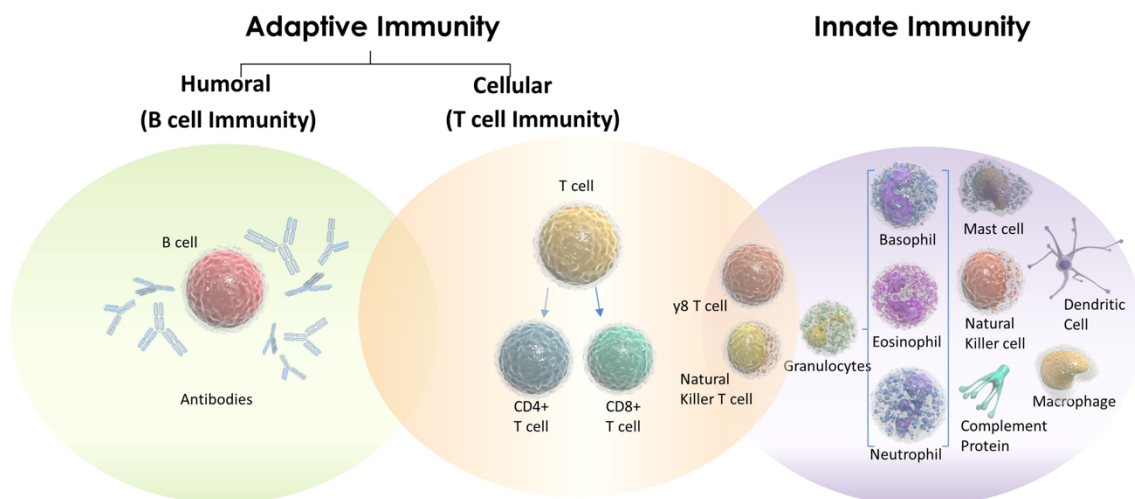


**Figure 1 The branches of the human immune system.** The adaptive immunity is subdivided into humoral and cellular immunity mediated by B and T lymphocytes, respectively. The different components of the innate immune system mediate eradication of pathogens as a first defense line and can further activate the adaptive immunity due to antigen presentation. Adapted from <http://www.oxfordimmunotec.com/international/science/technology-2/> [3].

### 1.1.1 ADAPTIVE IMMUNE RESPONSE

The most important properties of adaptive immunity are the development of immune memory, the tolerance to self-antigens, and specialization [1].

Immunological memory refers to the ability of the adaptive immune system to remember antigens, which it has encountered before and mount a more rapid and more vigorous response upon re-exposure to the same antigens. Immune memory responses form the basis of what make prophylactic vaccinations so effective in protecting individuals against pathogens [1].

Immunological self-tolerance is defined as the state of unresponsiveness of the immune system to self-antigens. However, tolerance is not simply a failure to recognize antigens, but involves active mechanisms whose end result is a lack of an immune response against those specific antigens. Immune tolerance is classified into central or peripheral tolerance, depending on where the state is originally induced. Central tolerance is generated in the bone marrow and thymus, and involves the deletion of autoreactive B and T lymphocytes prior to their maturation into fully competent immune cells. Peripheral tolerance develops in peripheral tissues and lymph nodes and plays an important role in limiting immune reactions in order to prevent tissue injury. Loss of self-tolerance results in autoimmune diseases [1], [4].

The specialization of the adaptive immune response refers to the organization and division of labor among highly specialized subsets of immune cells, allowing the immune system to respond to the multitude of diverse antigens present in the environment [5]. The humoral adaptive immunity is mediated by B lymphocytes, which are responsible for antibody production as a result of activation by CD4<sup>+</sup> helper T (Th) lymphocytes [6]. The various CD4<sup>+</sup> T cells subsets play distinct roles in modulating immune responses to different triggers. T follicular helper cells are crucial to formation and maintenance of germinal centers, which are necessary for the production of high-affinity antibodies by antigen-specific B cells. Th1 cells secrete IFN $\gamma$  and play a supporting role in defense against intracellular microbes, autoimmunity, and tissue damage. Th2 CD4<sup>+</sup> helper T lymphocytes protect against helminthic parasites. Th17 cells are important for fungi and extracellular bacterial infections. Th9 cells are involved in inflammation of the respiratory tract. Another important T cell subset are regulatory T cells (Tregs), which maintain immunologic tolerance and negatively regulate immune responses following the eradication of pathogens, in order to prevent tissue damage [7], [8]. While pathogen-specific antibodies are important for the neutralization, and the clearance of pathogens that are extracellularly located [6], intracellular pathogens, and even altered host cells (including tumor

cells), are recognized and eradicated by the cell-mediated adaptive immune response, of which CD8<sup>+</sup> T lymphocytes are the major key players [1].

#### 1.1.1.1 THE ROLE OF CD8<sup>+</sup> T LYMPHOCYTES IN CELL-MEDIATED IMMUNITY

Priming of naïve CD8<sup>+</sup> T lymphocytes is performed by antigen presenting cells (APCs) via formation of antigen-specific contacts in lymph nodes (LN) and spleen (SPL). This interaction leads to activation, expansion, and differentiation of naïve antigen-specific CD8<sup>+</sup> T lymphocytes into CD8<sup>+</sup> effector and memory T cells [9]. Interaction between APCs and T cells occurs with the formation of the so called immunological synapse, which is essential for signal transduction and activation of lymphocytes. This supramolecular interface incorporates 3 classes of receptor: (1) T cell receptor (TCR), which recognizes antigen associated with major histocompatibility complex (MHC) molecules, (2) adhesion molecules which are necessary for the initial formation and maintenance of the immunological synapse to enable sustained antigen recognition, and (3) costimulatory/checkpoint receptors which determine the final outcome of the response [10], [11]. MHC molecules display protein antigens for recognition by CD4<sup>+</sup> and CD8<sup>+</sup> T cells on the surface of APCs and host cells. There are two different classes of MHC molecules. MHC class II molecules (MHC II) display non-self protein antigens for recognition by CD4<sup>+</sup> T cells and are found primarily on the surface of APCs. In contrast, MHC class I molecules (MHC I) are found at the membrane of all nucleated cells of the body and present antigens derived from self proteins, as well as altered-self, and viral antigens. In short, MHC II display extracellular antigens that are phagocytosed and processed by APCs, whereas MHC I molecules present antigens which originate from cytosolic/intracellular proteins that are degraded via the proteasome, targeted to the endoplasmic reticulum (ER), and transported to the cell surface after loading to MHC I (Figure 2)[1].

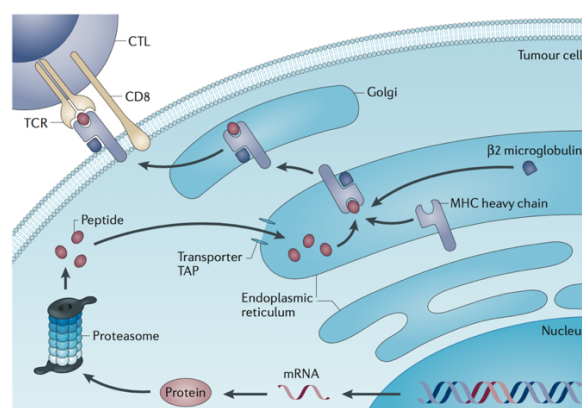


**Figure 2 Processing of cytoplasmic peptides for presentation on MHC I molecules on the cell surface.** Cytoplasmic-self, viral, as well as altered-self proteins get degraded to peptides by the proteasome, directed to the endoplasmic reticulum (ER) via transporter associated with antigen processing (TAP), loaded onto MHC I and transferred to the cell membrane for presentation to cytotoxic CD8<sup>+</sup> T lymphocytes (CTL) and their T cell receptor (TCR). Adapted from Coulie *et al.* 2014 [12].

The ability of a T cell to recognize antigen is dependent on the specificity of their TCR. TCRs recognize peptide epitopes that are 8-11 amino acids in length, but are additionally MHC-restricted in that they are specific for an MHC molecule expressed from a specific allele. Thus, both MHC restriction and the specificity of the TCR for the presented epitope are crucial determinants for initiating the formation of the immunological synapse that leads to the activation of CD8<sup>+</sup> T cells [1]. Additional to MHC/epitope – TCR interaction, the CD8 co-receptor on the surface of a T cell binds to the  $\alpha 3$  region of MHC I [13]. Full activation of naïve T cells also requires the engagement of co-stimulatory receptors. The ligands for these costimulatory molecules are provided on the surface of APCs. For example, CD80 (B7-1) and CD86 (B7-2) on APCs bind the costimulatory receptor CD28 on the T cell surface, leading to the induction of signaling pathways which promote cell proliferation and differentiation (effector and memory T cell) via the induction of survival proteins, cytokine receptors, and cytokines themselves. Additional costimulatory and adhesion molecules, like ICAM1/LFA1, CD2/CD59, integrin and family members of the tumor necrosis factor (TNF) family are known to be important for the maintenance of the immunological synapse [1], [10]. The support of so called CD4<sup>+</sup> T helper cells is also thought to be necessary for proper activation of CD8<sup>+</sup> T lymphocytes through APCs, especially for the eradication of tumors, viral infections, and in response to organ transplants. CD4<sup>+</sup> T cell help is mediated by the secretion of cytokines which can enhance APC differentiation and activation, resulting in more efficient CD8<sup>+</sup> T lymphocyte stimulation [1]. The differentiation of CD8<sup>+</sup> T cells into various subclasses is influenced by the cytokine milieu produced by APCs and CD4<sup>+</sup> T helper cells. The concentration of interleukin 2 (IL-2) has been shown to be crucial, with high concentrations resulting in an effector phenotype, whereas low levels are associated with a memory phenotype [14]. IL-12 and type I interferon (IFN) promote the development of CD8<sup>+</sup> cytotoxic effector cells (CTL), whereas IL-15 and IL-21 are important for memory cell survival and induction, respectively [1], [14].

Once a naïve CD8<sup>+</sup> T lymphocyte has been activated and undergone differentiation, clonal expansion occurs, and the effector T cell clones exit the lymph nodes and migrate into peripheral tissues upon increased expression of CXCR3, an inflammatory cytokine receptor [9]. Target cells, for example virally-infected cells and tumor cells, are recognized by specific CTLs by virtue of their MHC I and associated antigen. CTLs have the ability to kill only those target cells that present their cognate antigen on MHC I [1]. CTL mediated target cell killing is achieved through the action of lytic proteins such as granzymes and perforin [15], or via CD95/CD95L interaction. Both pathways lead to the induction of the caspase cascade and programmed cell death (apoptosis) in target cells [16], as shown in Figure 3.

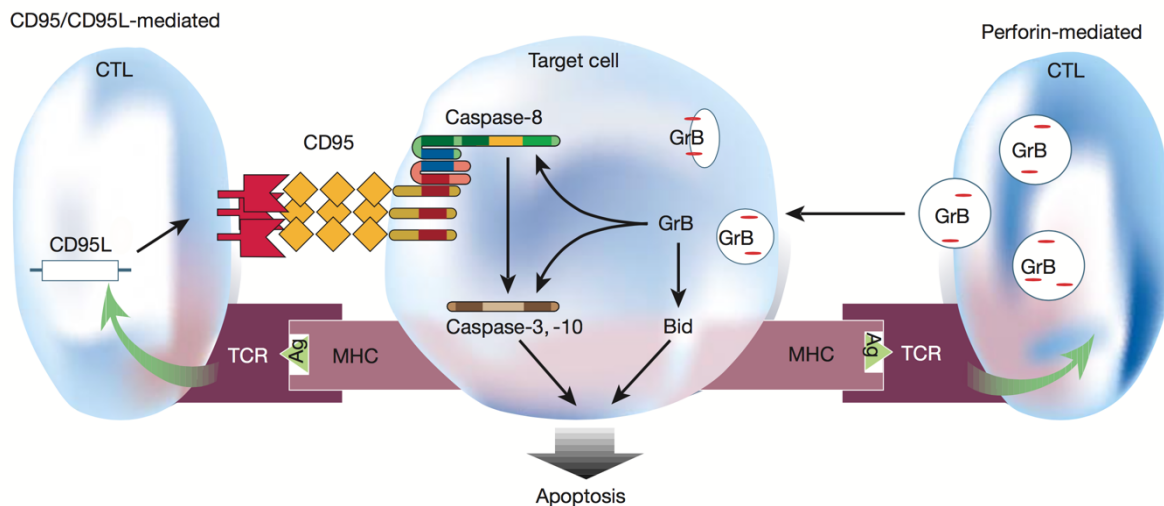


**Figure 3 The two pathways of CTL mediated target cell killing.** Target cell killing through CTLs is either mediated by the CD95L (red) and CD95 (yellow) pathway and following induction of a caspase cascade, or mediated by released granzyme B (GrB) that enters the target cell with help of perforin. GrB activates caspases by cleavage. Both pathways lead to apoptosis of the target cell induced by the signaling events. Adapted from Krammer *et al.* 2000 [16].

The precise execution of CTL effector function is also facilitated by the formation of the immunological synapse. Engagement of cognate TCR by MHC I/antigen and CD8 coreceptor triggers synapse formation and subsequent interaction between ICAM-1 (on the target cell) and LFA-1 (on the CTL), induces a signal cascade for recruitment of the secretory lysosome, which contains the lytic proteins granzyme A and B, as well as perforin. As a consequence of CTL activation, lytic proteins become secreted into the synapse, which facilitates the transfer of these proteins to the target cell [1], [17]. Increased  $Ca^{2+}$  concentrations contribute to conformational changes in perforin enabling the interaction with lipids of the target cell membrane as well as polymerization and development of 16 nm pores. Granzymes enter the cytosol of the target cell and induce apoptosis via an indirect and direct manner. Granzyme A nicks single stranded DNA, forcing target cells into programmed cell death due to obstruction of repair mechanisms. On the other hand, granzyme B acts through cleavage of procaspase-3 and the pro-apoptotic molecule Bid, in order to directly activate apoptosis [15], [17].

The second pathway by which CTLs direct cell killing is via engagement of the death receptor CD95/FAS on the target cell [1]. CD95-ligand (CD95L/FASL) expression is induced in CTLs upon activation. Ligand binding triggers FAS trimerization on the surface of the target cell and the formation of the death-inducing signaling complex (DISC), which additionally consists of FADD (FAS-associated death domain protein) and procaspase-8. Proteolytic processing leads to release of active caspase-8 from DISC, which subsequently activates the effector caspase, caspase-3, resulting in cell apoptosis [16]. Even small levels of cognate antigen-MHC I complexes expressed on the target cell surface are sufficient to trigger CTL-mediated killing by primed CTLs, depending on their sensitivity to antigen. Each immunological

synapse resolves within a few minutes, however, multiple synapses with several target cells can be formed simultaneously [10].

Activation of CD8<sup>+</sup> T cells, as well as stimulation with IL-12 and IL-18, also results in the production and secretion of IFN $\gamma$ . Natural killer (NK) cells and Th1 CD4<sup>+</sup> T cells also serve as a source for IFN $\gamma$  in the context of an immune response. IFN $\gamma$  leads to the enhanced expression of MHC I on target cells, with the consequence of rendering infected cells more “visible” to CTLs [18]. Additionally, CD95/FAS is expressed in numerous cells of the human body, and its expression is enhanced in response to IFN $\gamma$  and tumor necrosis factor [19].

Altogether, CD8<sup>+</sup> T lymphocytes play a vital role in host defense. They are necessary for the elimination of intracellular microbes, due to their ability to kill infected target cells, and are important in the recognition and eradication of tumor cells. They are key players in organ transplant rejection and tissue injury during the course of chronic inflammation [1]. In order to prevent the latter, a myriad of mechanisms exist to negatively regulate CD8<sup>+</sup> T cell responses, including the enhanced expression and engagement of inhibitory or checkpoint receptors, decreased IFN $\gamma$  production, and modulation by Tregs [20]. Checkpoint receptors (also discussed below) include programmed cell death protein 1 (PD-1) and cytotoxic T lymphocyte antigen 4 (CTLA-4). The cognate ligands for PD-1 are PD-ligand 1 and 2 (PD-L1 and PD-L2), whereas CTLA-4 shares the same ligands with CD28 (CD80 and CD86). Engagement of these checkpoint receptors on the surface of T cells leads to an inhibition of the signaling pathways involved in T cell activation. These different inhibitory mechanisms are often exploited by tumor cells to evade immune attack [21].

### **1.1.2 THE INTERACTION OF CELLS OF THE IMMUNE SYSTEM AND CANCER**

The tumor microenvironment is defined as the environment in which the tumor exists. It comprises of cellular components such as cancer-associated fibroblasts and various adaptive and innate immune cells, extracellular matrix, and a vascular system. The communication between the tumor and its microenvironment is a dynamic, bi-directional process that impacts tumor development and plasticity. Cytotoxic-, helper-, and regulator T lymphocytes, B lymphocytes, mast cells, macrophages, NK cells, and myeloid-derived suppressor cells (MDSCs) are all known to infiltrate tumors, exemplifying the dual role the immune system plays in cancer progression [22], [23]. On the one hand tumor-specific CTLs and T helper type 1 cells mediate anti-tumor effects via mechanisms similar to CTL-mediated killing of infected cells. These cells are supported by NK/NKT cells, mature DCs, and type 1 macrophages, which have demonstrated anti-tumor roles [23], [24]. On the other hand, type 2 macrophages, myeloid-

derived suppressor cells (MDSCs), T-helper type 2 (Th2) cells, and regulatory T (Treg) cells together orchestrate an environment rich in interleukins (IL) 10, IL-4, IL-5, IL-6, tumor growth factor beta (TGF-beta) which promotes angiogenesis and tumor cell proliferation. Additionally, Tregs inhibit the generation of CTLs, thus contributing to tumor survival [24]–[27]. Ultimately, the collective pressure these immune cells exert on tumors contributes to tumor evolution [28].

In 2002, the group of Dunn *et al.* at the Center of Immunology at the Washington University School of Medicine proposed a theory about the network of immune system and cancer cells, called immunoediting. Immunoediting is described as one of several processes by which the immune system not only eliminates tumors, but also shapes the immunologic phenotype of tumors. The process of immunoediting is divided in three phases: elimination, equilibrium and escape (Figure 4)[29].

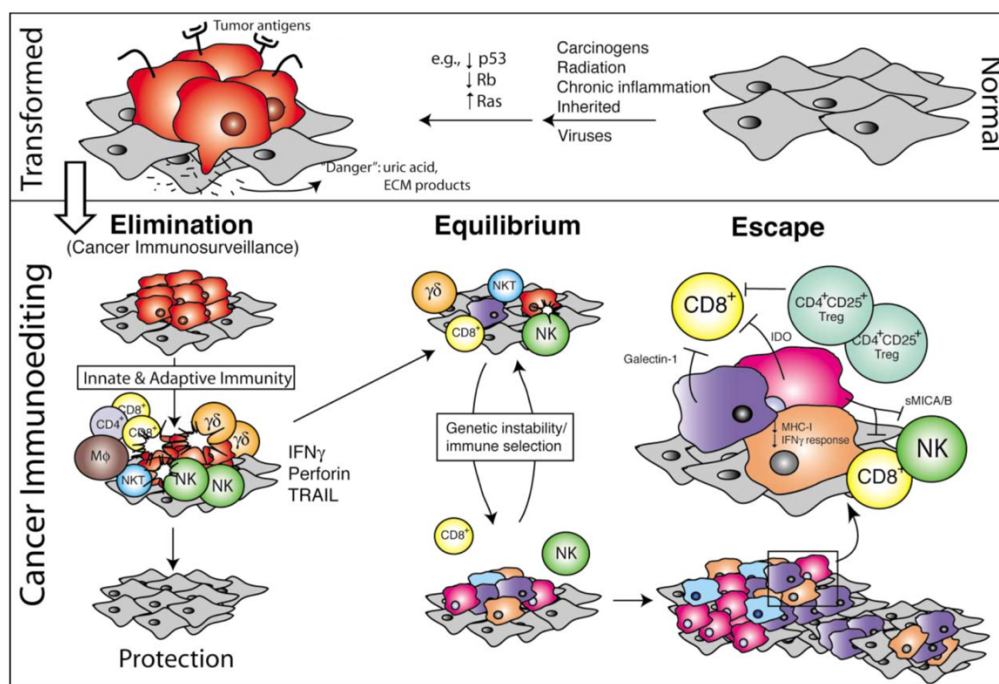


**Figure 4 The three phases of cancer immunoediting.** Normal cells (grey) mutate to tumor cells (red) upon oncogenic influences. At early stages, these cells may express tumor-specific markers that lead to the activation of the cancer immunoediting process mediated by cells of the innate and adaptive immunity, the immune surveillance network. In the initial phase, called elimination, immune cells fight the altered cells to protect the host from tumor formation. The stage of equilibrium is entered when the elimination process was without success. At this stage tumor cells are maintained chronically or get shaped from cells of the immune system to form different populations of tumor versions. The new variants possibly escape the immune control using different mechanisms and develop clinical detectable tumors in the escape phase. Adapted from Dunn *et al.* 2004 [30].

### 1.1.2.1 ELIMINATION – IMMUNE SURVEILLANCE OF CANCER

Tumor cells might express non-self-antigens derived from altered self-proteins or oncogenic viruses, or might present self-antigens at different tissues or at levels different to normal cells [31]. These characteristics make them recognizable to cells of the adaptive immune system, such as CD8<sup>+</sup> T lymphocytes, which work in concert with cells of the innate immune system, including NK cells, to destroy the tumor via perforin or granzyme B release and FASL-mediated apoptosis. Additionally, dendritic cells and macrophages are necessary for the presentation of antigen and expression of pro-inflammatory cytokines like type I interferon, GM-CSF, IFN $\gamma$  and IL-12 [32]. Tumor surveillance was shown for the first time by Shankaran *et al.* (2001) in RAG2 (recombination-activating gene-2) deficient, immunocompromised mice which lack mature lymphocytes. They investigated the role of lymphocytes and IFN $\gamma$  against tumor cells and could confirm the necessity of mature lymphocytes for tumor destruction, as RAG2<sup>-/-</sup> mice developed significantly more tumors following chemical induction compared to wildtype controls [33]. Furthermore, the expression of genes for Th1 adaptive immunity, such as CD8, IFN $\gamma$ , and granzyme B, correlate with better prognosis in colorectal cancer [34], as well as in non-small-cell lung cancer [35]. In the case of ovarian cancer, the presence of CD3<sup>+</sup> tumor-infiltrating T cells correlated with increased overall survival and delayed recurrence [36].

### 1.1.2.2 EQUILIBRIUM

In the course of the elimination phase, the majority of altered and potentially pre-malignant cells is eradicated. However, a few cells may survive the attack due to tumor heterogeneity. The equilibrium phase is described as the period of time that spans the end of the elimination phase up until the time the tumor is first clinically detectable. Tumor cells accumulate more mutations with time, facilitating immune escape and decreasing immunogenicity. Elimination of cancer, preservation of the equilibrium state, or escape from the immune system, are the three possible outcomes at the end of the equilibrium phase [30].

### 1.1.2.3 ESCAPE

Cancer cells exploit several different mechanisms in order to escape immune surveillance. A decrease in tumor immunogenicity has been reported to be caused by alterations within the cancer cells themselves. Differences in antigen presenting behavior due to loss of MHC I or impairment in the antigen processing machinery, facilitate immune cell evasion. Loss of IFN $\gamma$  receptor components results in resistance to IFN $\gamma$  [30]. The expression of IDO (indoleamine 2,3-dioxygenase) in tumor cells

or APCs leads to suppression of T cell functions. IDO reduces local levels of tryptophan resulting in suppression of T cell proliferation and enhanced T cell apoptosis, thus correlating with poor clinical outcome [37]. Expression of immunosuppressive cytokines such as TGF- $\beta$  or IL-10 by tumor cells further enhances tumor escape [30]. CD4<sup>+</sup> CD25<sup>+</sup> FoxP3<sup>+</sup> regulatory T cells (Tregs), accumulate in tumors, tumor-draining lymph nodes and in peripheral circulation where they exert an immunosuppressive effect on T cells, NK cells, B cells, and APCs, among others. As such, the depletion of Tregs has been shown to increase the effects of certain immunotherapies [30], [37]. Clark *et al.* (2008) investigated down-regulation of vascular E-selectin in blood vessels of squamous cell carcinoma (SCC) and recruitment of Tregs plays a role in immune evasion of SCC [38].

Additionally, to the adaptive immune cells, the innate immune system plays a role in tumor progression. Tumor cells are capable of inducing the differentiation of MDSCs, which have the ability to inhibit CD4<sup>+</sup> and CD8<sup>+</sup> T lymphocytes, independently of MHC, via NOS<sub>2</sub> and arginase [37]. Furthermore, nitration of tyrosine residues in TCR-CD8 complexes of CTLs leads to the destruction of specific binding to peptide MHC I complexes, and prevents CTLs from binding and responding to its cognate peptide [39]. It is also known that MDSCs contribute to the preparation of a pre-metastatic niche [25]. Macrophages are sub-classified into two subtypes: M1 which, indirectly support immune cytotoxic effects on cancer cells via secretion of cytokines such as IL-12, and M2, which include tumor associated macrophages (TAM) and secrete immunosuppressive cytokines that favor tumor growth. The presence of TAMs in tumors has been shown to predict poor tumor prognosis. Proteases secreted by TAMs increase metastases [22].

## 1.2 CANCER IMMUNOTHERAPY

Cancer immunotherapy, meaning to harness the immune system to fight cancer, was selected Science-Breakthrough of the year in 2013. In comparison to other cancer therapies, immunotherapy takes a different approach, namely to target the immune system and not the tumor itself. Different strategies have already shown success, although the impact is variable between different cancers and patients [40]. The term cancer immunotherapy includes checkpoint inhibition, adoptive T cell therapy, and cancer vaccination, to mention a few.

The underlying mechanism of all cancer immunotherapy strategies is the specific recognition of tumor-associated antigens (TAAs), either present on the tumor cell surface or associated with MHC I, by the immune system. TAAs can be derived from viral origin, depict epitopes of mutated or rearranged genes, represent abnormally expressed proteins, altered glycolipids or glycoprotein antigens, or are

cancer-germline antigens [1], [12]. More than 70 % of tumor antigens are derived from self-proteins [41]. Therefore, the tolerogenic mechanisms that prevent autoimmunity have to be circumvented for the success of immunotherapy approaches that target such antigens [22].

### 1.2.1 CHECKPOINT BLOCKERS

The immune checkpoint receptors, CTLA-4 and PD-1, play important roles in the induction of inhibitory feedback mechanisms that prevent autoimmunity and limit tissue damage during the course of prolonged immune activation, such as in chronic infections. Tumor cells exploit these mechanisms to avoid attacks of the host's immune system. CTLA-4 expression is limited to T cells, where it plays an antagonistic role to CD28 during the early stages of T cell activation. CTLA-4 shares the same ligands with CD28, namely CD80 and CD86. However, its affinity for these molecules is higher. Thus, CTLA-4 overcomes CD28 ligand binding by delivering inhibitory signals to the T cell that limits T cell activation. Additionally, it increases the activity of Tregs and lowers the support of CD4<sup>+</sup> helper T cells. In 2010 ipilimumab, an antibody that blocks CTLA-4, received approval from the Food and Drug Administration (FDA) for the therapy of patients with advanced melanoma [21]. Hodi and colleagues (2010) investigated the effect of ipilimumab on patients with previously treated metastatic melanoma and could show improved overall survival. Adverse events were severe, but also reversible [42].

PD-1 expression is enhanced in activated T cells and it functions to limit the activity of effector T cells in peripheral tissue in the context of an inflammatory response and to prevent autoimmunity. PD-L1 and PD-L2 are the two ligands of PD-1. PD-L1 is expressed on many cell types such as epithelial cells, endothelial cells, and tumor cells, and its expression is enhanced after IFN $\gamma$  exposure. Upon interaction with its ligands, PD-1 negatively influences signaling pathways mediated by the antigen receptor [21], [43]. Both antibodies for PD-1 and its ligand PD-L1 are currently investigated in clinical trials against various cancers [43]. A clinical phase I study with the PD-1 antibody nivolumab conducted by Topalian and colleagues (2012) showed objective responses in 18, 28 and 27 % of patients with non-small-cell lung cancer, melanoma, and renal cell cancer, respectively [44]. The combination of nivolumab (anti-PD-1) and ipilimumab in the treatment of melanoma in a study of 86 patients cause a tumor reduction of at least 80 % in 53 % of the patient group. The occurrence of adverse events was similar to the treatment with both antibodies alone [45].

### 1.2.2 ADOPTIVE T CELL THERAPY

Therapies for cancer treatment via transfer of adoptive T cells represent a highly personalized application [46]. Adoptive T cell therapy involves the isolation of autologous tumor-specific infiltrating lymphocytes from the patient, *ex vivo* expansion of T cells in the presence of IL-2, and subsequent re-infusion into the lymphodepleted patient. In a clinical trial including 93 patients with measurable metastatic melanoma, the application of this strategy resulted in complete regression in 22 % of the patients, with all but one complete responder remaining tumor-free beyond 3 years [47]. In recent years, this therapeutic strategy has advanced with our ability to genetically engineer T cells to express tumor-specific TCRs. Autologous T cells engineered to express a TCR specific for a MART-1 (melanoma antigen recognized by T cells) epitope complexed to MHC I is currently under evaluation for the treatment of metastatic melanoma [48]. The advent of chimeric antigen receptors (CARs) has further extended the applicability of this approach. Second/third generation CARs comprise a single chain of the variable fragment of an antibody specific for a tumor antigen, fused to the intracellular signaling domains of the TCR and costimulatory receptors. Thus, recognition of the antigen of the target cell is not MHC I dependent [48] and results in direct activation of the CAR-T cell without the need for a co-stimulatory signal. CAR-T cell therapy specific for CD19, a marker for B-cell malignancies, has shown promising results in the treatment of acute lymphoid leukemia (ALL). Levine *et al.* (2016) observed complete regression in 93 % of patients with ALL, however, cytokine release syndrome proved to be a common side effect [49].

### 1.2.3 CANCER VACCINATION

In a prophylactic setting, vaccination is administered prior to the first encounter with a pathogen (including oncogenic viruses), resulting in generation of immune memory that protects against subsequent infection. Upon a second exposure, a more rapid and robust response is triggered, leading to a more effective eradication of the invading pathogen. In contrast, therapeutic cancer vaccination is applied when the tumor has already manifested itself clinically, and aims to enhance the immune response against tumors. Although cancer vaccination results in the induction of antigen specific immune responses, namely increased levels of antibodies, elevated numbers of CTLs and CD4<sup>+</sup> T helper cells as well as specific T cell proliferation, clinically relevant effects against the tumor remain limited. In a study evaluating the efficacy of cancer vaccination against prostate cancer, a total of 1100 patients treated with different cancer vaccines resulted in only one complete and three partial responders [50]. Several factors may contribute to the lack of success of cancer vaccines in achieving clinical responses. One is the state of immune tolerance induced by the tumor, including the evasion mechanisms engaged by the tumor to escape detection [51]. Another factor that limits the success of cancer

vaccination is the fact that > 70 % of tumor antigens are derived from self-proteins that have gained central tolerance [41], [50], [52]. In this respect, circumventing these suppressive and tolerogenic mechanisms by combining checkpoint blockers with the activating function of vaccines depicts a therapeutic possibility [53].

### 1.3 MORPHOLOGY AND FUNCTION OF HUMAN SKIN

The skin represents the border of the human body to the environment. As such, the skin fulfils a variety of important functions, including protection from UV-light, mechanical stress, and invading pathogens, thermoregulation, and sensory functions. Additionally, it serves as a storehouse for water and metabolic substances. The skin is comprised of three major zones: the epidermis, which is exposed to the environment, followed by the dermis, which is separated from the epidermis via the basement membrane zone (BMZ) and the subcutis, which lies beneath the dermis (Figure 5) [54].

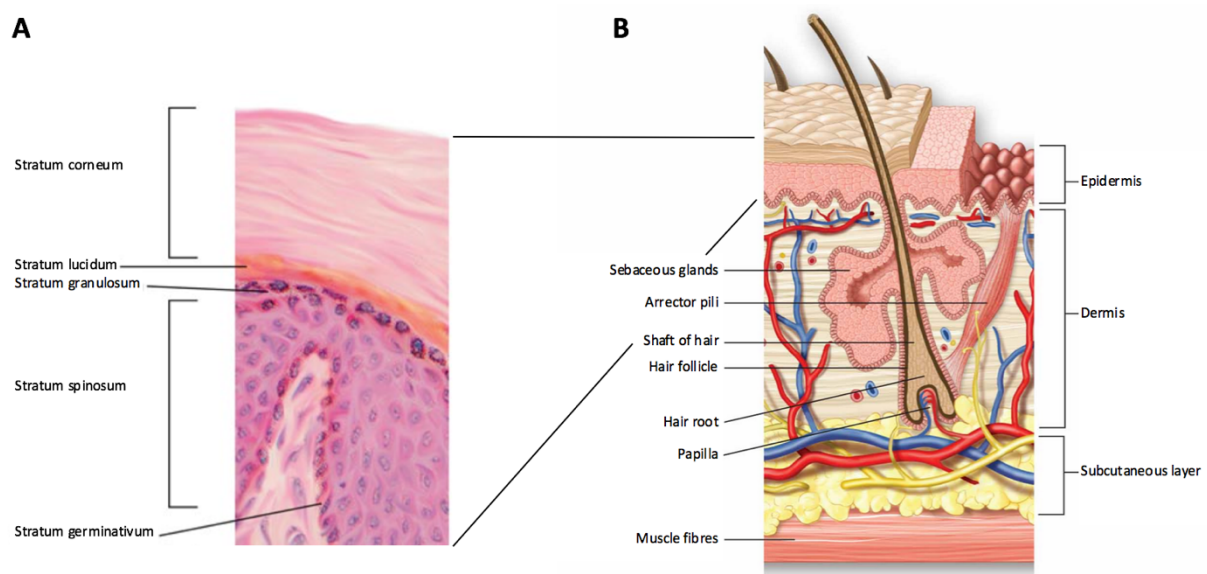


**Figure 5** Histological and schematic depiction of the human skin with its different layers and components. **A** The picture shows a magnification of the different layers of the epidermis beginning with the stratum corneum, followed by stratum lucidum, stratum granulosum and stratum spinosum. The stratum germinativum is the lowest layer of the skin and is also referred to as stratum basale. **B** The schematic shows the human skin including epidermis, dermis and the subcutaneous layer highlighting its most important components (e.g. sebaceous glands). Adapted from <http://biology-forums.com/index.php?action=gallery;cat=4> [55].

Constituting approximately 15 % of the total body weight of an adult, the skin is the most extensive organ of the human body and varies from 1.5 to 4.0 mm in thickness depending on body location [54], [56].

The epidermis represents the outermost layer and takes on the chemical-, biological-, immunological- and physical barrier functions of the skin. It is continually renewing and consists of five layers based on the differentiation status of the keratinocytes which comprise the major cell population (80 %). Figure 5A depicts the 5 layers of the epidermis, beginning with the innermost stratum germinativum (basal cell layer), to the stratum spinosum (squamous cell layer), the stratum granulosum (granular cell layer), the stratum lucidum, and finally the outermost stratum corneum (horny cell layer) [57], [58]. Keratinocytes originate from stem cells that reside at the basal layer and undergo biochemical and morphological changes as they migrate outwards through the various layers of the epidermis to the stratum corneum, where they reach terminal differentiation into flattened corneocytes, forming a toughened layer that prevents water loss and protects against invaders from the environment [56], [57].

The junction between the epidermis and dermis, known as the dermoepidermal junction (DEJ) or basement membrane zone (BMZ), is a structural and dynamic interface composed of multiple proteins [59]. It functions as a selective barrier for the transit of molecules according to their charge and size, enabling the migration of various cell types under normal and pathological conditions. As such, the BMZ plays a major role in wound healing, morphogenesis, remodeling, and development of the skin. It is divided into three zones: the lamina lucida, lamina densa, and sub-lamina densa. Maintenance of tissue integrity is achieved by various junctional complexes (e.g. hemidesmosomes, anchoring fibrils, and anchoring filaments) in the different zones of DEJ, that enable cellular adhesion to the extracellular matrix [60], [61].

The dermis is essential for the nourishment of the skin, as it harbors the vascular and nervous system. Furthermore, it is important for elasticity, tear strength, and plasticity. It is comprised of both cellular components and fibrous molecules, particularly different types of collagens and the ground substance (proteoglycans). Fibroblasts are the most common cell type found within the dermis. However, the dermis also houses numerous cell types of the immune system, including mast cells, dermal dendrocytes, and T cells [56], [57].

The subcutis represents the deepest layer of the skin. It is composed of fatty tissue, in which adipocytes are the main cell type. It is important for thermo-insulation and regulation, protection from mechanical violations, and storage of energy [56].

### **1.3.1 IMMUNOLOGICAL FUNCTIONS OF THE SKIN**

One of the skin's most important functions is immunological protection. The stratum corneum of the epidermis works as a mechanical barrier as well as a surface that is unwelcoming to pathogens due to its dry, acidic milieu and symbiotic microbiota [54]. Keratinocytes themselves are immune competent cells, able to react to wounds and invading pathogens with the secretion of antimicrobial peptides, as well as cytokines for the recruitment and promotion of innate and adaptive immune responses. The epidermis and dermis additionally house various immune cell subsets, including T cells, DCs, macrophages, and mast cells [1]. The different types of DCs found in the skin serve as professional APCs that continuously sample their surroundings for the presence of foreign antigen. The majority of T cells patrolling the epidermis express a T-memory/effector phenotype, capable of effector function upon re-activation [54], [56], [57].

#### **1.3.1.1 SKIN DENDRITIC CELLS**

The skin harbors several distinct DC subsets such as Langerhans cells (LC) that are found only in the epidermis, and conventional- (cDCs), monocyte-derived- (mdDCs) and plasmacytoid DCs (pDCs) in the dermis [62]. DCs act as an important link between the innate and adaptive immune systems. Immature DCs can respond to specific pathogen-associated molecular patterns (PAMPs) on microbes or to injury stimuli with the secretion of cytokines. Furthermore, they are able to ingest non-self-proteins, migrate to the skin-draining LNs where they then present these processed non-self epitopes loaded onto MHC molecules to naïve T cells [1]. LCs in the epidermis interact closely with keratinocytes, and are described to stimulate CD8<sup>+</sup> T cells and NK cells via secretion of IL-15, play a role in the development of Th17 responses, as well as suppress immune responses induced by cDCs [62], [63]. Conventional DCs are divided into different subtypes according to the expression pattern of surface molecules. These play a role in cross-presentation, the induction of Th1 responses and the induction of Tregs. Furthermore, cDCs are important in the prevention of autoimmunity, as they are able to present skin derived self-antigens to the lymph nodes, where they lead to the death of autoreactive T cells [62]. Finally, pDCs are recruited into inflamed skin to support wound healing, but are absent under normal conditions [62].

#### **1.3.1.2 TISSUE RESIDENT MEMORY T CELLS**

There are nearly 20 billion T cells residing in the human skin. This number represents approximately twice the number of T cells found in the entire circulation [64], underscoring the importance of

immune surveillance in the skin. These so-called tissue resident memory T cells ( $T_{RM}$ ) have gained increasing interest in recent years.

Watanabe *et al.* (2015) recently described four populations of resident and recirculating memory T cells that are important for human skin protection. Two of these are true  $T_{RM}$  and two are short-term residents and have the ability to migrate between the skin and the blood and lymph nodes. These various subsets of skin resident T cells were identified using an immunodeficient mouse into which human T cells had been engrafted. When these mice were treated with the anti-human CD52 antibody alemtuzumab, capable of depleting all recirculating T cells, a small subset of T cells, the true  $T_{RM}$ , remained unaffected in the skin [65].  $T_{RM}$  are located at epithelial barriers, like gut, respiratory tract, reproductive organs, and skin. The majority are specific for antigens that previously induced an immune response, and are therefore capable of rapidly responding to a repeated infection.  $T_{RM}$  can be  $CD4^+$  or  $CD8^+$ , depending on the pathogen that led to their development. Epidermal  $T_{RM}$  are  $CD69^+ CD103^+ CCR7^-$  whereas dermal  $T_{RM}$  are  $CD69^+ CD103^- CCR7^-$ .  $CD69$  is important for the resident state of  $T_{RM}$  as its expression interferes with the function and expression of the G protein-coupled receptor for sphingosine 1 phosphate (S1P1).  $CD103$  expression is increased in  $CD8^+$  compared to  $CD4^+ T_{RM}$ . It is a ligand for E-cadherin, which is present on the surface of epithelial cells found in many barrier tissues. Upregulation of  $CD103$  is induced upon migration to the epidermis and local signaling by  $TGF\beta$  expressed by keratinocytes.  $CCR7$  on the other hand, is important for cells to exit the skin and migrate to LN.  $CD103^+ T_{RM}$  showed potent effector functions but a decreased proliferative phenotype compared to  $CD103^- T_{RM}$ . Recirculating memory T cells that are  $CCR7^+$  and  $CD62L^+$  (also known as L-selectin) are called central memory T cells ( $T_{CM}$ ).  $T_{CM}$  circulate between skin, blood, and skin-draining as well as distant LN.  $CCR7^+ CD62L^-$  migratory memory T cells ( $T_{MM}$ ) are also able to recirculate, but not to distant LN, due to the lack of L-selectin expression. Additionally, they are suggested to migrate more slowly [65]–[67]. The four distinct T cell populations are depicted in Figure 6.

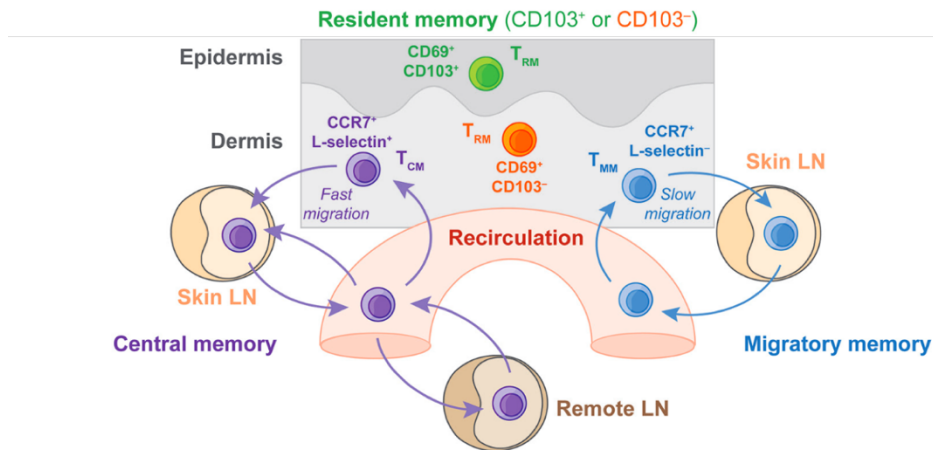


**Figure 6** A schematic depiction of four subpopulations of memory T cells with different recirculation, proliferation and functional behavior. Non circulating  $T_{RM}$  cells in dermis (orange) and epidermis (green), differing in CD103 expression. TCM (purple) and TMM (blue) showing distinct migratory patterns. Adapted from Hochheiser, K. *et al.* 2015 [67].

## 1.4 EPIDERMOLYSIS BULLOSA

Inherited genetically and clinically heterogeneous diseases, where blisters and erosions form on patient's skin and mucous membranes after minor trauma are comprised in the term epidermolysis bullosa (EB). Cutaneous findings that are associated with inherited EB are among others blistering, milia, alopecia, congenital absence of skin, mottled pigmentation, atrophy, scarring and contractures [68], [69]. EB is classified as a rare disease with an estimated incidence of 50 per one million live births according to the National EB Registry [70]. In Europe there are about 30,000 EB patients living whereof 500 EB patients are registered in Austria [71].

EB is divided into four major types: EB simplex (EBS), junctional EB (JEB), dystrophic EB (DEB) and Kindler syndrome (KS). These EB types vary not only genetically or phenotypically but especially in regard to the site of blister formation and cleavage in the different skin layers [69]. Blistering is restricted to the epidermis in all subtypes of EBS. JEB is characterized by blister formation in the lamina lucida. In all subtypes of DEB, blisters develop underneath the lamina densa. Finally, kindler syndrome shows blistering at several levels within and/or underneath the BMZ [72]. The major types of EB and the associated affected proteins in the different layers of the skin are shown in Figure 7.

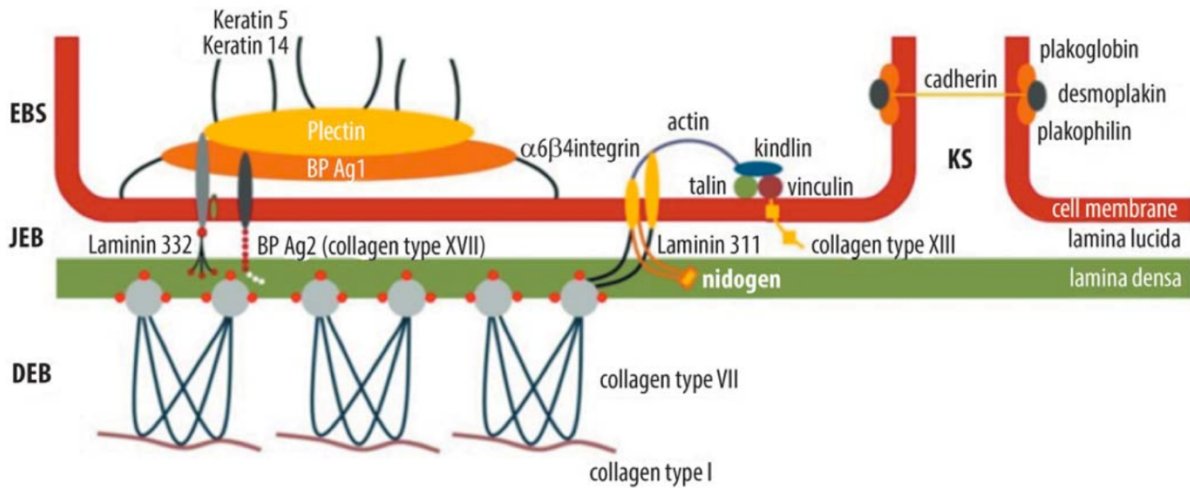


**Figure 7 Schematic representation of proteins that are affected in different types of EB.** The affected proteins are located in different layers of the basement membrane zone. EBS: epidermolysis bullosa simplex, JEB: junctional epidermolysis bullosa, DEB: dystrophic epidermolysis bullosa, KS: kindler syndrome. Adapted from Boeira *et al.* 2013 [70].

The phenotypic differences between the various EB types can be accounted for mutations in different genes encoding structural proteins that are responsible for maintaining adhesion between the various skin layers. 18 different genes have been found to be causally associated with 30 different subtypes of EB [73]. In Table 1 the major types of EB with related subtypes, the associated mode of inheritance, levels of cleavage and blistering, and affected proteins are listed.

**Table 1 Current classification of inherited EB divided in types and subtypes with affected proteins.** AD = autosomal dominant, AR = autosomal recessive. Adapted from Boeira *et al.* 2013 [70].

major EB type	major EB subtype	mode of inheritance	level of skin cleavage	usual level of blister formation	affected proteins
EBS	suprabasal EBS	AD	intraepidermal	subbasal epidermis	transglutaminase 5, plakophilin 1, desmoplakin, plakoglobin
	basal EBS	AD	intraepidermal	basal epidermis	keratin 5 and 14, plectin, exophilin 5 (Slac2-b), bullous pemphigoid antigen1
JEB	JEB, generalized	AR	intralamina lucida	Intralamina lucida	laminin-332, collagen XVII, α6β4 integrin, α3 integrin subunit
	JEB, localized	AR	intralamina lucida	Intralamina lucida	collagen XVII, laminin-332, α6β4 integrin
DEB	DDEB	AD	lamina densa	sublamina densa	collagen VII
	RDEB	AR	lamina densa	sublamina densa	collagen VII
Kindler syndrome		AR	multiple levels		Fermitin family homolog 1 (kindlin-1)

In addition to macroscopic analysis of the skin for the diagnosis of a patient, transmission electron microscopy (TEM) and immunofluorescence mapping (IFM) are vital techniques that allow identifying

the different levels of skin cleavage. TEM enables to visualize and semi quantitative assess specific structures, whose alteration is known to be linked to the different subtypes of EB. The use of specific monoclonal antibodies for IFM can also lead to an insight into structural proteins that are known to be altered in EB. Differences in relative expression or distribution of proteins within the skin can also be analyzed with this technique. To determine the mode of inheritance and the exact site of mutation within the genomic sequence, mutational analysis depicts the method of choice [74].

Epidermolysis bullosa simplex is characterized by blistering within the epidermis, scarce systemic involvement and skin lesions that usually vanish without scarring. EBS is mainly inherited in an autosomal dominant manner. Cleavage at intraepidermal levels in EBS is caused by mutations in the *keratin (K) 5* and *K14* genes encoding proteins of type I and II intermediate filament (IF) and keratin. Keratinocytes in the epidermis express those proteins, which assemble to heterodimers and form 10-nm-wide cytoskeletal IF. There are several clinical subtypes of EBS described. EBS localized is the most common subtype with an incidence of two-thirds among EBS patients and blisters are restricted to the feet and hands. Patients with generalized EBS show blistering all over the body whereas blisters appear in a more clustered pattern in patients with EBS generalized severe. Some EBS subtypes show additional clinical complications such as EBS with muscular dystrophy [69], [70], [75].

Junctional epidermolysis bullosa (JEB) is inherited in an autosomal recessive manner and cleavage occurs at the site of the lamina lucida in the DEJ [70]. Mutations in the genes *LAMA3*, *LAMB3* or *LAMC2*, coding for the  $\alpha 3$ ,  $\beta 3$  and  $\gamma 2$  chains of laminin 5 and in the *COL17* gene are the most common ones in JEB [76]. The two major types of JEB are defined as JEB generalized (JEB-gen) and JEB localized (JEB-loc) and differ in their severity. JEB generalized severe (JEB-gen sev) constitute one of the most severe forms of EB since all skin areas are affected and blistering already occurs after birth. Patients mostly die within the first years of life due to sepsis, failure to thrive or tracheolaryngeal obstruction [69].

The gene that is affected by mutations in dystrophic epidermolysis bullosa is *COL7A1*. It codes for type VII-collagen, which is the main component of anchoring fibrils of the basement membrane that attach the epidermis to the underlying dermis [68]. Mutations within the *COL7A1* gene lead to loss or non-functionality of type VII-collagen and to reduced or complete absence of anchoring fibrils and therefore to cleavage in the sub-basal lamina [70], [77]. According to the type of inheritance, DEB is classified in two major subtypes: the autosomal dominant inherited form, dominant dystrophic EB (DDEB), and the autosomal recessive form, recessive dystrophic EB (RDEB). Further subdivision is ensued by severity and clinical phenotype of the disease [69]. In DDEB generalized blisters occur after birth or during childhood but blisters appear more localized when patients are getting older. Patients

with RDEB show mild to severe manifestation of the disease, with localized or generalized blisters, respectively [70]. A more detailed description of RDEB is given in chapter 1.4.1.

Kindler syndrome is a rare autosomal recessive inherited disease and the clinical phenotype can be similar to all three major types of EB. A mutation in the gene encoding Kindlin-1, which is a central component of the inter keratinocyte contact [70], results in destruction of the basement membrane and impaired type VII-collagen deposition [78]. In contrast to photosensitivity and poikilodermatous pigmentations that develop in later stages, generalized blistering occurs by birth [69].

#### 1.4.1 RECESSIVE DYSTROPHIC EPIDERMOLYSIS BULLOSA

RDEB is divided into three major subtypes – RDEB generalized severe (RDEB-gen sev), RDEB generalized intermediate (RDEB-gen intermed) and RDEB inversa (RDEB-I). The forms differ in severity although blisters already occur immediately after birth in all subtypes [69]. RDEB is caused by mutations within the gene *COL7A1*, coding for type VII-collagen, which results in blister formation within the basal membrane. Depending on the alteration in type VII-collagen and the resulting nascence or reduced numbers of anchoring fibrils, the clinical severity differs between the groups (Table 2)[79].

**Table 2 Subtypes of recessive dystrophic epidermolysis bullosa (RDEB)**, adapted from Fine *et al.* 2014 [72].

All subtypes	
<b>RDEB</b>	RDEB, generalized severe
	RDEB, generalized intermediate
	RDEB, inversa
	RDEB, localized
	RDEB, pretibial
	RDEB, pruriginosa
	RDEB, cetripetalis
	RDEB, bullous dermolysis of the newborn

Generalized RDEB-gen sev is the most severe form of RDEB. It is caused by frameshift mutations that lead to a preterminal termination stop codon (PTC) [80]. The clinical picture of the disease includes excessive scarring of the blistered skin, growth retardation, multifactorial anemia, esophageal strictures and pseudosyndactyly (fusion of the digits). The latter ones arise early in infancy and impact the quality of life of affected patients. Furthermore, blistering of skin and mucous membranes lead to chronic blood loss, inflammation, infection, poor nutrition, delayed puberty and osteoporosis [69], [81].

RDEB-gen intermed is a more common and a less severe subtype as the risk for esophageal strictures and the deformation of the limbs is decreased. In patients suffering from RDEB-I, the site of blister development is mainly limited to intertriginous skin sites, the base of the neck, the uppermost back and the lumbosacral area [69].

Despite the complications of RDEB in early childhood the risk of infantile death is low [69]. However, RDEB-gen sev patients may die in early adulthood due to complications with the kidneys or development of an aggressive malignant cutaneous squamous cell carcinoma (cSCC) at the site of erosions and recurrent scarring [69], [81]. Patients suffering from RDEB-gen intermed show also a high susceptibility to form cSCC but the risk of death due to this cancer is decreased. Patients with RDEB-I develop cSCC to an even smaller extent [69].

#### 1.4.1.1 CUTANEOUS SQUAMOUS CELL CARCINOMA IN EB

Aggressive, cutaneous squamous cell carcinoma (cSCC) represents the most serious complication in patients with EB. cSCC arises primarily in RDEB, to a lower extent in JEB-gen sev and can be rarely seen in EBS and DDEB patients [82]. SCC is a cancer of squamous cells of the epidermis and primarily arise at UV-exposed areas but can also be observed at mucous membranes and genitals [83]. However, in RDEB patients cSCC are predominantly formed at sites of long-term skin wounds (63.2–100 %) and long-term cutaneous scars (20–26.7 %) [82].

Fine *et al.* (2009) investigated the risk of incidence of the first SCC in RDEB patients compared with the risk of death from SCC. The results are summarized in Figure 8.

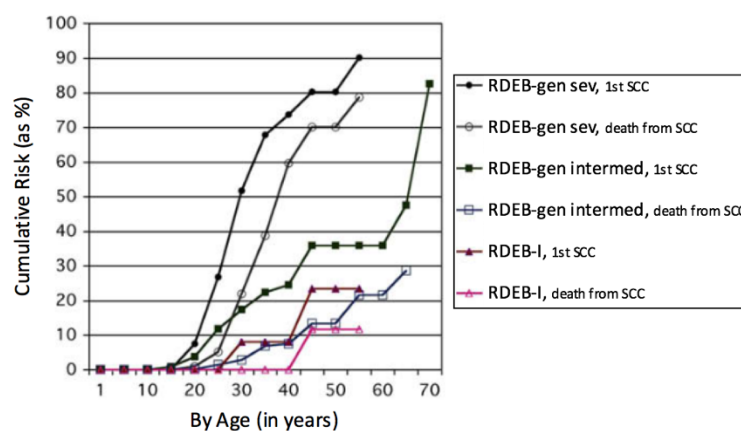


**Figure 8** Cumulative risk of the development of a first SCC and death from SCC depicted for the major subtypes of RDEB. RDEB-gen sev (RDEB generalized severe); RDEB-gen intermed (RDEB generalized intermediate); RDEB-I (RDEB inversa). Adapted from Fine *et al.* 2009 [82].

The cumulative risk to develop a first SCC for patients with RDEB-gen sev is 7.5 % at the age of 20 years. This risk increases tremendously by ages 35, 40, 45, and 55 giving an incidence to develop a first SCC of 17.8 %, 73.4 %, 80.2%, and 90.1 %, respectively. The risk for RDEB-gen intermed and RDEB-I is similar but to a lower extent, with its peak at 82.5 % for RDEB-gen intermed patients by age of 75. The risk of death from SCC correlates with the risk of developing a first SCC. The earliest death caused by SCC occurs in RDEB-gen sev patients followed by RDEB-gen intermed and RDEB-I [82]. When compared to non-EB patients, 80 % of non-melanoma skin cancers (including SCC and basal cell carcinoma, BCC) arise later in life, at the age of 60 or older [84]. In this context it is also worth noting that immunosuppressed patients, like organ transplant recipients, are also at elevated risk (250x) to develop cSCC thereby pointing to a possible relation between cSCC and the immune suppressive effects also in RDEB patients [85].

The genetic background of RDEB-SCC is yet not fully understood, but gene profiling experiments comparing RDEB-SCC tumors with UV-induced SCC tumors in the general population demonstrated that RDEB-SCC and UV-SCC keratinocytes are largely genetically indistinct with only a handful of genes differentially expressed between the two tumor types [86]. More recent data indicate that the dermal matrix in RDEB predisposes to cancer development. Gene expression profiling revealed striking similarities between RDEB dermal fibroblasts and UV-SCC tumor associated fibroblasts. Knockdown of *COL7A1* expression in human dermal fibroblasts (to simulate the genetic defect in RDEB) induced a phenotypic change in these cells resembling that of tumor-associated fibroblasts which promoted keratinocyte invasion and tumor progression [87]. Furthermore, repeated injury in RDEB has been shown to promote dermal stiffening which in turn enhanced integrin  $\beta$ 1/pFAK/pAKT signaling in SCC cells [88]. Thus, loss of type VII collagen in RDEB leads to a global remodeling of the dermal microenvironment that is primed for tumor development [89].

It is known that healthy, sun-exposed human skin is freckled with cells that harbor mutations in oncogenic genes but still fulfil their function in the epidermis [90]. In this context some oncogenic mutations have already been described. For example, Arbiser *et al.* (2004) described that alterations in tumor suppressor genes, such as p53 mutations or *p16ink4a* hypermethylation, are associated with RDEB-SCC [91]. Therefore, Uitto *et al.* (2016) suggested that the increased incidence for SCC in RDEB is due to a special microenvironment that is not able to rein alterations in differentiation and proliferation resulting from mutations in oncogenes for instance p53 and NOTCH1 [73].

Microbial infection of wounds is one of the burdens of RDEB patients [68]. Recently, a possible link between bacterial infection, inflammation and tumor development has been identified. Hoste *et al.*

(2015) used a mouse model of chronic inflammation and wound associated cancer formation. They could show that signaling via toll-like receptor 5 (TLR-5), upon exposure to flagellin, lead to upregulation of high mobility group box 1 (HMGB1). It is secreted upon inflammation and was already described to play a role in tumor formation [92] for example, in maintaining the inflammatory tumor microenvironment, by increasing the IL-10 secretion of Tregs, and promoting invasion and metastasis through expression of matrix metalloproteinases, which degrade extracellular matrix proteins. However, it is also described to interact with tumor suppressor protein Rb in breast cancer and increase autophagy and therefore additionally exhibit antitumor functions [93]. Interestingly, RDEB tissue also revealed high levels of HMGB1 [92].

#### **1.4.1.2 TREATMENT OF EPIDERMOLYSIS BULLOSA ASSOCIATED SCC**

The most common treatment for SCCs in RDEB patients represents surgical excision over a wide area. Nevertheless, removal of a well differentiated SCC does usually not result in a cure. Unlike UV induced SCC in non-RDEB patients, the tumor recurs with elevated numbers of primary SCCs and a high metastasizing potential [94]. Non-surgical treatments like radio- or chemotherapies have been used to treat metastasis but with lower success due to side effects such as toxicity. Furthermore, radiotherapy can worsen wound healing and desquamation which is of course a big issue in EB, but has already been well tolerated when applied in smaller fractions [94], [95]. Treatment with cetuximab, a monoclonal antibody that binds to the epidermal growth factor (EGFR), represents an option of treatment of SCCs that do not have a mutation in *ras* and express EGFR. Arnold *et al.* (2009) observed tumor size reduction in a 25-year old RDEB patient after cetuximab treatment in combination with radiotherapy [96]. However, cetuximab is known to cause wound healing complications [97] which we also observed in an RDEB-SCC patient treated with cetuximab. This could be in part circumvented by using a lower concentration of the drug but simultaneously decreasing the anti-tumor effect thereby limiting its long-term use.

The absence of an effective treatment and the fact that the majority of RDEB-gen sev patients die within 5 years after diagnosis of the first SCC due to its aggressive, metastatic nature [82], underlines the urgent need for a consistent therapy of SCC in RDEB patients.

## 1.5 HYPOTHESIS

Given the abundance of highly specialized immune cell subsets that are resident in the skin, immunotherapy represents an appealing alternative strategy for the treatment of aggressive cutaneous carcinomas such as RDEB-SCC. As a barrier tissue tasked with protecting the host from invading pathogens, the skin is home to numerous memory T cells primed to recognize and respond to recall antigens it has previously encountered. This would include viral epitopes against which the majority of the general population has been vaccinated. We hypothesize that this pre-existing immunity can be exploited and re-directed against tumor cells by manipulating these malignant cells to express the cognate viral epitopes. The mechanisms engaged in this type of tumor destruction would likely be similar to the cytolytic killing of virus infected cells. We believe that the use of a recall antigen that is non-self circumvents many of the tolerogenic mechanisms engaged by tumors and triggers a rapid and vigorous memory response that will effectively control or eliminate the tumor. To test this hypothesis, we first need to establish a mouse model with specific CTL immunity against known viral epitopes which can then be used for the further development of this therapeutic strategy.

## 2 SPECIFIC AIMS AND SCOPE OF THIS THESIS

The overall goal of the study was the establishment of a mouse model that would allow us to evaluate the quality and robustness of immune responses to known immunogenic viral CTL epitopes. Subsequently, the model could then be used as the basis for the development of an anti-tumor therapeutic strategy against RDEB-SCC. Specifically, we had three specific aims, namely

1. the generation and characterization of specific viral CTL immunity in mice,
2. the stable expression of the cognate CTL epitopes in a syngeneic tumor cell line, and
3. the demonstration of anti-neoplastic activity of our approach.

To this end, we designed and generated DNA plasmid vaccines, and established an immunization protocol making use of the Helios gene gun system for administration of our vaccines. The quality of the immunity generated by vaccination was monitored by cytokine release, as well as functional cellular assays both *in vitro* and *in vivo*. The stable expression of cognate viral CTL epitopes in tumor cells was achieved by retroviral transduction. Finally, the anti-neoplastic activity of our strategy was evaluated *in vivo* in tumor challenge experiments in immunized mice.

### 3 MATERIALS AND METHODS

#### 3.1 REAGENTS

##### 3.1.1 MEASLES VIRUS PEPTIDES

CTL epitopes N52 (LDRLVRIG) and N81 (VESPGQLI) of the measles virus (MV) nucleocapsid protein were commercially synthesized by Proimmune (Oxford, UK) at a purity of approximately 96 %. Lyophilized peptides were reconstituted at a concentration of 10 mg/ml with DMSO (Sigma-Aldrich, St. Louis, MO, USA) and stored at  $-20^{\circ}\text{C}$ . SIINFEKL, the immunodominant CTL peptide of ovalbumin served as control peptide and was a generous gift from Dr. Stöcklinger from Paris Lodron University Salzburg.

##### 3.1.2 DEXTRAMER

For the identification of N81-specific CTLs, a customized N81-H-2K<sup>k</sup>-dextramer was synthesized and purchased from Immudex (Copenhagen, DNK). It comprises a dextran backbone carrying MHC class I molecules (H-2K<sup>k</sup>) loaded with N81 peptide and fluorochrome FITC molecules [98]. This N81-H-2K<sup>k</sup>-dextramer specifically binds to CD8<sup>+</sup> T cells expressing N81-specific TCR.

#### 3.2 DNA PLASMIDS

All primers used for cloning are listed in detail in Table 5, chapter 10.1.

##### 3.2.1 PLASMID CONSTRUCTS FOR DNA IMMUNIZATION

For DNA vaccination plasmids based on the mammalian expression vector pCI (Promega, Madison, WI, USA) were cloned consisting of a murine Interleukin 2 signal sequence (IL2ss) followed by a MV specific CTL epitope and a measles virus specific T-helper epitope (MVTh) at the C-terminus. The IL2ss is needed for enhanced targeting to the ER [99] and loading onto MHC class I of the downstream cloned MV specific epitopes comprising the nucleotide sequence of nucleocapsid protein H-2K<sup>k</sup> restricted epitopes N52, N81 or a fusion of both N52N81 [100]. To support the generation of a CTL response to the nucleocapsid protein epitopes [101], the MVTh (F288) was fused downstream [102].

At the beginning the following double stranded oligonucleotides have been hybridized: IL2ss<sub>sense</sub>: 5'-CTAGCGCCACCATGTACAGCATGCAGCTCGCCAGTTGCGTGACCCCTGACCCCTGGTG-CTGCTGGTG-3', IL2ss<sub>antisense</sub>: 5'-AATTCACCAGCAGCACCAGGGTCAGGGTCACGCAACTGGCGAGCTGCATGCTGTACATGGTGCG-3', N52<sub>sense</sub>: 5'- AATCCCTGGACAGGCTGGTGAGGCTGATCGGC-3', N52<sub>antisense</sub>: 5'-GCCGATCAGCCTCACCAGCCTGTCCAGGG-3', N81<sub>sense</sub>: 5'- AATCCGTGGAGAGCCCCGCCAGCTGATC-3',



retroviral transfection was used. Our retroviral vector system (pMX\_IRES-GFP vector, Cell Biolabs, San Diego, CA, USA) comprises GFP as marker for selection of positively transduced cells. Since GFP itself is known to elicit an immune response *in vivo*, which might contribute to tumor rejection, we inserted loxP sites at the flanks of the IRES-GFP sequence. After viral transduction cells were treated with a plasmid encoding the Cre recombinase (pCMV\_Cre, Biocat, Heidelberg, GER) for three times and finally GFP negative cells were sorted and used for further studies.

### 3.2.2.1 CLONING OF PMX\_LOXP-GFP

The mammalian retroviral transduction vector pMX\_IRES-GFP was purchased from Cell Biolabs. loxP sites (ATAACTTCGTATAGCATAACATTATACGAAGTTAT) were cloned upstream and downstream of the IRES-GFP sequence of the vector, to facilitate deletion of the IRES-GFP sequence upon Cre transfection, in the stably transduced target cells. First, an IRES specific forward primer (loxP\_IRES\_fwd) and a GFP specific reverse primer (GFP\_loxP\_rev) were generated incorporating loxP sites and restriction sites Sall (FastDigest, Thermo Scientific, Waltham, MA, USA) and SnaBI (FastDigest, Thermo Scientific), respectively (primer sequences are given in , chapter 10.1). PCR amplification was performed using KOD Polymerase (MerckMillipore, Darmstadt, GER), dNTPs and pMX\_IRES-GFP as template. The conditions for the amplification of the PCR product were set as follows: 95 °C for 2 minutes, followed by 5 cycles of 95 °C for 20 s, 51 °C for 10 s and 70 °C for 30 seconds, followed by 20 cycles of 95 °C for 20 s, 70 °C for 10 s and 70 °C for 30 s. The PCR was terminated with 70 °C for 5 minutes and 4 °C for an infinite time. The integrity of the PCR product was verified by an 1% agarose gel. The NucleoSpin Gel and PCR Clean-up Kit (Machery-Nagel, Düren, GER) was used for purification of the PCR product according to the manufacturer's protocol.

Restriction digest of 3 µg of pMX\_IRES-GFP and the purified PCR product was performed using Sall (Thermo Scientific) and SnaBI (Thermo Scientific) in a double digestion mix for 45 minutes at 37 °C. The pMX backbone and loxP flanked IRES-GFP insert were ligated with T4 DNA ligase (Thermo scientific) for 90 minutes at room temperature followed by overnight incubation at 4 °C. Then, the ligated plasmid was transformed into One Shot™ *E. coli* Top10 chemical competent cells (Invitrogen, Carlsbad, CA, USA) and positive clones were screened after 24 hours using a standard colony PCR reaction. After verification of the correct plasmid sequence by direct sequence analysis using pMX\_seq\_fwd primer (as described in chapter 3.2.3), a plasmid preparation was performed with NucleoBond PC100 Midiprep Plasmid Purification Kit (Machery-Nagel) according to the manufacturer's protocol. The generated plasmid was named pMX\_loxP-GFP.

### 3.2.2.2 CLONING OF PMX\_N81\_LOXP-GFP

A IL2ss, MV-specific CTL epitope (N81) and a MVTh epitope sequence were cloned into pMX\_loxP-GFP vector upstream of the loxP site flanking IRES-GFP using pCI\_N81 vector as template. An IL2ss specific forward primer (BamHI\_IL2ss\_fwd) and a MV T-helper epitope specific reverse primer (MVTh\_XhoI\_rev) were used for the amplification of the expression cassette from pCI\_N81 vector. After verification of the correct size of the PCR product on an agarose gel, the purified PCR product as well as 3 µg of pMX\_loxP-GFP were digested with the restriction enzymes BamHI and XhoI (FastDigest, Thermo Fisher Scientific) for 60 minutes at 37 °C. The digested PCR product was further cloned into pMX\_loxP-GFP using T4 DNA ligase (Thermo Scientific). The correct insertion of the MV expression cassette into the pMX\_loxP-GFP vector was verified by sequence analysis using pMX\_seq\_fwd primer.

### 3.2.3 SEQUENCE ANALYSIS

The integrity of all DNA plasmids was verified by direct sequencing using the BigDye Terminator sequencing kit (Applied Biosystems, Waltham, MA, USA). The reaction was performed with sequencing premix, 5x Sequencing buffer, forward or reverse primer (10µM) and ≥ 100 ng/ml plasmid DNA or PCR product subjected to PCR reaction. Cycling conditions were set to 96 °C for 1 min followed by 30 cycles of 96 °C for 10 seconds, 50 °C for 5 seconds and 60 °C for 90 seconds. Sequencing was routinely performed on the in-house sequencer (3500 Genetic Analyzer, Applied Biosystems/Hitachi, Tokyo, JPN) and results were analyzed using Chromas 1.56 (Technelysium Pty Ltd, South Brisbane, AUS).

## 3.3 CELL CULTURE

### 3.3.1 PRIMARY CELLS AND CELL LINES

Primary splenocytes as well as lymphocytes from C3H mice were cultured in RPMI 1640 (Thermo Fisher Scientific) medium supplemented with 10 % FCS (Biochrom, Berlin, GER), 1 % penicillin/streptomycin (Biochrom), 1 % sodium-pyruvate (Sigma-Aldrich), 1 % MEM non-essential amino acids (Sigma-Aldrich), 0.0669 mM β-mercaptoethanol (Sigma-Aldrich) and 1% L-glutamine (Thermo Fisher Scientific) at 37 °C and 5 % CO<sub>2</sub>. This medium is referred to as “RPMI complete” throughout this thesis.

The murine cancer cell line SCCVII was kindly provided by Prof. Scott Strome (University of Maryland, USA) and was also cultured in RPMI complete medium. SCCVII cells have been isolated from a

spontaneously arisen squamous cell carcinoma in a C3H mouse and are characterized by poor immunogenicity and expression of MHC class I molecules [104].

Sub-culturing of SCCVII cells was performed after washing the cells with duplecco's phosphate buffered saline (DPBS, Sigma-Aldrich). Solution A + Trypsin (0,05 %) EDTA (0,02 %) (Biochrom) was used to detach the cells from the flask and by adding Solution A + 10 % FCS (Biochrom) the trypsinization reaction was stopped. After centrifugation at 350 g for 5 minutes, cells were resuspended in RPMI complete for further cultivation.

All cells were cultured at 37°C under 5% CO<sub>2</sub> in a humidified incubator (Thermo Electron Corporation, Forma Series II Jacketed CO<sub>2</sub> incubator, Thermo Fisher Scientific).

### **3.4 GENERATION OF CELL LINES**

#### **3.4.1 VIRAL TRANSDUCTION**

Retroviral transduction of mammalian cells is routinely performed in the lab by our technician. Briefly, Phoenix Cells (ATCC, Manassas, VA, USA), at a confluency of 60-70 %, were transfected with either 15 µg pMX\_N81\_loxP-GFP or 15 µg pMX\_loxP-GFP (mock) using calcium-phosphate and incubated over night at 37 °C with DMEM (Thermo Fisher Scientific) + 10 % FCS and Penicillin/Streptomycin (Biochrom). Medium was changed and every 8 hours thereafter virus supernatants were collected, filtered through a 0.22 µm filter and spinfected with 5 µg/ml polybrene onto SCCVII target cells. Successful transduction resulted in GFP expression by cells, which was assessed by flow cytometric analysis (FC500, Beckman Coulter). GFP positive SCCVII\_N81 and SCCVII\_mock cells were then sorted, via gating on GFP positive cells with duplet discrimination, with a FACS Aria™ machine (BD Biosciences, San Jose, CA, USA).

#### **3.4.2 TRANSIENT TRANSFECTION**

In order to erase the GFP sequence from stably transduced cells we performed a transient transfection using a plasmid expressing Cre recombinase. Transfection of GFP positively sorted SCCVII\_N81 and SCCVII\_mock cells were performed three times, in a two days interval, using the Xfect™ transfection reagent (Clontech, Mountain View, CA, USA) according to manufacturer's protocol. Briefly, 7 µg pCMV\_Cre plasmid DNA (Biocat) was mixed with 2,1 µl of Xfect polymer and cells (50% confluent) were incubated with the transfection solution for 5 hours at 37°C. Afterwards, the medium was changed

and loss of GFP signal was verified 24 h after each transfection round. The cells were detached from the culture flask, as described before and washed with DPBS. The amount of GFP positive cells was investigated via flow cytometry (FC500, Beckman Coulter, Krefeld, GER). Further on, the GFP negative population was sorted from the whole cell bulge with duplet discrimination (FACS Aria™, BD Biosciences) and correct excision of IRES-GFP was verified by PCR analysis.

### 3.5 CHARACTERIZATION OF CELL LINES

The murine SCCVII cell line was engineered to stably express N81 (SCCVII\_N81). The generation of a SCCVII cell line, transduced with the empty vector pMX\_loxP-GFP (SCCVII\_mock) served as control (Table 3). Both cell lines were characterized regarding the proper integration of the gene of interest, as well as their immunological phenotype.

**Table 3** Retroviral transduced murine SCC cell lines used for *in vivo* tumor experiments.

Parental cell line	Viral plasmids introduced	Name of new cell line
SCCVII	pMX_N81_loxP-GFP	<b>SCCVII_N81</b>
SCCVII	pMX_loxp-GFP	<b>SCCVII_mock</b>

#### 3.5.1 INTEGRATION PCR

Successful stable integration of the gene of interest was investigated on genomic level. Therefore, genomic DNA was isolated from  $1-4 \times 10^6$  retroviral stably transduced SCCVII\_mock and SCCVII\_N81 cells before and after pCMV\_Cre transfection using the PureLink® Genomic DNA Mini Kit (Invitrogen), according to the manufacturer's protocol. The parental SCCVII cells served as a control. KOD DNA polymerase was used to amplify the target gene using an IL2ss specific forward primer (int\_IL2ss\_fwd) and a MVTh specific reverse primer (int\_MVTh\_rev). For the confirmation of the IRES-GFP knock-out, an IRES specific forward primer (int\_IRES\_fwd) and a reverse primer binding downstream of GFP (int\_GFP\_rev) were used. PCR conditions were set to: 95 °C for 1 min, 30 cycles of 95 °C for 15 seconds, 62 °C for 15 seconds and 72 °C for 10 seconds, followed by 5 minutes at 72 °C and was terminated with at 4 °C.

The IL2ss specific forward primer (int\_IL2ss\_fwd) as well as the primer binding downstream of GFP (int\_GFP\_rev) was also used to verify the knock-out of the IRES-GFP by sequence analysis. Therefore, the PCR product was cleaned up using the illustra™ ExoStar™ Kit (GE Healthcare, Vienna, AUT), followed by sequence analysis as described in chapter 3.2.3.

### 3.5.2 REVERSE TRANSCRIPTASE PCR (RT-PCR)

55,000 SCCVII cells/well were seeded into a 6-well plate and incubated for 48 hours in the presence of either 100 or 500 U/ml murine recombinant IFN $\gamma$  (Peprotech, Vienna, AUT). Cells were washed once with DPBS and then lysed using RLT buffer + 1 %  $\beta$ -mercaptoethanol (Sigma-Aldrich) according to the manufacturer's protocol of RNeasy Mini Kit (QIAGEN). Lysed cells were then scraped from the plates and frozen at  $-20^{\circ}\text{C}$  overnight. RNA extraction was performed using RNeasy Mini Kit (QIAGEN) according to the manual. Afterwards residual DNA was digested using DNase I kit (Sigma-Aldrich) and cDNA synthesis was performed with iScript cDNA synthesis kit (Bio-Rad, Hercules, CA, USA) according to the manufacturer's protocol.

69 ng cDNA were then used for each reverse transcriptase (RT)-PCR reaction. GoTaqG2 Polymerase (Promega) was used for the amplification of the specific PCR fragments, according manufacturers protocol. Fragments of targeted genes were amplified using mCD137L\_fwd and mCD137L\_rev, mCD80\_fwd and mCD80\_rev, mCD95\_fwd and mCD95\_rev, mPD-L1\_fwd and mPD-L1\_rev, mGAPDH\_fwd and mGAPDH\_rev primer. Following cycle conditions were used:  $94^{\circ}\text{C}$  for 2 min, 40 cycles of  $94^{\circ}\text{C}$  for 30 seconds,  $60^{\circ}\text{C}$  for 30 seconds and  $72^{\circ}\text{C}$  for 20 seconds, followed by 5 minutes at  $72^{\circ}\text{C}$  and was terminated with infinite time at  $4^{\circ}\text{C}$ . The size of the PCR products was verified with a 1.5 % agarose gel.

### 3.5.3 FACS ANALYSIS

SCCVII cells were characterized regarding co-stimulatory and inhibitory molecules expressed on their surface. SCCVII cell lines were treated with 100 U/ml recombinant murine IFN $\gamma$  (Peprotech) over a period of 48 or 96 hours. After trypsinization, cells were washed with DPBS and single stained with anti-mouse CD137 Ligand (4-1BB ligand) PE (rat IgG2a kappa, clone: TKS-1, eBioscience, Vienna, AUT), rat IgG2a kappa isotype control (clone: RTK2758, Biolegend, San Diego, CA, USA), anti-mouse CD80 PE (armenian hamster IgG, clone: 16-10A1, eBioscience), armenian hamster IgG isotype control (clone: HTK888, Biolegend), anti-mouse PD-L1 PE (rat IgG 2b, clone: 10F.9G2, Biolegend) or rat IgG2b isotype control PE (clone: eB149/10H5, eBioscience), for 20 minutes at  $4^{\circ}\text{C}$  protected from light. Additionally, cells were stained with either purified anti-mouse H-2K<sup>k</sup> (clone: AF3-12.1, Santa Cruz, Dallas, TX, USA) mouse monoclonal antibody, purified anti-mouse I-A<sup>k</sup> (A $\beta$ k) (clone: 10-3.6, Biolegend) mouse monoclonal antibody or anti-mouse CD95 purified monoclonal antibody (clone: SA367H8, Biolegend). Alexa Fluor488 goat anti-mouse IgG (life technologies) was used as secondary antibody. Each staining step was performed for 20 minutes at  $4^{\circ}\text{C}$  in the dark. Finally, cells were washed with DPBS, analyzed

by flow cytometry (Gallios™, Beckman Coulter) and analyzed using Kaluza 1.3 software (Beckman Coulter).

### 3.6 ANIMALS

4–6 weeks old female C3H/HeNCrl mice were purchased from Charles River (Sulzfeld, Germany) and housed at the animal facility of the Paracelsus Medical University (PMU) Salzburg in the conventional area. Treatment protocols were reviewed and approved by the local authorities (Land Salzburg; GZ). C3H is an immunocompetent, inbred mouse strain carrying the MHC haplotype H-2K<sup>k</sup>.

#### 3.6.1 IMMUNIZATION PROTOCOL

A DNA immunization protocol was established to generate a MV specific immune response against H-2K<sup>k</sup>-restricted epitopes N52, N81 or N5281 in C3H mice. Mice were immunized three times in an interval of 14 days using the Helios gene gun transfection system from Bio-Rad (Figure 10).

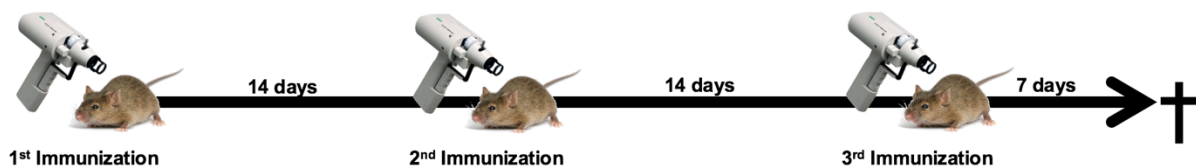


**Figure 10** Immunization protocol for the generation of MV specific immunity in C3H mice. Immunization of mice was performed three times with an interval of 14 days between each immunization using the Helios gene gun system.

#### 3.6.2 PREPARATION OF BULLETS FOR THE GENE GUN SYSTEM AND *IN VIVO* GENE GUN TRANSFECTION

For the transdermal delivery of the plasmids into murine skin, gene gun immunization was performed as described previously [105]. Briefly, 25 mg of 1.6  $\mu\text{m}$  gold carriers (Bio-Rad) were mixed with 100  $\mu\text{l}$  of 0.1 M spermidine (Sigma-Aldrich) and vortexed for a few seconds. Gold clumps were broken up by sonification. 50  $\mu\text{g}$  plasmid-DNA and ice cold 2.5 M  $\text{CaCl}_2$  (200  $\mu\text{l}$ ) were added to precipitate the DNA onto the gold particles. After three washing steps with 100 % dried ethanol the pellet was resuspended in 100 % ethanol (MerckMillipore) and the suspension was further subtracted to coating into a plastic tubing (Bio-Rad). Briefly, a piece of tubing was inserted into the support cylinder and the tubing was dried for at least 15 minutes by adjusting the nitrogen flow to 0.3 – 0.4 LPM. Next the DNA/carrier

solution was loaded into the tubing with a syringe and after the microcarriers were settled the ethanol was carefully removed. The tubing was dried using the nitrogen flow (0.25 – 0.3 LPM) while continued rotation for 3–5 minutes. Finally, the tubing was cut into bullets of about 1 cm in length, leading to a bullet loaded with 1 µg of plasmid DNA.

To verify quality of bullets, DNA was extracted from one bullet by incubation with ~ 30 µl H<sub>2</sub>O and analyzed using agarose gel electrophoresis. Bullets were stored at –20 °C in a 50 ml tube containing a desiccant. Groups of female C3H mice were immunized into shaved ventral side via two gene gun shots using bullets coated with 1 µg total DNA at a pressure of 400 psi.

### **3.7 BLOOD SAMPLING**

#### **3.7.1 BLOOD SAMPLING FROM THE VENA SAPHENA**

For the monitoring of the development of MV epitope specific immune response in immunized mice, peripheral blood was sampled. Therefore, mice were restrained in a 50 ml tube containing a hole for air supply. The left hind limb was immobilized in an extended position and shaved using a surgical blade (Braun, Maria Enzersdorf, AUT) in the direction of the hair. Using a 27G needle (Braun) the saphenous vein was punctured, approximately 100 µl peripheral blood were collected and immediately mixed with 30 µl PBS/EDTA to prevent clotting of the blood cells. Red blood cells were lysed with ACK-buffer for 5 minutes at room temperature. Then the cell suspension was washed twice with DPBS to get rid of dead cells. PBMCs were either stained for flow cytometry analysis to identify specifically generated CD8<sup>+</sup> T lymphocytes as described in chapter 3.12, or restimulated with peptide for the monitoring of specific IFN $\gamma$  secretion via enzyme linked immune absorbent assay (ELISA), as described in chapter 3.8.

#### **3.7.2 COLLECTION OF SERUM**

Immunized mice were sacrificed and peripheral blood was sampled from vena cava inferior using a 70G syringe (Braun). Collected blood was incubated for 30 minutes at room temperature to induce clotting of the blood cells. Blood samples were centrifuged for 25 minutes at 13,200 rpm at 4 °C and supernatant (= serum) was collected and stored with sodium azide, at a final concentration of 0,02 % at 4 °C.

### 3.8 IFN $\gamma$ ELISA

PBMCs were isolated and cells of up to 3 mice of the same cohorts were pooled, in order to examine the generated immune response. Therefore  $1 \times 10^5$  cells were plated in each well of a 96-well round bottom plate in RPMI complete and restimulated with either 10  $\mu\text{g/ml}$  N52, N81, N52 and N81, or SIINFEKL for 24 hours at 37 °C and 5 % CO<sub>2</sub>. Cells incubated with medium alone served as negative control. Supernatants were collected and an IFN $\gamma$  “Sandwich”-ELISA (Ready-Set-Go! IFN $\gamma$  ELISA, eBioscience) was carried out in duplicates according to the manufacturer’s protocol.

Briefly, 96-well flat bottom plates (nunc maxisorp, Thermo Fisher Scientific) were coated with 2  $\mu\text{g/ml}$  anti-IFN $\gamma$  monoclonal capture antibody over night at 4 °C, followed by blocking with 1 x ELISA/ELISPOT diluents (eBioscience) for 30 minutes at room temperature. 50  $\mu\text{l}$  of supernatants from stimulated PBMCs were added to the wells of the plate. Then the plate was incubated over night at 4°C. After three washing steps with DPBS + 0.05 % Tween-20 (MerckMillipore), anti-IFN $\gamma$  monoclonal detection antibody conjugated with biotin was added to each well (50  $\mu\text{l}$ ) for one hour at room temperature. After three washing steps, peroxidase-conjugated streptavidin diluted 1:250 in 1 x ELISA/ELISPOT diluents was added and incubated for 30 minutes at room temperature. The assay was developed with tetramethylbenzidine (TMB) substrate (eBioscience) and the reaction was stopped with 2N H<sub>2</sub>SO<sub>4</sub>. Absorbance was measured at 450 nm (reference wavelength: 570 nm) using a multiplate reader (Spark 10M, Tecan, Zürich, CHE).

### 3.9 ANTIBODY ELISA

96-well Nunc maxisorp plates (Thermo Fisher Scientific) were coated with 2  $\mu\text{g/ml}$  N81 peptide, or OVA protein as a positive control, and incubated over night at 4 °C. After washing once with PBS, plates were blocked with DPBS + 0.1 % Tween-20 (PT) for 1 hour at room temperature. Serum samples, prepared as described in chapter 3.7.2, were diluted in PT + 1% BSA (Sigma-Aldrich) 50, 100 or 500 fold. After one hour incubation at room temperature, plate was washed three times with PT and then incubated at room temperature with anti-mouse IgG1 (H+L) HRP antibody (1:3,000, Thermo fisher scientific), followed by five washing steps with PT. Then TMB substrate (eBioscience) was added. The reaction was stopped after 15 minutes with 2N H<sub>2</sub>SO<sub>4</sub> and absorption was measured at 450 nm (reference wavelength: 570 nm) on a multiplate reader (Spark 10M, Tecan).

### 3.10 PREPARATION OF MURINE LYMPHOID ORGANS AND CELL ISOLATION

C3H mice were sacrificed with an overdose of CO<sub>2</sub> and lymphoid organs including spleen, axillary, brachial as well as inguinal lymph nodes of each mouse were collected. Spleen and lymph nodes were mashed in DPBS using the stopper of a 2 ml syringe and filtered through a 40 µm nylon cell strainer (Becton Dickinson) to remove residual tissue and obtain single cell suspensions. Residual red blood cells were lysed using ACK-buffer for 5 minutes at room temperature. The reaction was stopped using twice the amount of DPBS and cells were centrifuged at 300 g for 5 minutes. Lysis of red blood cell was not necessary when harvesting cells from lymph nodes. The cell suspensions were washed twice with culture medium or DPBS according to the following experiment.

### 3.11 IFN $\gamma$ ELISPOT

ELISpot (Enzyme Linked Immuno Spot Assay) was used to assess differences in IFN $\gamma$ -secreting lymphocytes or splenocytes from immunized and naïve mice, seven days after the final immunization step. ELISpot was performed as described previously by Stöcklinger *et al.* (2007) [106]. Briefly, 96-well filter bottom multiscreen plates (MerkMillipore) were coated with 2 µg/ml capture anti - IFN $\gamma$  monoclonal antibody (clone: AN-18, eBioscience) in DPBS and incubated over night at 4°C. Plates were blocked with RPMI 1640 + 5 % FCS for 1 hour at 37 °C. Single cell suspensions of lymphoid organs were prepared as described previously. Lymphocytes or splenocytes were resuspended in RPMI complete and plated into the 96-well plates at a density of  $2 \times 10^5$  cells/well. Additionally, wells were stimulated with the specific antigen N52, N81 at a concentration of 10 µg/ml or kept untreated. Then the plate was incubated overnight at 37 °C in a humidified chamber. The assay was carried out in duplicates. Plates were washed with DPBS + 0.1 % Tween (PT) and biotin conjugated anti-mouse IFN $\gamma$  monoclonal antibody (clone: R4-6A2, Biolegend) was diluted in DPBS + 1% BSA (2 µg/ml) and added to each well. After three washing steps with PT, peroxidase-conjugated streptavidin (eBioscience) diluted 1:250 in DPBS + 1% BSA was added and the plate was incubated at room temperature for 2 hours. Plates were washed with PT and detection of cytokine was performed by 3-amino-9-ethylcarbazol (AEC) substrate (Sigma-Aldrich). After spots could be clearly identified the reaction was stopped by washing the plate with water. Spots were scanned (resolution 1200 dots per inch) and counted using Image Tool software (UTHSCSA, San Antonio, TX, USA).

### 3.12 IDENTIFICATION OF MV SPECIFIC CTLs

1 x 10<sup>6</sup> PBMCs or a CD8<sup>+</sup> T cell fraction were labelled with the fixable viability dye (FVD) eFluor780 (eBioscience) to discriminate live and dead cells at a concentration of 1 µl in 1 ml PBS, for 15 minutes at 4 °C. After washing with DPBS + 5 % FCS cells were stained with 5 µl of the H-2K<sup>k</sup> N81 specific dextramer in 50 µl DPBS + 5 % FCS for 10 minutes at room temperature and additionally stained with the following monoclonal antibodies for 20 minutes at 4°C: anti-mouse CD3 PE (clone: 17A2, Biolegend), anti-mouse CD4 PE/Cy7 (clone: RM4-5, Biolegend), and anti-mouse CD8a APC (clone: 53-6.7, eBioscience). After washing with DPBS + 5 % FCS, cells were resuspended in a suitable amount of DPBS and measured using flow cytometry (Gallios™, Beckman Coulter). Data were analyzed with Kaluza 1.3 software (Beckman Coulter). The frequency of dextramer-positive CD8<sup>+</sup> T cells was determined by gating on live CD3, CD8 double-positive cells.

### 3.13 T CELL PROLIFERATION ASSAY

In order to detect MV antigen (N81) specific proliferation of lymphocytes *in vitro* a T cell proliferation assay was performed. Splenocytes from immunized C3H mice were harvested as described before and stained with 10 µM eFluor450 (eBioscience), according to the manufacturer's protocol. In addition, CD8<sup>+</sup> T cells were isolated from the splenocyte suspension using the murine CD8<sup>+</sup> T cell enrichment Kit (eBioscience), according to the manufacturer's protocol. Splenocytes from syngeneic, naïve donor mice were used as APCs. APCs were pulsed either with peptide N81 (1 µg/ml) for 60 minutes at 37°C or left untreated as control. The enriched CD8<sup>+</sup> T cell fraction was adjusted to 1.6 x 10<sup>6</sup> cells/ml and 500 µl were co-incubated with N81 pulsed or unpulsed APCs at a ratio of 1:1 for 7–14 days at 37 °C. Recombinant murine IL-2 (50 U/ml, Peprotech) was added to the wells at day 3 and 10. At day 7 and 14 the cells were harvested and stained with FVD and monoclonal antibodies against CD3, CD4 and CD8 as well as the H-2K<sup>k</sup>-N81 specific dextramer for flow cytometry analysis, as described in chapter 3.12.

### 3.14 *IN VIVO* CTL KILLING ASSAY

Syngeneic donor splenocytes from naïve C3H mice were isolated from spleens and red blood cells were lysed using ACK-buffer. After two washing steps with DPBS, whole splenocytes were divided into four populations and each was stained with different concentrations of CFSE (eBioscience) or eFluor450 (eBioscience) respectively. CFSE<sup>hi</sup> or eFluor450<sup>hi</sup> splenocytes were stained with 5 µM of each dye whereas 0.5 µM of each dye was used to stain the CFSE<sup>low</sup> or eFluor450<sup>low</sup> splenocytes. Staining was

performed for 10 minutes at 37 °C. The cell suspensions were vortexed several times during the incubation step. Finally, the staining was stopped by adding an equal amount of DPBS followed by two washing steps with RPMI complete. The CFSE<sup>low</sup> and eFluor450<sup>low</sup> fraction was additionally pulsed with 100 µg/ml peptide, N81 or N52 respectively, for 1 h at 37 °C in RPMI complete. The cell suspensions were vortexed several times during the incubation step and afterwards washed twice with DPBS. CFSE<sup>hi</sup>, CFSE<sup>low</sup>, eFluor450<sup>hi</sup> and eFluor450<sup>low</sup> fractions were mixed together at equal amounts, reaching a final concentration of 4 x 10<sup>7</sup> cells/ml each. The ratio of the labelled splenocytes was examined by flow cytometry (Gallios, Beckmann Coulter). Then, 100 µl of this mixture was injected intravenously (i.v.) into pre-immunized or naïve C3H mice one week after the third gene gun immunization. 16 hours after cell transfer, mice were sacrificed and spleens and lymph nodes were harvested as described before. 2 x 10<sup>6</sup> splenocytes and lymphocytes were analyzed using flow cytometry (Gallios, Beckman Coulter) and percent specific lysis of fluorescent donor cells in each mouse was calculated using the formula in Figure 11.

$$\text{specific lysis} = 100 - \left[ \frac{\frac{\text{CFSE}^{\text{high}}_{t0}}{\text{CFSE}^{\text{high}}_{t16h}} \times \text{CFSE}^{\text{low}}_{t16h} \times 100}{\text{CFSE}^{\text{low}}_{t0}} \right]$$

**Figure 11 Formula for the calculation of specific lysis of peptide pulsed target cells in an *in vivo* CTL assay.** Syngeneic splenocytes of a naïve mouse were pulsed with 5 (CFSE<sup>high</sup>) or 0.5 (CFSE<sup>low</sup>) µM CFSE. CFSE<sup>low</sup> fraction was additionally pulsed with 100 µg/ml peptide. t0 indicates the amount of events, measured for the corresponding cell population via flow cytometry, at the time point of injection. t16h indicates the events measured in single cell suspensions of sacrificed mice.

### 3.15 *IN VIVO* CTL BLOCKING ASSAY

*In vivo* CD8<sup>+</sup> T cell blocking was performed to confirm that CD8<sup>+</sup> T cells are responsible for *in vivo* cell killing activity in our vaccination approach. Therefore, mice were injected intra peritoneal (i.p.) with 500 µg of a purified anti-mouse CD8a monoclonal antibody (functional grade, clone: 53-6.7, eBioscience) six days after the final immunization step. On the following day an *in vivo* CTL killing assay was performed as described previously in chapter 3.14.

### 3.16 *IN VIVO* TUMOR CHALLENGE

The generated SCCVII cells expressing the MV epitope N81 (SCCVII\_N81) or SCCVII\_mock cells were used for an *in vivo* tumor challenge. C3H mice were immunized with either the pCI\_EV or pCI\_N52N81 plasmid and seven days after the third gene gun immunization tumor cells were inoculated into mice.

5,000 cells in 20 $\mu$ l DPBS were injected intradermally (i.d.) at the ventral side of C3H mice. SCCVII\_mock cells were used as a control. Tumor growth was monitored twice a week using a digital calliper and tumor volume (mm<sup>3</sup>) was calculated with the following formula: length x width<sup>2</sup>/2. Mice were sacrificed after one month of treatment or when the tumor reached a volume of about 500-600 mm<sup>3</sup>.

### 3.17 FLUORESCENCE MICROSCOPY

Tumors were snap frozen in liquid nitrogen after excision from sacrificed mice and then stored at -80 °C. Then 6  $\mu$ m sections were generated using a cryomicrotome (MICROM HM 550, Thermo Fisher Scientific, Runcorn, UK) and stored at -80 °C. Sections were either stained with H/E as described in chapter 3.18, or fixed with ice-cold acetone:methanol (1:1) for 10 minutes at -20 °C. Fixed sections were washed for 5 minutes in PBS and blocked with 5 % BSA (Sigma-Aldrich) in DPBS for 1 hour at room temperature. Primary antibodies were incubated overnight at 4 °C diluted in 1 % BSA/DPBS and 0.3 % TritonX-100 (Sigma-Aldrich). Rat anti-mouse CD8a purified (clone: 53-6.7), was kindly provided by Dr. Stöcklinger (Paris Lodron University Salzburg) and used as monoclonal primary-antibody. After 3 washing steps for 5 minutes each in PBS, slides were incubated with mouse anti-rat IgG AF488 (eBioscience) secondary antibody for 1 hour at room temperature diluted 1:250 in 1 % BSA in PBS. Washing was performed again 3 times for 5 minutes in PBS, followed by staining with DAPI solution (3  $\mu$ g/ml, 1:1,500, Sigma-Aldrich) for 10 minutes at room temperature. Slides were washed three times and once rinsed with tap water, followed by mounting with Fluorescence mounting medium (Dako, Glostrup, DNK). Slides were stored at 4 °C in the dark until final analysis by fluorescence microscopy with a confocal laserscanning unit (Axio Observer Z1 attached to LSM710, Zeiss, Göttingen, Germany) and ZEN 2009 software by Carl Zeiss.

### 3.18 H/E STAINING OF SKIN SECTIONS

4 mm<sup>2</sup> punch biopsies were taken from ungunned and gunned abdominal murine skin and embedded in OCT medium (Tissue Tek, Sakura, Leiden, NL) and immediately frozen and stored at -80 °C. Out of these biopsies 8  $\mu$ m sections were then generated using a cryomicrotome (MICROM HM 550, Thermo Fisher Scientific, Runcorn, UK) and stained with hematoxylin and eosin.

Briefly, slides were thawed and air-dried for 15 minutes. Then, slides were rinsed by dipping the slides thirty times in tap water and afterwards incubated in hematoxylin solution (Merck) for 6 minutes. Further on the slides were washed by dipping the slides into tap water twenty times and differentiated in 0.3 % HCl alcohol. Slides were again washed by dipping the slides into tap water for forty times and then stained with 0.5 % eosin for 2 minutes. Washing was performed again via dipping the slides thirty

times into tap water followed by dehydration due to 10 dips in absolute isopropyl alcohol for three times. Finally, slides were cleared with xylene and air-dried. H/E stained slides were then mounted using Fluorescence mounting medium (Dako). Slides were stored at 4 °C until further analysis using light microscopy (LSM710, Zeiss) and Axio Vision Rel 4.8 software.

### **3.19 STATISTICAL ANALYSIS**

Statistical analysis was performed using Graphpad Prism 7 Software. Data were checked for normal distribution using Shapiro-Wilk normality test. Upon normal distribution of data within the two groups to be compared, an unpaired, two-tailed t-test was applied to calculate the significant differences of the cohorts. In case of a non-normal distribution of either one of the groups to be compared or in case of low sample size, a non-parametric t-test (Mann-Whitney test) was used. Overall survival curves of the different cohorts were compared using Log-rank (Mantel-Cox) test. Results were considered significant when  $P < 0.05$ .

## 4 RESULTS

### 4.1 PRELIMINARY CONSIDERATIONS

At the start of the project, several considerations needed to be taken into account, including: (1) the choice of mouse model, (2) the choice of viral epitopes, and (3) the design and route of administration of the vaccine.

Fully immunocompetent mice represent the best means to study immune reactions, as the multifactorial complexities of the immune system cannot be readily mimicked in an *in vitro* cell culture system. We chose the C3H/HeNCrl mouse strain because a tumor cell line that was derived from a spontaneously arising squamous cell carcinoma in this strain had been established [104]. This allows for the transplantation of syngeneic tumor cells into recipient mice without the need for prior immunosuppression of the mice. Transplantation of syngeneic tumors was preferable to chemical induction of skin tumors as the use of chemical inducers is likely to alter the immune composition of the skin, making data interpretation difficult.

Because the C3H mouse has an H-2K<sup>k</sup> haplotype, we were restricted to viral epitopes that could be presented by this MHC I complex. An extensive literature research revealed that the nucleocapsid protein of measles virus contains epitopes that elicit a CTL response in mice. Two CTL epitopes in particular, N52-59 and N81-88, were shown to be immunogenic in BALB/c and CBA mice, exhibiting an MHC I restriction to H-2K<sup>k</sup> and H-2L<sup>d</sup> [100], which we additionally confirmed using a CTL prediction software (IEDB Analysis Resource). Therefore, we chose these two measles virus CTL epitopes for our study.

Measles virus (MV) is the cause of measles, one of the most common childhood diseases preventable by vaccination. For the purposes of this proof-of-principle study, measles virus antigens are epitopes of choice, since the majority of the population has already been vaccinated against it during childhood [107]. In the course of a routine health check of RDEB patients seen at our institute, we evaluated the measles virus antibody titer in 6 patients and observed high titers of MV-specific antibodies in 4 out of 6 RDEB patients (Figure 12), indicating that they have been vaccinated or previously exposed to the virus. Thus, for the majority of RDEB patients as well as the general population, MV-derived epitopes would depict recall antigens capable of reactivating an immune memory resulting in rapid and potent immune responses.

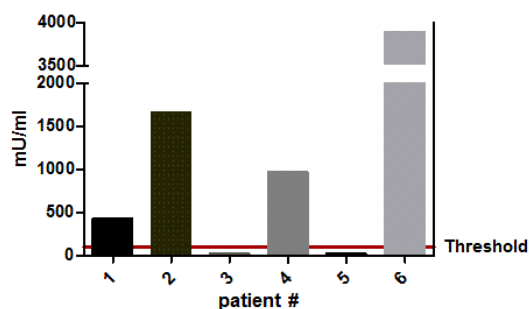


**Figure 12 Antibody titer (IgG) against MV detected in sera from 6 different RDEB patients.** Measles virus titer was measured in course of a routine examination at the EB House Outpatient Unit upon written informed consent of the patient. An antibody titer result < 150 mIU/ml was considered as negative.

Finally, we decided on a DNA vaccine design and gene gun administration. A DNA vaccine platform was chosen for reasons of cost-efficiency and ease of manipulation. DNA plasmids are cheaper to produce than highly-purified custom-synthesized peptides. Additionally, in this exploratory phase of the project, DNA plasmids allow us to easily evaluate several different configurations of a vaccine in a cost-effective manner. For designing our DNA vaccines, we used the pCI vector as a mammalian expression plasmid. The signal sequence of the murine interleukin 2 (IL2<sub>ss</sub>) was cloned upstream of the MV CTL epitopes and was included for enhanced targeting of the epitopes to the TAP transporter (transporter associated with antigen processing) and proper loading onto MHC I in the endoplasmic reticulum as previously shown by Lindinger *et al.* (2003) [99]. The different MV-CTL epitopes were fused C-terminally to the IL2<sub>ss</sub>, alone or in a tandem configuration (Figure 9). Furthermore, a promiscuous murine MVTh epitope was added C-terminal to the CTL epitopes to support the generation of the MV specific CTL response [99]–[102]. Codon usage was optimized for expression in mice using the Integrated DNA Technologies Codon Optimization Tool.

The various DNA vaccine vectors were administered to mice using the Helios<sup>R</sup> gene gun system of Bio-Rad. Gene gun administration of DNA vectors was a technique already established in the lab [105]. The gene gun system enables efficient transdermal delivery of DNA coated onto gold particles. In comparison to intradermal injection of naked DNA, gene gun-mediated bombardment of DNA-coated gold particles induces more potent danger signals and a stronger local inflammatory response, leading to the efficient activation and maturation of skin dendritic cells (DCs) [108]. Skin DCs are transfected and migrate to the skin draining lymph nodes where they present the encoded antigens to naïve T cells [109]. In contrast to speculation, Stöcklinger *et al.* (2007) showed that the professional skin homing DCs, the so called LCs, are not necessary for an immune response induced by gene gun vaccination [106].

## 4.2 GENE GUN IMMUNIZATION IS SUCCESSFUL IN THE GENERATION OF FUNCTIONAL MV-SPECIFIC CD8<sup>+</sup> T LYMPHOCYTES IN C3H MICE

The first aim of this study was to generate an MV specific cellular adaptive immune response in a mouse model. For that purpose, DNA vaccination was performed using the gene gun system from Bio-Rad. The vaccination strategy we adopted is depicted in Figure 13A. Mice were vaccinated a total of three times with an interval of 14 days in between immunizations. The successful transdermal delivery of the DNA coated gold particles was confirmed by H/E staining of cryosections of mouse skin corresponding to the areas that had been “gunned” (Figure 13B). The epidermis with the stratum corneum is depicted on the top of the pictures. Black arrows point to gold particles located in the dermis of vaccinated mice.

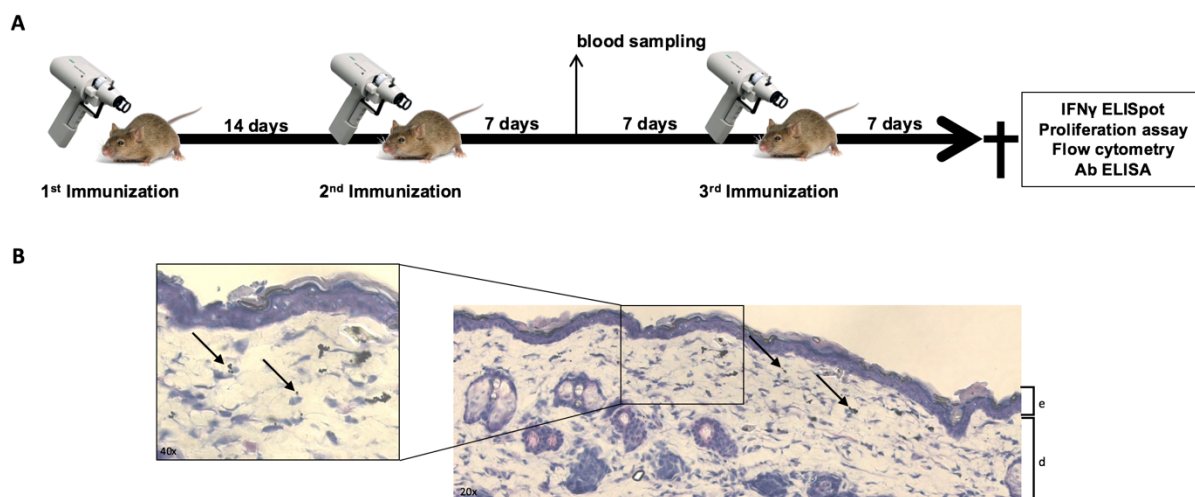


**Figure 13 DNA immunization protocol of C3H/HeNcrI mice for the generation of a MV specific immunity.** **A** C3H mice were shaved abdominally and gene gun immunization was performed three times with an interval of 14 days. Seven days after the second immunization step, blood sampling via the vena saphena was performed to investigate specific interferon  $\gamma$  (IFN $\gamma$ ) production. Seven days after the final gene gun immunization, mice were sacrificed and axillar and brachial lymph nodes as well as the spleen were harvested for further investigation. **B** H/E staining of a skin section of an immunized mouse one week after the third immunization step (20x, zoom out 40x). The gold particles (black arrows) are located in the upper dermis (d) and at the edges of the epidermis (e).

### 4.2.1 MONITORING OF THE DEVELOPING MV SPECIFIC IMMUNE RESPONSE

IFN $\gamma$  is secreted by CD4<sup>+</sup> Th1, NK, and CD8<sup>+</sup> T cells and plays an important role in the development of an immune response against intracellular pathogens [1]. We therefore used IFN $\gamma$  expression as a readout for developing immunity in response to our vaccination protocol. IFN $\gamma$  expression was monitored at two different time points in our immunization regimen: in peripheral blood mononuclear

cells (PBMCs) at day seven after the second immunization, and at day seven after the final immunization, in lymph node cells and splenocytes isolated from the mice after sacrifice.

Blood was sampled from the mice via the vena saphena at day seven after the second vaccination and the blood from each vaccination cohort was pooled in order to obtain sufficient numbers of PBMCs for the assay. PBMCs were cultured in the absence or presence of target- or irrelevant peptides, and the cell culture supernatants were collected after 24 hours for detection of secreted IFN $\gamma$  by ELISA. In comparison to results obtained from naïve mice or mice vaccinated with empty plasmid vector (pCI\_EV), specific IFN $\gamma$  secretion could be detected in PBMCs from mice immunized with pCI\_N52N81 upon restimulation with N81 or the combination of N52 and N81. Furthermore, culturing these PBMCs with an irrelevant peptide (SIINFEKL) or in medium alone did not result in significant IFN $\gamma$  production. In contrast to mice immunized with the tandem configuration, immunization with pCI\_N52 or pCI\_N81 alone did not result in increased IFN $\gamma$  production at this time point, as measured by this assay (Figure 14).

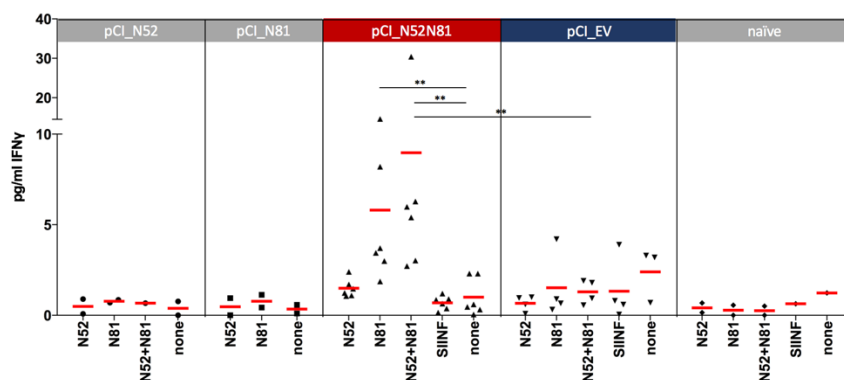


**Figure 14 IFN $\gamma$  release by PBMCs upon restimulation with relevant peptides.** Blood was collected from the vena saphena seven days after the second immunization and PBMCs of the different experimental cohorts were pooled and were either restimulated with 10  $\mu$ g/ml of indicated peptides or cultured without any restimulation. After 24 hours supernatants were used for detection of specifically secreted IFN $\gamma$  using an ELISA. The red lines indicate the mean pg/ml IFN $\gamma$  for each condition. Significant differences were calculated using an unpaired nonparametric t-test (Mann-Whitney test). \*\* p value = 0.0087 for pCI\_N52N81 vaccinated mice restimulated with N81 or without restimulation. \*\* p value = 0.0022 for pCI\_N52N81 immunized mice restimulated with N52+N81 or without restimulation and \*\* p value = 0.0095 for pCI\_N52N81 with pCI\_EV both restimulated with N52+N81.

We additionally assayed for IFN $\gamma$  production one week after the final immunization in skin-draining lymph nodes as well as the spleens harvested from the mice after sacrifice. Single cell suspensions of these organs were prepared and cultured overnight in an IFN $\gamma$ -specific ELISpot plate in the absence or presence of target peptide. In this assay, secreted IFN $\gamma$  becomes immobilized onto specific antibodies on membranes at the bottom of each well and a subsequent enzymatic reaction leads to the formation

of precipitates that are visible to the naked eye. Each spot, therefore, represents one IFN $\gamma$ -secreting cell (Figure 15A). As expected, lymph node (LN) and splenic (SPL) cells isolated from naïve and pCI\_EV-vaccinated mice were largely devoid of IFN $\gamma$ -producing cells under all restimulation conditions tested (Figure 15B and C). In contrast, we observed a significant increase in IFN $\gamma$ -spot forming units (SFU) in LN (Figure 15B) and SPL (Figure 15C) cells derived from pCI\_N52N81 immunized mice when restimulated with N81 peptide. Restimulation of LN and SPL cells from pCI\_N52N81-vaccinated mice with N52 peptide also resulted in increased numbers of IFN $\gamma$ -SFUs, although to a lesser extent than that observed with N81. Similarly, LN and SPL cells from pCI\_N52- and pCI\_N81-vaccinated mice showed only a slight increase in number of IFN $\gamma$ -SFUs when restimulated with the corresponding target peptides.

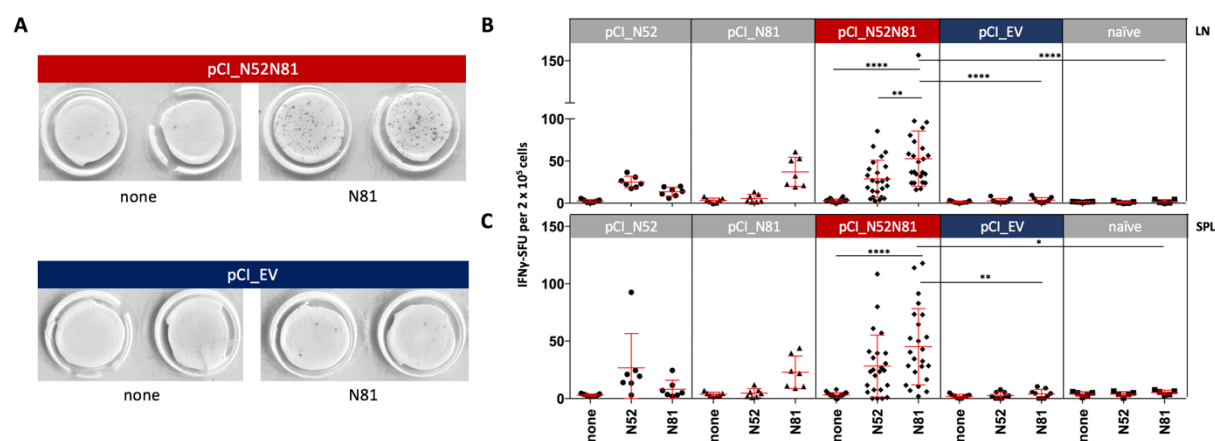


**Figure 15 Specific IFN $\gamma$  secretion by LN and SPL cells after restimulation with relevant peptides.** **A** Representative picture of IFN $\gamma$  spots formed after stimulation of lymph node (LN) or splenic (SPL) cells with either N81 (10  $\mu$ g/ml) or no peptide. Spots were counted manually. A significant increase of SFU (spot forming units) could be observed in LN (**B**) and SPL (**C**) cells derived from pCI\_N52N81 (n=24) immunized mice, compared to pCI\_EV (n=9) immunized or naïve (n=5) mice. LN and SPL cells from pCI\_N52 (n=7) and pCI\_N81 (n=7) immunized mice also showed specific IFN $\gamma$  spots. **B** For statistical analysis an unpaired nonparametric t-test (Mann-Whitney test) was applied. \*\*\*\* p value = <0.0001; \*\* p value = 0.0041. **C** An unpaired t-test was used for the determination of statistical differences. \*\*\*\* p value = <0.0001; \*\* p value = 0.0045; \* p value = 0.0362.

These data demonstrate a measurable response in IFN $\gamma$  production as a consequence of our immunization protocol. In this context, we achieved the best response in mice vaccinated with pCI\_N52N81 and further observed that in these mice the contribution of immune responses to N81 were considerably more significant than those to N52. Based on these observations, we chose N81 as the immunodominant peptide of interest, and the pCI\_N52N81 plasmid or pCI\_EV as our DNA vaccines in subsequent experiments.

#### 4.2.2 IDENTIFICATION OF FUNCTIONAL N81 SPECIFIC CD8<sup>+</sup> T CELLS IN IMMUNIZED MICE

IFN $\gamma$  production in peripheral blood-, lymph node-, and splenic cells in response to vaccination with pCI\_N52N81 provided indication of the successful generation of specific CTL immunity against our viral epitope of interest. We therefore aimed to identify the generated MV specific CD8<sup>+</sup> T cells themselves. As N81 proved to be the immunodominant epitope from our previous experiments, we purchased a customized FITC-labelled dextramer comprising a dextran polymer backbone with an optimized number of H-2K<sup>k</sup>-N81 peptide complexes (Immudex) [98]. Peripheral blood cells and splenocytes from mice vaccinated with pCI\_N52N81 or with pCI\_EV were labelled with antibodies against CD3, CD4, CD8, a fixable viability dye, and the N81 dextramer (Dex) and analyzed by flow cytometry. We observed an increase in the number of Dex<sup>+</sup> CD8<sup>+</sup> T cells in mice that had been vaccinated with pCI\_N52N81 compared to EV-vaccinated controls (Figure 16A). Approximately about 0.31 to 0.35 % of isolated live CD3<sup>+</sup> CD8<sup>+</sup> T cells were N81 specific in mice vaccinated three times with pCI\_N52N81. In contrast to that, mice that had been vaccinated with the empty vector solely, could only show about 0.05 % Dex<sup>+</sup> CD8<sup>+</sup> T cells.

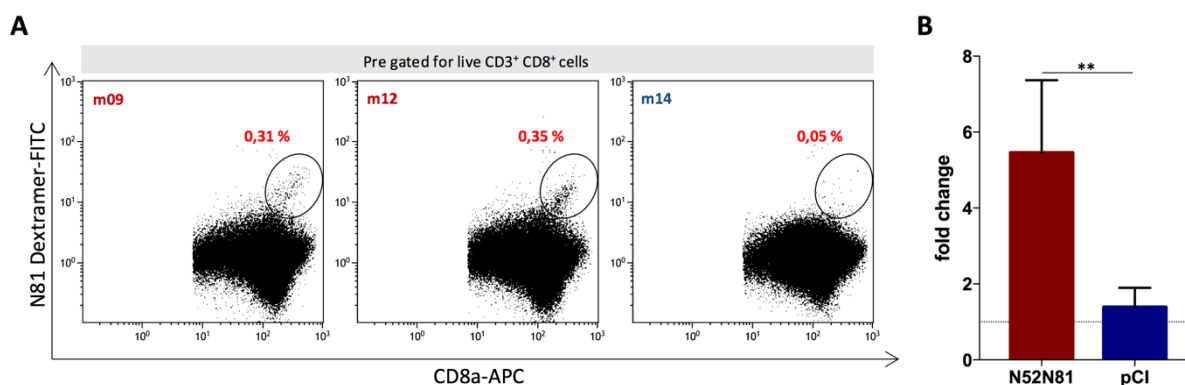


**Figure 16 Identification of functional N81 specific CD8<sup>+</sup> T cells in vaccinated mice.** **A** With the help of a customized dextramer specific for the N81 specific TCR on T cells, epitope specific CD8<sup>+</sup> T cells could be identified in splenocytes of pCI\_N52N81 (mouse 9 and 12) and were absent in pCI\_EV (mouse 14) immunized mice. Data of three representative mice are depicted. **B** Incubation of the CD8<sup>+</sup> T cell fraction with N81 pulsed syngeneic donor splenocytes for seven days, led to specific proliferation of N81 specific CD8<sup>+</sup> T cells of N52N81 (n=6) vaccinated mice compared to the control (pCI, n=4). Unpulsed donor splenocytes served as a control and were used for normalization. An unpaired, non-parametric t-test (Mann-Whitney test) was performed (\*\* p value = 0.0061).

Moreover, these Dex<sup>+</sup> CD8<sup>+</sup> T cells could be stimulated to proliferate *in vitro* when co-cultured with syngeneic donor splenocytes pulsed with N81 for 7–14 days, resulting in a mean relative increase of 5.5-fold compared to the negative control (co-culture with unpulsed splenocytes). In contrast, we observed a mean 1.4-fold increase in relative numbers of Dex<sup>+</sup> CD8<sup>+</sup> T cells in pCI\_EV-immunized mice when stimulated in the same manner. Thus, it could be demonstrated that vaccination with

pCI\_N52N81 successfully generated Dex<sup>+</sup> CD8<sup>+</sup> T cells that respond specifically to cognate antigen *ex vivo*.

#### 4.2.3 GENE GUN VACCINATION WITH MV CTL EPITOPES EVOKES CELLULAR ADAPTIVE IMMUNITY ONLY

CD8<sup>+</sup> CTLs have been shown to play prominent roles in the clearance of virus and virus-infected cells from the body. However, a significant proportion of the protection bestowed by viral vaccines is attributed to antibody-mediated mechanisms [1]. As we were interested in evaluating the contribution of CTL-mediated killing to effective tumor surveillance, we included only CTL- and T helper epitopes in our DNA vaccines. To confirm that our vaccination protocol generated only cell-mediated, and not humoral immunity, we analyzed serum from pCI\_N52N81- and EV-vaccinated mice for specific antibodies against our cognate antigen N81 or the unrelated protein ovalbumin (OVA) by ELISA. To validate our assay, we used serum from mice vaccinated with pCI\_OVA as a technical control. Figure 17A confirms the functionality of the assay, as OVA-specific IgG could be detected in serial dilutions of serum collected from OVA-vaccinated mice. In contrast, no OVA-specific antibodies were detected in N52N81-vaccinated, EV-vaccinated, or naïve mice. Notably, N81-specific IgG could not be detected in any of the serum tested (Figure 17B), confirming that vaccination with pCI\_N52N81 did not generate N81-specific humoral immunity.

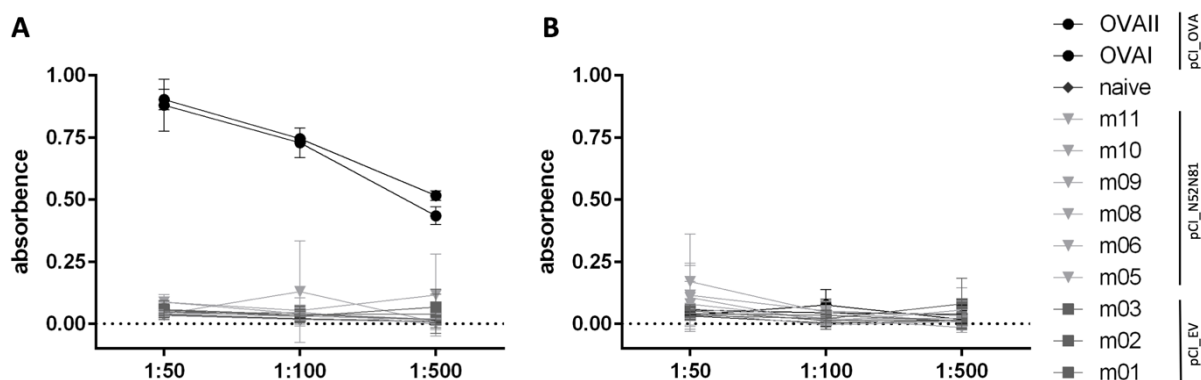


**Figure 17 Detection of N81 specific IgG in serum of vaccinated mice by ELISA.** Serum was sampled seven days after the final immunization step and subjected to an N81 specific antibody ELISA. Squares indicate pCI\_EV gunned mice, triangles indicate pCI\_N52N81 gunned mice and dots indicate pCI\_OVA gunned mice, which served as a positive control. The diamond represents a naïve mouse. Serum was diluted 1:50, 1:100 and 1:500 and was incubated on plates coated with (A) OVA or (B) N81 peptide. No N81 specific IgG could be detected in any of the analyzed mice.

### 4.3 THE GENERATED MV SPECIFIC IMMUNE RESPONSE IS CAPABLE OF SPECIFIC TARGET CELL KILLING *IN VIVO*

Since our aim was to generate an immune response that is capable of CTL-mediated specific killing of target cells, we tested this in *in vivo* CTL killing assays. To this end, we labelled syngeneic splenocytes with two different intensities of CFSE (CFSE<sup>high</sup> and CFSE<sup>low</sup>) and pulsed the CFSE<sup>low</sup> cells with N81 peptide. Both fractions were mixed at a ratio of 1:1 and approximately  $2 \times 10^6$  cells were injected intravenously into pCI\_N52N81- or pCI\_EV-vaccinated mice one week after the final immunization (Figure 18). After 16 hours, the mice were sacrificed, spleen and skin draining lymph nodes were harvested and single cell suspensions of these organs analyzed by flow cytometry for the fluorescently labelled cells. A decrease in the relative percentage of N81-pulsed CFSE<sup>low</sup> and a corresponding increase in the relative percentage of unpulsed CFSE<sup>high</sup> cells indicated specific lysis of peptide pulsed target cells. The percent specific lysis of peptide pulsed target cells was then calculated as using the input ratio (at time point 0 hours) as reference (Figure 19A).

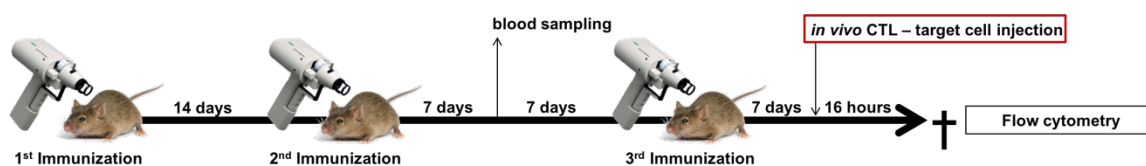


**Figure 18 Treatment protocol for *in vivo* CTL experiment.** Mice were vaccinated three times with an interval of 14 days with the Helios gene gun system of Bio-Rad, thereby applying two abdominal shots of 400 psi/immunization time point. Blood sampling via vena saphena was done seven days after the second immunization. Seven days after the final immunization fluorescent labelled syngeneic target cells were injected i.v. into mice. After 16 hours mice were sacrificed, spleens and lymph nodes were harvested and investigated for the remaining target cells via flow cytometry.

We observed up to a mean 80 % lysis of N81 pulsed injected target cells in lymph nodes (Figure 19B) and spleens (Figure 19C) after overnight incubation in mice which had been vaccinated with pCI\_N52N81. No difference in N81 specific lysis could be observed upon injection of an additional proportion of target cells pulsed with N52. In contrast, naïve mice, or those vaccinated with pCI\_EV, showed no specific target cell lysis in lymph nodes and spleens.

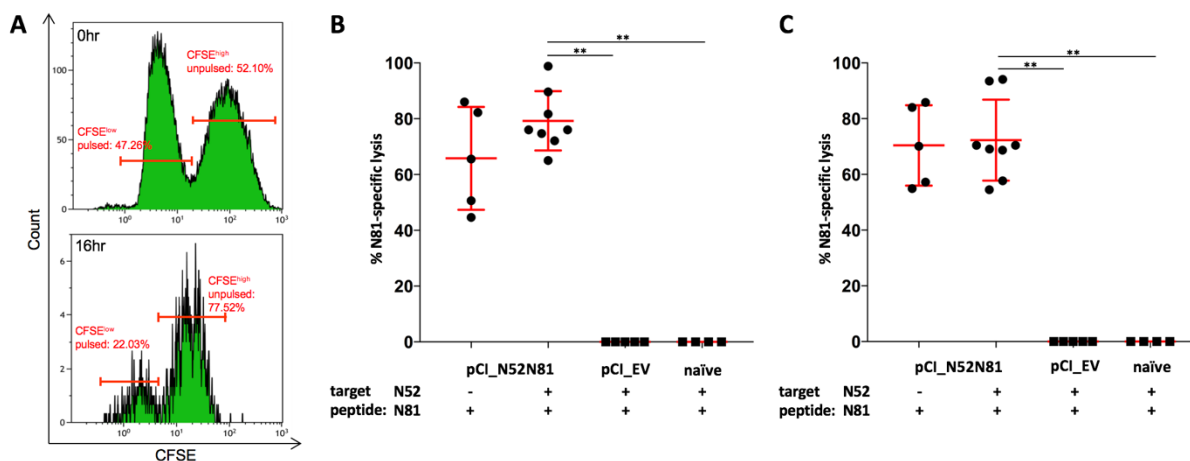


**Figure 19 Gene gun vaccination induces generation of MV specific CD8<sup>+</sup> T cells capable of target cell killing *in vivo*.** **A** Ratio of CFSE labelled peptide pulsed/unpulsed target cell mixture before (0 hours) and after (16 hours) i.v. injection in pCI\_N52N81 vaccinated mice seven days after the final immunization. Target cells were labelled with CFSE and either pulsed with N81, N52 peptide or left untreated. After 16 hours mice were sacrificed, lymph nodes and spleens were collected to analyze single cells for fluorescently labelled target cells using flow cytometry. Percent specific lysis of N81-CFSE target cells was then calculated in LN (**B**) and SPL cells (**C**). To calculate statistical significance an unpaired nonparametric t-test (Mann-Whitney test) was performed. The % N81-specific lysis of mice vaccinated with pCI\_N52N81 (n = 8) and inoculated with both target cell populations (N52 and N81) was significantly higher when compared to pCI\_EV (n = 5, \*\* p-value = 0.0016) and to naïve mice (n = 4, \*\* p-value = 0.0020) in cells from LN, as well as in spleen pCI\_EV vs. pCI\_N52N81 (n = 8, \*\* p value = 0.0016) and naïve vs. pCI\_N52N81 (\*\* p value = 0.0040).

#### 4.3.1 CD8<sup>+</sup> T CELLS ARE RESPONSIBLE FOR MV SPECIFIC TARGET CELL KILLING *IN VIVO*

To confirm that this specific lysis of target cells was mediated by CD8<sup>+</sup> T cells, we used a monoclonal anti-mouse CD8a antibody (clone 53-6.7) to block the interaction of CD8 with MHC I. Recipient mice were injected intraperitoneally (i.p.) with the antibody 24 hours [110] prior to injection of the fluorescently labelled target cells. Mice were sacrificed 16 hours later and specific CD8<sup>+</sup> T cell blocking, as well as target cell killing, were investigated in lymph nodes and spleen by flow cytometry.

Successful blocking of CD8<sup>+</sup> T cells could be confirmed by the reduced staining intensity of CD8<sup>+</sup> T cells with the same antibody clone, conjugated to APC, in flow cytometric analyzes (Figure 20A and B). While pCI\_N52N81-vaccinated mice, in this experiment, showed a mean 57 - 65 % specific killing of N81-pulsed target cells (in spleen and lymph node respectively), pre-treatment with the CD8 blocking antibody led to a significant reduction in specific target cell killing down to 10 - 20 % (spleen and lymph node) (Figure 20C and D). These results indicate that interaction of CD8 with MHC I is necessary to achieve target cell killing, and that the observed cell lysis is likely mediated by CD8<sup>+</sup> CTLs.

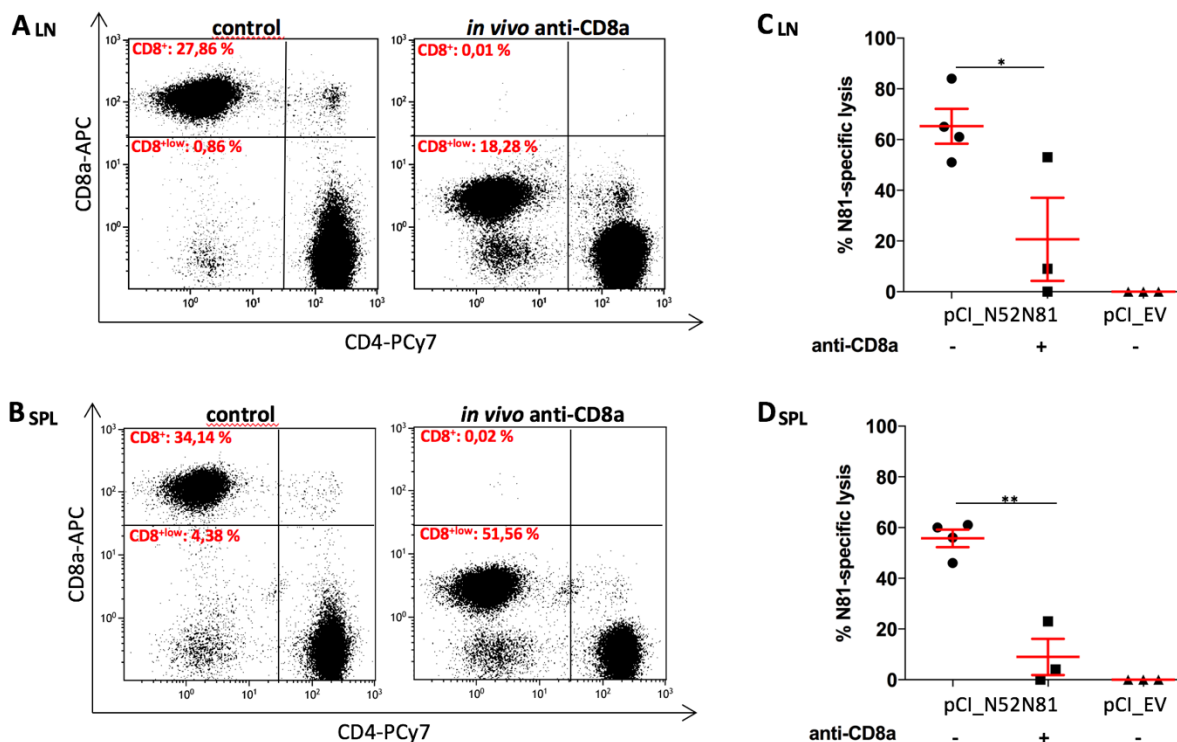


**Figure 20** Blocking of CD8<sup>+</sup> T cells *in vivo* leads to reduced killing of MV specific target cells. 500 µg anti-mouse CD8a (clone: 53-6.7) monoclonal antibody was injected i.p. in vaccinated mice five days after the final immunization. After 24 hours target cells for *in vivo* CTL assay were injected i.v. and 16 hours thereafter mice were sacrificed. The blocking of the CD8<sup>+</sup> T cells could be confirmed in cells from lymph node (LN, **A**) and spleen (SPL, **B**) via flow cytometry, by reduced binding of the anti-CD8a APC antibody (clone: 53-6.7). Significant reduction of target cell killing could be observed in LN (**C**) and (**D**) of MV immunized mice, which received the blocking antibody compared to the untreated group. An unpaired t-test was performed to determine the statistical difference between blocked pCI\_N52N81 (n = 3) and unblocked pCI\_N52N81 (n = 4) mice in lymph node (\* p value = 0.0382) and spleen (\*\* p value = 0.0013).

#### 4.4 GENERATION OF A MV EPITOPE-EXPRESSING SCCVII CELL LINE

Having successfully established a DNA vaccine and vaccination regimen that results in the generation of specific CTL immunity, we wanted to investigate whether this immunity would be sufficient to control growth of tumor cells expressing the cognate antigen. We therefore had to generate a syngeneic tumor cell line expressing the N81 epitope in order to perform these tumor challenge experiments. For this purpose, we used a syngeneic squamous cell carcinoma cell line that has spontaneously arisen in C3H mice, namely SCCVII [104]. We cloned the IL2ss-N81-T helper epitope cassette upstream of a floxed IRES-GFP coding sequence into a retroviral vector for stable integration into SCCVII cells. Positively transduced cells were FACS-sorted to > 98 % purity based on GFP expression. To eliminate the probability of immune responses against GFP contributing to tumor rejection [111], the IRES-GFP cassette was deleted by transfecting cells with an expression vector for

Cre recombinase [112]. This time, cells that had lost GFP expression were isolated by FACS-sorting (Figure 21).

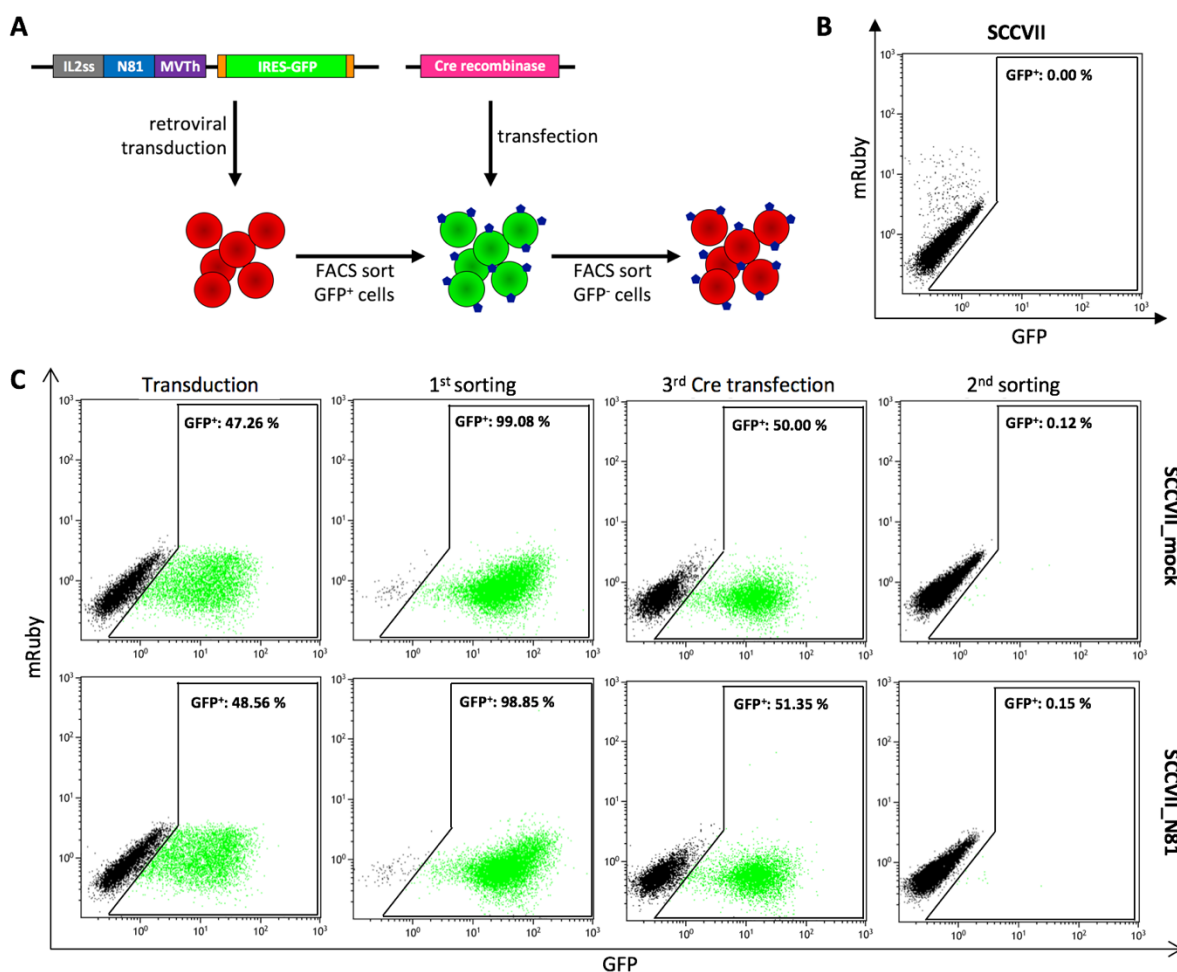


**Figure 21** Generation of a MV expressing SCCVII cell line. **A** Schematic of the experimental design for the generation of SCCVII cells stably expressing N81. Retroviral transduction was used for the stable integration of the IL2ss-N81-MVTh into the genome of the murine SCC cell line. Cre recombinase was used for floxing of loxP- (orange) flanked IRES-GFP. FACS sorting was performed to obtain highly pure cell lines. **B** FACS dot blot visualizing SCCVII parental cells did not show GFP expression. **C** GFP expression of SCCVII cells after viral transduction with mock (SCCVII\_mock) or N81 (SCCVII\_N81) expressing vector after 1<sup>st</sup> sorting, 3<sup>rd</sup> Cre transfection and after the 2<sup>nd</sup> sorting procedure. X-axis: GFP expression; Y-axis: mRuby expression.

We additionally confirmed the presence or absence of the GFP cassette and the N81 sequence in genomic DNA isolated from cells after each sort by PCR (Figure 22A and B). Accordingly, we amplified products of 133 and 633 bp, corresponding to N81 or to confirm the loss of the GFP cassette in these cells, using int\_IL2ss\_fwd and int\_MVTh\_rev or int\_IRES\_fwd and int\_GFP\_rev primers, respectively. We additionally sequenced the genome of our genetically engineered SCCVII\_N81  $\Delta$ GFP cells after final sorting to verify deletion of the IRES-GFP cassette (Figure 22C).

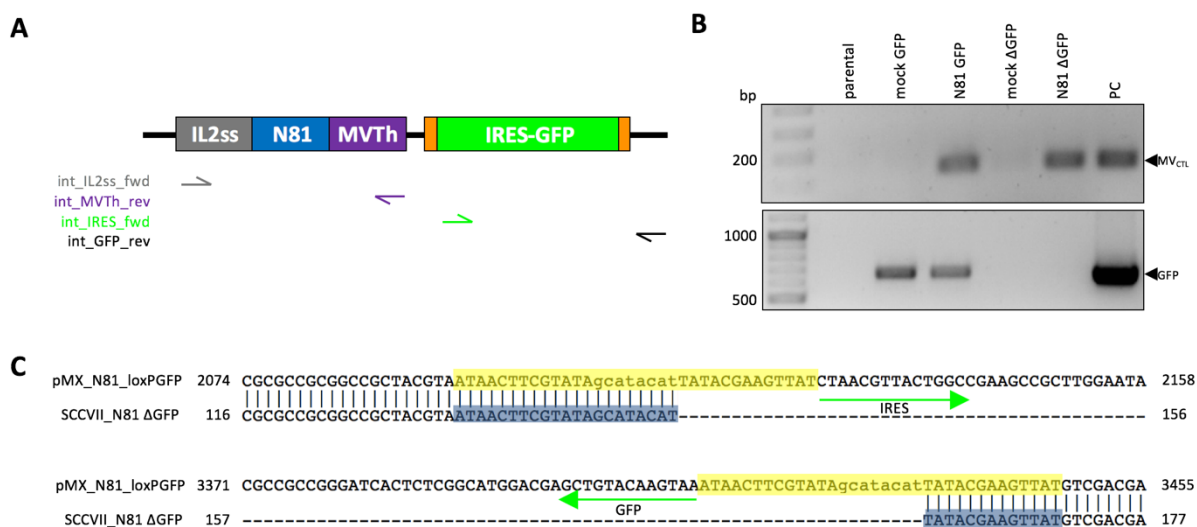


**Figure 22 Integration PCR of virally transduced SCCVII cells before and after transfection with Cre recombinase. A** Schematic depiction of the binding site of the different primer sets used for the confirmation of the proper integration of IL2ss-N81-MVTh and successful floxing of IRES-GFP in the genomic DNA of SCCVII\_mock and SCCVII\_N81. **B** PCR amplification of N81 (MV<sub>CTL</sub>) from genomic DNA of transduced SCCVII cells (133 bp). PCR amplification of GFP from genomic DNA of transduced SCCVII cells (631 bp). PC = positive control vector (pMX\_N81\_loxP-GFP) **C** Sequence alignment of the transduced pMX\_loxP\_GFP vector sequence used for viral transduction (top) and the genomic sequence of Cre recombinase treated, genetically engineered SCCVII\_N81 ΔGFP cell line (bottom). Green arrows indicate the start of IRES or end of GFP sequence, respectively. Yellow boxes highlight the two loxP-sites that flank IRES-GFP. The blue boxes indicate the remaining loxP-site after the recombination event through the Cre recombinase.

#### 4.4.1 SCCVII CELLS OFFER AN IMMUNOLOGICAL RELEVANT PHENOTYPE

The first description of the SCCVII cell line characterized these tumor cells as lowly immunogenic, due to the absence of expression of CD80 and CD86 [104], co-stimulatory molecules that provide the second activation signal to T cells via CD28 [1]. In this respect, the SCCVII cell line represented an ideal target for the development of strategies to overcome the low immunogenicity of tumors. To confirm the original findings from Khurana *et al.* (2001), we checked for surface expression of MHC I, MHC II, CD80, and CD86, under normal culture conditions and in the presence of recombinant murine IFN $\gamma$  (100 – 500 U/ml), to stimulate inflammatory conditions. We additionally evaluated the expression of other surface molecules that could enhance or modulate the antigen-specific CTL response, including CD95, PD-L1, ICAM-1, LFA-3, and CD137L.

Flow cytometric analyses of parental SCCVII cells, as well as those stably integrated with the N81 (SCCVII\_N81) and empty vector cassettes (SCCVII\_mock), confirmed the expression of MHC I as well as the absence of MHC II and CD86. In contrast to previous reports, however, we detected CD80 expression on the surface of all cell lines investigated (Figure 23A). Treatment of the various SCCVII cell

lines with IFN $\gamma$ , which is secreted by various immune cell subsets during the course of an anti-tumor response [113], did not alter the expression levels of these cell surface molecules.

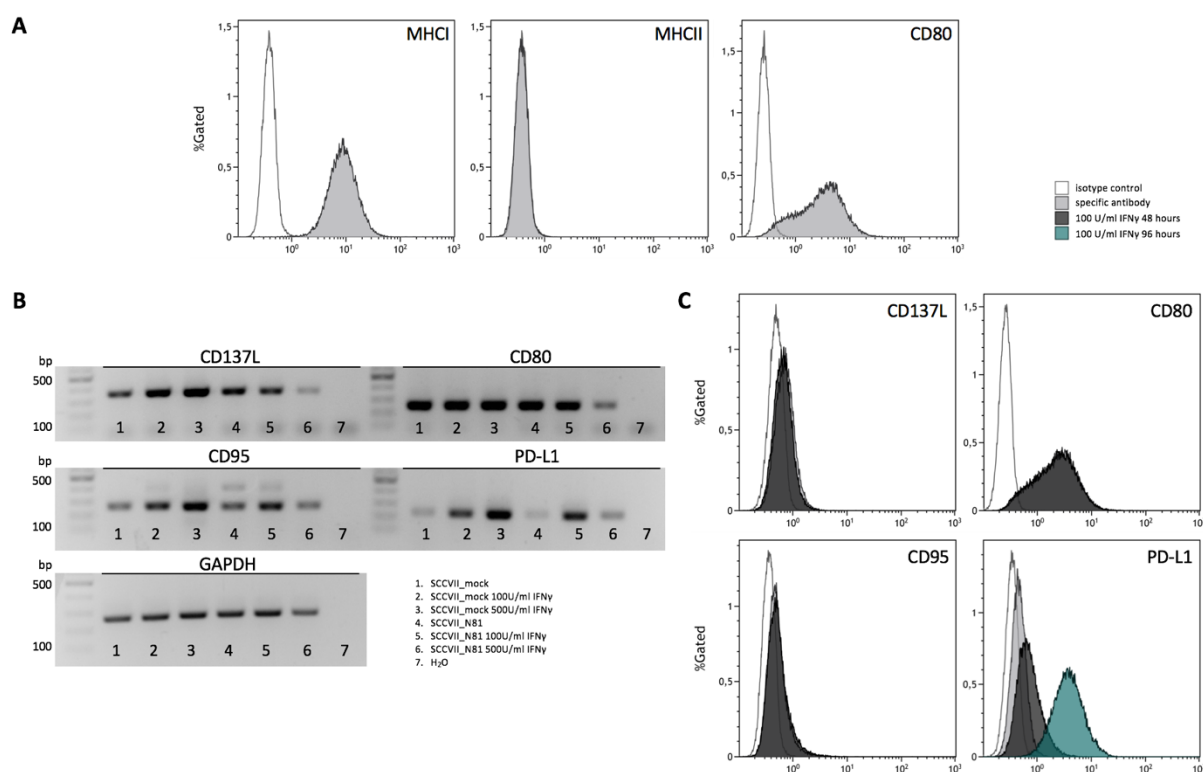


**Figure 23 Immunological phenotyping of SCCVII cell lines.** **A** SCCVII parental cells show positive cell staining for MHC I and CD80 but not for MHC II as demonstrated by flow cytometry. **B** RT-PCR products of various immunomodulatory surface molecules separated on a 1.5 % agarose gel. SCCVII\_mock and SCCVII\_N81 cells were treated with 100, 500 U/ml murine IFN $\gamma$  or left untreated and subjected to RT-PCR amplification of CD137L (366 bp), CD80 (251 bp), CD95 (237 bp) and PD-L1 (190 bp). GAPDH served as loading control. **C** FACS histogram blots of SCCVII\_mock cells stained for CD137L, CD80, CD95 or PD-L1 after stimulation with 100U/ml IFN $\gamma$  for 48 hours (black) or 96 hours (blue). White curve represents the isotype control.

Because the parental SCCVII cell line was initially described to be negative for both CD80 and CD86, we investigated other molecules that have been reported to support CTL-mediated killing. ICAM-1 and LFA-3, for example, bind to LFA-I and CD2 on the T cell surface, and these interactions were previously shown to play a role in the cytotoxic activity of virus-specific CTLs [114], similarly, CD137L (a.k.a. 4-1BBL) in the cytotoxicity of tumor-specific CTLs [115]. RT-PCR analyses of total RNA, as well as flow cytometric analyses (for ICAM-1) demonstrated that neither ICAM-1 nor LFA-3 is expressed in our SCCVII cell lines in the absence or presence of IFN $\gamma$  (data not shown). However, we detected expression of CD137L and the CD95/FAS receptor (death receptor) in all SCCVII cell lines on the mRNA level. CD95 was additionally upregulated in the presence of IFN $\gamma$  (Figure 23B). Surprisingly, in contrast to mRNA data, we could not detect expression of either of these proteins by flow cytometry (Figure 23C),

therefore, the significance of the observed induction of gene expression of these molecules remains unclear.

Finally, we also examined the expression of PD-L1, a ligand for the checkpoint receptor PD-1 found on the surface of T cells. PD-L1 is often upregulated in tumor cells as a mechanism to evade immune detection [21]. We observed low levels of PD-L1 on the mRNA in all SCCVII cell lines that were enhanced in a dose-dependent manner with increasing concentrations of IFN $\gamma$  (Figure 23B). These results were confirmed by flow cytometric analyses of PD-L1 expression on the surface of SCCVII cells under the various culture conditions tested (Figure 23C).

#### 4.5 PREVIOUSLY GENERATED IMMUNITY PROTECTS MICE FROM TUMOR DEVELOPMENT

To demonstrate that the CTL-immunity generated in pCI\_N52N81-vaccinated mice could contribute to the control or elimination of tumors expressing cognate antigen, we challenged these mice with SCCVII\_N81 cells seven days after the final immunization. These mice represented our experimental group. Additionally, various control cohorts were set up according to Table 4 to interrogate the specificity of the expected immune response. The common denominator among all control cohorts was the absence of MV-specific immune memory and tumors expressing cognate-antigen within the same mouse. For these experiments,  $5 \times 10^3$  tumor cells were injected intradermally (i.d.) into the abdomen of recipient mice. Tumor development was monitored twice per week for approximately 35 days, or until a tumor volume of about 500–600 mm<sup>3</sup> was reached, at which point the mice were sacrificed (Figure 24).

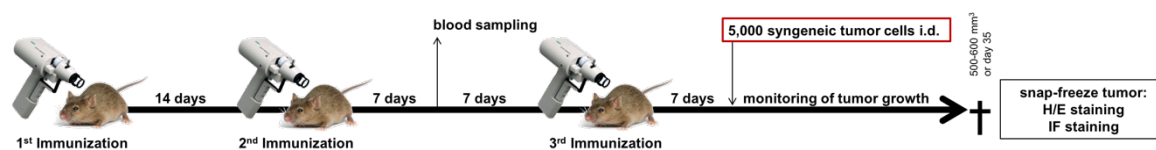


**Figure 24 Experimental design of syngeneic SCCVII tumor challenge in C3H mice.** Mice were vaccinated three times at intervals of 14 days with the Helios gene gun system performing two abdominal shots of 400 psi per immunization time point. Seven days after the final immunization mice got challenged with 5,000 syngeneic SCCVII cells i.d. and tumor growth was monitored henceforth for a period of 35 days or until the tumor reached a volume of about 500-600 mm<sup>3</sup>.

Table 4 and Figure 25 summarize the results obtained from the tumor-challenge study. With these small sample numbers, we observed no significant difference in tumor-free skin survival between all four control cohorts (Figure 25A) (Log-rank (Mantel-Cox) test, p value = 0.5875). The median time to

tumor development in the control cohorts ranged from 9 – 14.5 days, and the percentage of tumor-free mice at day 35 ranged from 0 – 40 %.

**Table 4 Summary of experimental and control cohorts of the tumor challenge study.**

Cohort	n	Control/ Experimental	Immunization status	Tumor cell challenge	Median time to tumor development (days)	Number (%) tumor- free at day 35
1	3	Control	naïve	SCCVII_N81	13	0/3 (0 %)
2	5	Control	pCI_EV	SCCVII_mock	9	1/5 (20 %)
3	5	Control	pCI_EV	SCCVII_N81	21	2/5 (40%)
4	6	Control	pCI_N52N81	SCCVII_mock	11	1/6 (16.7 %)
5	7	Experimental	pCI_N52N81	SCCVII_N81	undefined	6/7 (85.7 %)

We then compared the tumor-free skin survival of our experimental cohort, pCI\_N52N81-vaccinated mice that had been challenged with N81-expressing tumors, with that of all control groups combined (Figure 25B). We observed a significant increase in tumor-free skin survival in our experimental group (Log-rank (Mantel-Cox) test, \*\* p value = 0.0073). Only 1 out of 7 mice developed a tumor, while the remaining 85.7% stayed tumor-free for the entire observation period.

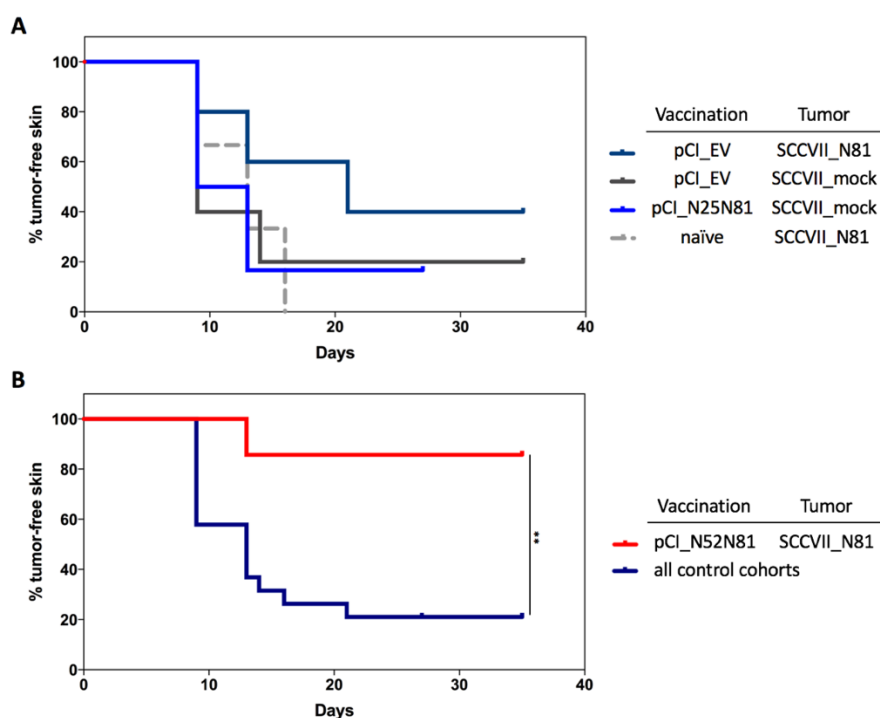


**Figure 25 Gene gun vaccination with MV antigens protects mice against SCCVII\_N81 tumor formation.** Seven days after the final immunization step mice were challenged i.d. with 5,000 SCCVII\_mock or SCCVII\_N81 cells. Tumor development and growth was monitored twice a week. Tumor development was detected upon first sight. **A** The percentage of tumor free skin from five different control cohorts over a period of 35 days is shown. Log-rank (Mantel-Cox) test showed no significant differences between the control groups. **B** Percent tumor free skin of the experimental cohort (pCI\_N52N81 immunized mice challenged with SCCVII\_N81 cells) was compared to merged control cohorts. Log-rank (Mantel-Cox) test was performed to detect significant differences (\*\* p-value = 0.0058).

H/E staining of the tissue sections from tumors that developed in the control groups confirmed the intradermal location of the tumors (Figure 26A). We additionally stained tumor cryosections with a CD8-specific antibody to evaluate the presence of CD8<sup>+</sup> T cells infiltrating the tumor. We observed CD8<sup>+</sup> T cell infiltration to various extents in all tumor sections analyzed (Figure 26B-D).

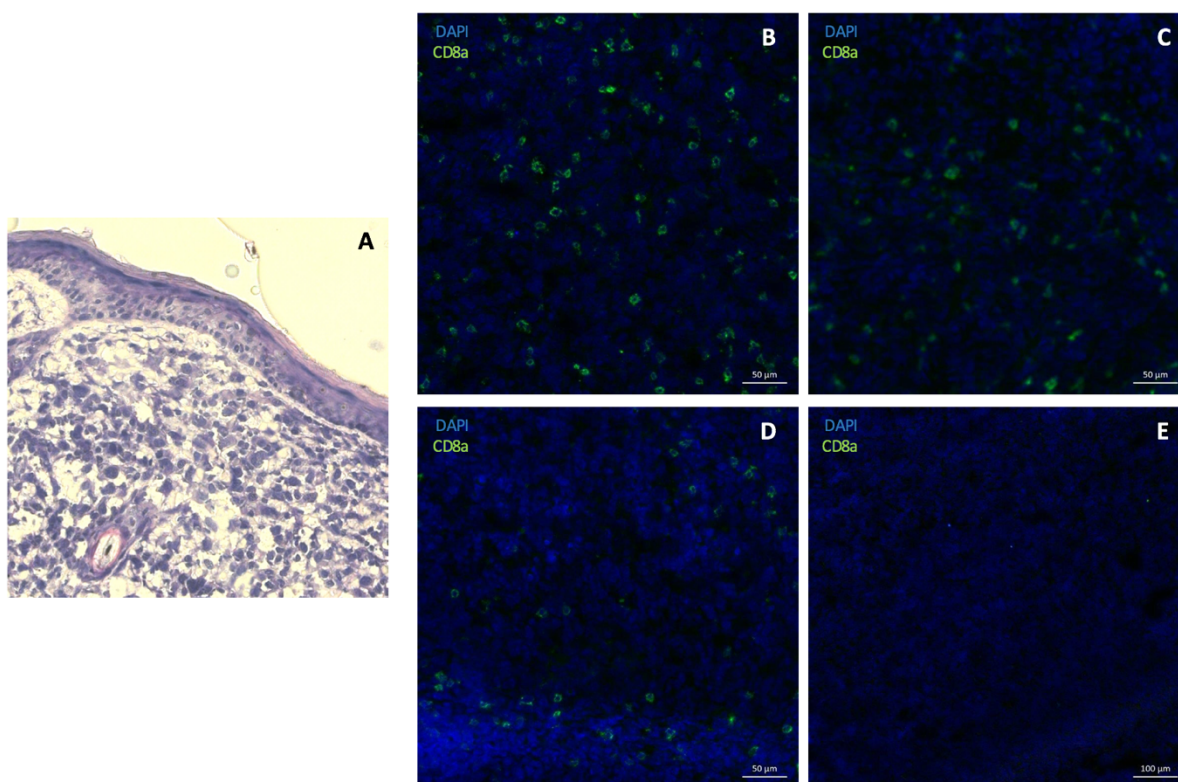


**Figure 26** CD8<sup>+</sup> T cells infiltrate tumors of MV vaccinated and empty vector gunned mice. **A** H/E stainings of 6 μm cryosections confirmed intradermal localization of tumors within mouse skin. Tumor sections were further stained for CD8<sup>+</sup> T cell infiltrates (green). Immunofluorescence analysis showing CD8<sup>+</sup> T cells in tumors arisen from SCCVII\_N81 (**B**) or SCCVII\_mock cells (**C**) in pCI\_EV gunned mice. In addition, tumors from pCI\_N52N81 immunized mice challenged with SCCVII\_mock cells (**D**) were included in the analysis. Nuclei staining of cells were performed with 4'-6-diamidin-2-phenylindol (DAPI, blue). A second step control confirmed specificity of antibody staining (**E**).

## 5 DISCUSSION

Epidermolysis bullosa is an inherited skin disease characterized by tissue fragility and blistering following minor trauma. The underlying cause lies in the absence or malfunction of proteins, which are important for proper cohesion of the different skin layers. The most severe form, recessive dystrophic EB is caused by mutations in type VII collagen [70]. RDEB is characterized by chronic and long-standing wounds that are the sites for the development of aggressive squamous cell carcinoma in early adulthood. This cancer is the primary cause for premature death in these patients [69], [81]. Current data reports that 90 % of RDEB patients will develop SCC [82], making this patient group, in our opinion, an ideal target for cancer vaccination strategies.

Our long-term goal is the development of cancer immunogene therapeutic strategies against RDEB-SCC. Our strategy builds upon the success of widespread prophylactic vaccination programs in imparting significant protection against infectious childhood diseases. We wish to exploit the pre-existing immune memory against known viral CTL epitopes and redirect this response to target tumor cells expressing the cognate antigen. We believe that: (1) such an approach takes advantage of the immune memory generated during vaccination which is more rapid and robust than the primary response, and (2) that the use of a viral antigen circumvents existing tolerance mechanisms against self-proteins from which over 70 % of tumor-associated antigens are derived [22], [41].

Measles is one of the most common childhood diseases that is preventable by vaccination. Before the introduction of widespread vaccination campaigns, mortality due to the disease was estimated at 2.6 million deaths per year. Between 2000 and 2014, vaccination against the virus is estimated to have prevented 17.1 million deaths [116]. The majority of the general population in the western world has been vaccinated against the measles virus. This includes RDEB patients, as we could show that 4 out of 6 RDEB patients tested positive for anti-measles antibodies, indicating a previous exposure to the virus either via vaccination or infection. Studies have demonstrated that MV-specific functional CD4<sup>+</sup> and CD8<sup>+</sup> memory T lymphocytes persist in MV vaccinated as well as naturally infected 15 to 25 and 25 to 42 years old patients, respectively, indicating a long-term cellular immune memory to MV [117], [118]. Thus in most people, measles virus antigens represent epitopes capable of rapidly recalling a robust cytolytic immune memory response [100]. This pre-existing immunity can be harnessed to kill tumor cells provided that the cancer cells can be made to express these CTL epitopes.

As a first step and to provide proof-of-principle, we demonstrate the successful establishment of a fully immunocompetent mouse model with immunity against CTL epitopes derived from the

nucleocapsid protein of MV. Immunity was generated via DNA vaccination with vectors designed to encode the IL2 $\alpha$  for proper targeting to the ER and loading onto MHC I [99], the MV nucleocapsid CTL epitopes N52-59 and N81-88 in a tandem configuration [100], and a promiscuous MVTh epitope to elicit CD4 $^{+}$  help for the efficient generation of CTL memory T cells [101], [102]. The DNA plasmids were delivered directly to the DC-rich region of the dermis via the gene gun system. Additionally, microscopic damage due to the pressurized bombardment of DNA coated gold particles elicits a danger signal and local inflammation [108]. This contributes to efficient DC activation, which enhances the uptake and processing of antigens, as well as migration to skin-draining lymph nodes where they provide the appropriate signals required for activation of naïve T cells into memory and effector cells [109]. Gene gun DNA vaccination has already been shown to be successful in the generation of functional CD8 $^{+}$  T cells capable of target cell killing [106], [119]. We monitored the quality of the elicited immune responses by performing IFN $\gamma$  immunoassays, T cell proliferation, and *in vivo* CTL killing assays. IFN $\gamma$  secretion was enhanced in peripheral blood-, lymph node-, and splenic cells isolated from MV-vaccinated mice upon restimulation with the N81 peptide, which we observed to be the immunodominant antigen of the two MV CTL epitopes tested. Using a customized FITC-labelled N81-H-2K $^k$  dextramer, we could identify an increased subpopulation of N81-specific CD8 $^{+}$  T cells in immunized mice that responded to restimulation with cognate peptide in *in vitro* T cell proliferation assays. Finally, we achieved up to 80% specific lysis of N81-loaded target cells in *in vivo* CTL assays that could be inhibited by pre-treatment of the mice with CD8-blocking antibody. Thus, our vaccination strategy resulted in the successful generation of CTL immunity against the N81-88 epitope derived from MV nucleocapsid protein.

To investigate whether these immune responses would be potent enough to mediate tumor-cell killing, we challenged immunized mice with syngeneic tumors that expressed the cognate epitope. 85.7 % of immunized mice were able to reject the engraftment of tumor cells expressing the cognate antigen in comparison to 21.1 % in control groups. Thus, the CTL immunity generated by our vaccination protocol was enough to protect mice from tumor development as long as these tumor cells express the cognate epitope. This mouse model therefore represents an important tool that can be utilized to evaluate the efficacy of various *in situ* strategies for the delivery and proper presentation of cognate antigen to tumor cells.

Indeed, the targeted expression of cognate antigen in tumor cells represents a big caveat for the success of our approach. There are several potential applications one could employ to present peptide epitopes on the surface of SCC cells. The simplest method would be to inject peptide epitopes directly into the tumor for loading onto MHC I molecules on the tumor surface, similar to the “pulsing” of

target cells with peptide *in vitro*. Intratumoral injection of peptide has already been tested in a mouse model by Nobuoka *et al.* (2012) who could confirm proper loading of peptides onto MHC I. Following intratumoral injection with antigenic peptides *in vivo*, tumors were excised and single cell suspensions made. The isolated tumor cells were then used as target cells for peptide-specific CTLs, and could induce IFN $\gamma$  secretion in these cells in *in vitro* ELISPOT assays. Furthermore, intratumoral injection of the immunogenic peptides was successful in inducing migration of peptide-specific CTLs into the tumor following adoptive T cell transfer resulting in CTL-mediated tumor lysis and enhanced overall survival of the mice [120]. In this study, it could also be shown that intratumoral injection of the peptide did not result in presentation by normal tissue as no destruction could be observed in different organs examined. However, a second injection of tumor cells into the opposite flank resulted in rejection of those cells, indicating that antigen spreading had occurred [120]. Notably, this effect would be important for RDEB associated SCC, as it is a highly metastasizing tumor. Experiments investigating the efficacy of peptide presentation on tumor cells following intratumoral injections of peptide in our established mouse model are currently underway.

*In vivo* DNA transfection of tumors with plasmids encoding the antigenic epitopes depict another possibility. *In vivo* gene delivery represents one of the biggest hurdles to gene therapy, with numerous different nanoparticle platforms being investigated and developed for this purpose. In the context of our therapeutic application, only a minimal DNA sequence, encoding the IL2 leader sequence and CTL epitope, needs to be introduced. This is significantly smaller in size than the DNA vectors needed for many gene therapy applications aimed at correcting disease-causing genetic mutations. A small vector size greatly facilitates efficient delivery, however, the matter of tumor specificity remains to be addressed. There are several methods under investigation that rely on the application of external forces to selectively target delivery of therapeutic molecules to the desired location in the body. For example, magnetic nanoparticles can be used for site-directed delivery of drugs to tumors by local application of magnetic fields [121]. Clinical contrast agents or microbubbles have been formulated to be capable of carrying a therapeutic payload that is selectively released in the target tissue upon local ultrasound application [122]. Both these guided delivery systems offer the additional advantage of being able to reach tumors in hard-to-target and inaccessible internal organs. However, even with a highly efficient delivery method, a 100 % transfection of all tumor cells cannot be expected *in vivo*. The question therefore remains whether expression of CTL epitopes in only a fraction of the tumor cells would be enough to result in complete tumor regression. To address this question in our established mouse model, we will inject SCCVII parental and N81-expressing tumor cells, mixed at defined ratios, into the flanks of vaccinated mice and monitor for tumor development. While CTL-mediated killing is antigen-specific, the lysis of even a fraction of tumor cells that express the cognate epitope may lead

to release and cross-presentation of N81 and other tumor associated antigens, as well as the activation of innate mechanisms due to the resulting danger signals. The combination of antigen-specific and non-antigen-specific mechanisms could therefore result in complete tumor regression. Such an experiment would give us an insight into the transfection efficiencies we would need to achieve for successful application of our strategy.

In this study, we could ascribe specific lysis of target cells to the action of CD8<sup>+</sup> CTLs as demonstrated by our CD8-blocking experiments. In the last few years, new sub-populations of memory T cells have been defined including skin-resident memory T cells [65], thereby begging the question as to which cell subset is critical for the observed anti-tumor effect. The route of vaccination, the intradermal localization of the tumor, and the results of our *in vivo* CTL assays, all suggest that the anti-tumor effects are likely mediated by the skin-resident CD8<sup>+</sup> T<sub>RM</sub> cells. Flow cytometric analyses of surface markers on T cells isolated from the skin of vaccinated mice and those infiltrating the tumors, as well as blocking or depletion of specific immune cell subsets in tumor challenge experiments, would facilitate the confirmation this suggestion. An important T cell marker to investigate is the checkpoint receptor PD-1. We observed an upregulation of PD-L1 in SCCVII cells when cultured in the presence of IFN $\gamma$ , a cytokine involved in CTL responses [1]. The upregulation of PD-L1 on tumor cells represents a mechanism by which these cells evade immune attack. Engagement of PD-L1 by PD-1 on T cells results in a dampening of T cell activation and decreased effector function, resulting in what is known as an “exhausted” phenotype [21]. Therefore, the induction of PD-1 expression on N81-specific CTLs would indicate a decline in the anti-tumor function of these cells. In this case, combining our immunotherapy strategy with the application of immune checkpoint blockers such PD-L1/PD-1 blocking antibodies should be considered.

One major future aim will be the translation of our findings into the human system. Mice are not natural hosts for MV [123] and we were severely limited in the choice of CTL epitopes with known H-2k<sup>k</sup> restriction. Thus, while our C3H model will continue to be useful for the mechanistic studies described above, it is neither appropriate for the pre-clinical development of this therapeutic approach nor for predicting the success of such a strategy in humans. For these purposes, the use of a “humanized” transgenic mouse that expresses human MHC I (HLA-A2.1), human MHC II (HLA-DP4), and human CD4, as developed by Ru *et al.* (2012), is preferable. HLA-A2.1 is the most frequent MHC I molecule, estimated to be present in 30–50% of the human population. Likewise, the HLA-DP4 MHC II is one of the most abundant alleles, expressed in 20–80 % of humans. Additionally, these mice lack expression of murine MHC II and  $\beta$ 2-microglobulin [124], allowing for the study of “human” immune functions without the interference of murine MHC responses [125]. Numerous MV CTL epitopes have

already been identified as immunogenic in humans. Most of these are derived from the hemagglutinin protein of MV [126]. Likewise, CTL epitopes from many other viruses have been identified. The potencies of these epitopes and the quality of the CTL responses they generate can be investigated in HLA-A2/DP4 mice in order to predict the success of the therapeutic approach. In parallel, we need to confirm the presence of functional immune memory against these CTL epitopes in RDEB patients, as well as in the general population. To this end, CD8<sup>+</sup> T cells isolated from peripheral blood samples could be restimulated with the various CTL epitopes of interest in *in vitro* T cell proliferation assays. *In vitro* CTL assays would further show, if the isolated CTLs were still functional and able to specifically kill peptide-pulsed target cells.

To conclude, in this project we have attempted to lay down the foundation for extending the way we view prophylactic vaccination against childhood diseases to include the possibility of being an anti-cancer strategy. Current vaccination strategies focus on the development of vaccines against tumor antigens in order to provide protection by clearing potentially malignant cells before the establishment of a tumor mass. Our strategy is not preventative as it depends on introducing a recall antigen into tumor cells, and can only be applied once a lesion or suspected lesion has been established. Nevertheless, we feel our approach offers several advantages. Forced expression of known viral epitopes in tumor cells can circumvent some of the issues of tumor heterogeneity. Moreover, viral epitopes generally induce more potent immune responses and have the advantage of being entirely non-self, thereby circumventing the tolerance mechanisms that have been established against self-derived epitopes. Finally, the sudden and robust expression of viral epitopes in tumor cells, as we hope to achieve, makes these cells highly immunogenic and visible to the immune system, thereby greatly increasing the odds of successful clearance. With our increased understanding of tumor-induced immune tolerance mechanisms, the design of better vaccines and improved delivery routes, and the continuing advancement in *in vivo* drug delivery systems, we believe our approach has the potential to be broadly applicable to many tumor types in the future.

## 6 BIBLIOGRAPHY

- [1] A. K. Abbas, A. H. Lichtman, and S. Pillai, *Cellular and Molecular Immunology*, Eighth Edition. Elsevier Saunders, 2015.
- [2] T. H. Mogensen, "Pathogen Recognition and Inflammatory Signaling in Innate Immune Defenses," *Clin. Microbiol. Rev.*, vol. 22, no. 2, pp. 240–273, Apr. 2009.
- [3] "Technology | Oxford Immunotec International." [Online]. Available: <http://www.oxfordimmunotec.com/international/science/technology-2/>. [Accessed: 02-Aug-2016].
- [4] C. C. Goodnow, J. Sprent, B. F. de St Groth, and C. G. Vinuesa, "Cellular and genetic mechanisms of self tolerance and autoimmunity," *Nature*, vol. 435, no. 7042, pp. 590–597, Jun. 2005.
- [5] S. Waggoner, "Specialization in Adaptive Immunity," in *Pathobiology of Human Disease: A Dynamic Encyclopedia of Disease Mechanisms*, Elsevier, 2014.
- [6] C. A. Janeway, P. Travers, M. Walport, and M. J. Shlomchik, *Immunobiology: The Immune System in Health and Disease*, vol. 5th edition. New York: Garland Science, 2001.
- [7] K. Hirahara and T. Nakayama, "CD4+ T-cell subsets in inflammatory diseases: beyond the Th1/Th2 paradigm," *Int. Immunol.*, vol. 28, no. 4, pp. 163–171, Jan. 2016.
- [8] R. V. Luckheeram, R. Zhou, A. D. Verma, and B. Xia, "CD4+ T cells: Differentiation and Functions," *J. Immunol. Res.*, vol. 2012, p. e925135, Mar. 2012.
- [9] N. Zhang and M. J. Bevan, "CD8+ T Cells: Foot Soldiers of the Immune System," *Immunity*, vol. 35, no. 2, pp. 161–168, Aug. 2011.
- [10] J. B. Huppa and M. M. Davis, "T-cell-antigen recognition and the immunological synapse," *Nat. Rev. Immunol.*, vol. 3, no. 12, pp. 973–983, Dec. 2003.
- [11] M. L. Dustin, "The Immunological Synapse," *Cancer Immunol. Res.*, vol. 2, no. 11, pp. 1023–1033, Nov. 2014.
- [12] P. G. Coulie, B. J. Van den Eynde, P. van der Bruggen, and T. Boon, "Tumour antigens recognized by T lymphocytes: at the core of cancer immunotherapy," *Nat. Rev. Cancer*, vol. 14, no. 2, pp. 135–146, Feb. 2014.
- [13] R. D. Salter *et al.*, "Polymorphism in the  $\alpha 3$  domain of HLA-A molecules affects binding to CD8," *Nature*, vol. 338, no. 6213, pp. 345–347, Mar. 1989.
- [14] M. A. Cox, L. E. Harrington, and A. J. Zajac, "Cytokines and the Inception of CD8 T Cell Responses," *Trends Immunol.*, vol. 32, no. 4, p. 180, Apr. 2011.
- [15] Z. Fan and Q. Zhang, "Molecular mechanisms of lymphocyte-mediated cytotoxicity," *Cell. Mol. Immunol.*, vol. 2, no. 4, pp. 259–264, Aug. 2005.
- [16] P. H. Krammer, "CD95's deadly mission in the immune system," *Nature*, vol. 407, no. 6805, pp. 789–795, Oct. 2000.
- [17] G. Bossi and G. M. Griffiths, "CTL secretory lysosomes: biogenesis and secretion of a harmful organelle," *Semin. Immunol.*, vol. 17, no. 1, pp. 87–94, Feb. 2005.
- [18] J. R. Schoenborn and C. B. Wilson, "Regulation of Interferon- $\gamma$  During Innate and Adaptive Immune Responses," vol. 96, B.-A. in *Immunology*, Ed. Academic Press, 2007, pp. 41–101.

- [19] F. Leithäuser *et al.*, “Constitutive and induced expression of APO-1, a new member of the nerve growth factor/tumor necrosis factor receptor superfamily, in normal and neoplastic cells,” *Lab. Invest. J. Tech. Methods Pathol.*, vol. 69, no. 4, pp. 415–429, Oct. 1993.
- [20] E. J. Wherry and M. Kurachi, “Molecular and cellular insights into T cell exhaustion,” *Nat. Rev. Immunol.*, vol. 15, no. 8, pp. 486–499, Aug. 2015.
- [21] D. M. Pardoll, “The blockade of immune checkpoints in cancer immunotherapy,” *Nat. Rev. Cancer*, vol. 12, no. 4, pp. 252–264, Apr. 2012.
- [22] M. L. Disis, “Immune Regulation of Cancer,” *J. Clin. Oncol.*, vol. 28, no. 29, pp. 4531–4538, Oct. 2010.
- [23] A. M. Monjazeb, A. E. Zamora, S. K. Grossenbacher, A. Mirsoian, G. D. Sckisel, and W. J. Murphy, “Immunoediting and Antigen Loss: Overcoming the Achilles Heel of Immunotherapy with Antigen Non-Specific Therapies,” *Front. Oncol.*, vol. 3, Jul. 2013.
- [24] S. K. Biswas and A. Mantovani, “Macrophage plasticity and interaction with lymphocyte subsets: cancer as a paradigm,” *Nat. Immunol.*, vol. 11, no. 10, pp. 889–896, Oct. 2010.
- [25] T. Condamine, I. Ramachandran, J.-I. Youn, and D. I. Gabrilovich, “Regulation of Tumor Metastasis by Myeloid-derived Suppressor Cells,” *Annu. Rev. Med.*, vol. 66, pp. 97–110, Jan. 2015.
- [26] M. Johansson, D. G. DeNardo, and L. M. Coussens, “Polarized immune responses differentially regulate cancer development,” *Immunol. Rev.*, vol. 222, no. 1, pp. 145–154, Apr. 2008.
- [27] A. Mantovani, P. Allavena, A. Sica, and F. Balkwill, “Cancer-related inflammation,” *Nature*, vol. 454, no. 7203, pp. 436–444, Jul. 2008.
- [28] M. R. Junttila and F. J. de Sauvage, “Influence of tumour micro-environment heterogeneity on therapeutic response,” *Nature*, vol. 501, no. 7467, pp. 346–354, Sep. 2013.
- [29] G. P. Dunn, A. T. Bruce, H. Ikeda, L. J. Old, and R. D. Schreiber, “Cancer immunoediting: from immunosurveillance to tumor escape,” *Nat. Immunol.*, vol. 3, no. 11, pp. 991–998, Nov. 2002.
- [30] G. P. Dunn, L. J. Old, and R. D. Schreiber, “The immunobiology of cancer immunosurveillance and immunoediting,” *Immunity*, vol. 21, no. 2, pp. 137–148, Aug. 2004.
- [31] H. J. Steer, R. A. Lake, A. K. Nowak, and B. W. S. Robinson, “Harnessing the immune response to treat cancer,” *Oncogene*, vol. 29, no. 48, pp. 6301–6313, Dec. 2010.
- [32] S. I. Grivnenkov, F. R. Greten, and M. Karin, “Immunity, Inflammation, and Cancer,” *Cell*, vol. 140, no. 6, pp. 883–899, Mar. 2010.
- [33] V. Shankaran *et al.*, “IFN $\gamma$  and lymphocytes prevent primary tumour development and shape tumour immunogenicity,” *Nature*, vol. 410, no. 6832, pp. 1107–1111, Apr. 2001.
- [34] J. Galon *et al.*, “Type, Density, and Location of Immune Cells Within Human Colorectal Tumors Predict Clinical Outcome,” *Science*, vol. 313, no. 5795, pp. 1960–1964, Sep. 2006.
- [35] P. Roepman *et al.*, “An Immune Response Enriched 72-Gene Prognostic Profile for Early-Stage Non-Small-Cell Lung Cancer,” *Am. Assoc. Cancer Res.*, vol. 15, no. 1, pp. 284–290, Jan. 2009.
- [36] L. Zhang *et al.*, “Intratumoral T Cells, Recurrence, and Survival in Epithelial Ovarian Cancer,” *N. Engl. J. Med.*, vol. 348, no. 3, pp. 203–213, Jan. 2003.
- [37] N. Bhardwaj, “Harnessing the immune system to treat cancer,” *J. Clin. Invest.*, vol. 117, pp. 1130–1136, 2007.

- [38] R. A. Clark *et al.*, "Human squamous cell carcinomas evade the immune response by down-regulation of vascular E-selectin and recruitment of regulatory T cells," *J. Exp. Med.*, vol. 205, no. 10, pp. 2221–2234, Sep. 2008.
- [39] S. Nagaraj *et al.*, "Altered recognition of antigen is a novel mechanism of CD8+ T cell tolerance in cancer," *Nat. Med.*, vol. 13, no. 7, pp. 828–835, Jul. 2007.
- [40] J. Couzin-Frankel, "Cancer Immunotherapy," *Science*, vol. 342, no. 6165, pp. 1432–1433, Dec. 2013.
- [41] M. A. Cheever *et al.*, "The Prioritization of Cancer Antigens: A National Cancer Institute Pilot Project for the Acceleration of Translational Research," *Am. Assoc. Cancer Res.*, vol. 15, no. 17, pp. 5323–5337, Sep. 2009.
- [42] F. S. Hodi *et al.*, "Improved Survival with Ipilimumab in Patients with Metastatic Melanoma," *N. Engl. J. Med.*, vol. 363, no. 8, pp. 711–723, Aug. 2010.
- [43] P. Sharma and J. P. Allison, "The future of immune checkpoint therapy," *Science*, vol. 348, no. 6230, pp. 56–61, Apr. 2015.
- [44] S. L. Topalian *et al.*, "Safety, Activity, and Immune Correlates of Anti-PD-1 Antibody in Cancer," *N. Engl. J. Med.*, vol. 366, no. 26, pp. 2443–2454, Jun. 2012.
- [45] J. D. Wolchok *et al.*, "Nivolumab plus Ipilimumab in Advanced Melanoma," *N. Engl. J. Med.*, vol. 369, no. 2, pp. 122–133, Jul. 2013.
- [46] S. A. Rosenberg and N. P. Restifo, "Adoptive cell transfer as personalized immunotherapy for human cancer," *Science*, vol. 348, no. 6230, pp. 62–68, Apr. 2015.
- [47] S. A. Rosenberg *et al.*, "Durable Complete Responses in Heavily Pretreated Patients with Metastatic Melanoma Using T Cell Transfer Immunotherapy," *Clin. Cancer Res. Off. J. Am. Assoc. Cancer Res.*, vol. 17, no. 13, pp. 4550–4557, Jul. 2011.
- [48] C. S. Hinrichs and S. A. Rosenberg, "Exploiting the curative potential of adoptive T-cell therapy for cancer," *Immunol. Rev.*, vol. 257, no. 1, pp. 56–71, Jan. 2014.
- [49] B. L. Levine *et al.*, "Durable Remissions with Control of Cytokine Release Syndrome (CRS) Using T Cells Expressing CD19 Targeted Chimeric Antigen Receptor (CAR) CTL019 to Treat Relapsed/Refractory (R/R) Acute Lymphoid Leukemia (ALL)," *Cytotherapy*, vol. 18, no. 6, pp. S14–S15, Jun. 2016.
- [50] J. J. L. Jacobs, C. Snackey, A. A. Geldof, D. Characiejus, R. J. a. V. Moorselaar, and W. D. Otter, "Inefficacy of Therapeutic Cancer Vaccines and Proposed Improvements. Casus of Prostate Cancer," *Anticancer Res.*, vol. 34, no. 6, pp. 2689–2700, Jan. 2014.
- [51] K. Oleinika, R. J. Nibbs, G. J. Graham, and A. R. Fraser, "Suppression, subversion and escape: the role of regulatory T cells in cancer progression," *Clin. Exp. Immunol.*, vol. 171, no. 1, pp. 36–45, Jan. 2013.
- [52] M. Y. Mapara and M. Sykes, "Tolerance and Cancer: Mechanisms of Tumor Evasion and Strategies for Breaking Tolerance," *J. Clin. Oncol.*, vol. 22, no. 6, pp. 1136–1151, Mar. 2004.
- [53] S. H. van der Burg, R. Arens, F. Ossendorp, T. van Hall, and C. J. M. Melief, "Vaccines for established cancer: overcoming the challenges posed by immune evasion," *Nat. Rev. Cancer*, vol. 16, no. 4, pp. 219–233, Apr. 2016.
- [54] P. Fritsch, *Dermatologie und Venerologie*. Berlin Heidelberg: Springer Lehrbuch, 1998.

- [55] "Medicine - Biology Forums Gallery." [Online]. Available: <http://biology-forums.com/index.php?action=gallery;cat=4>. [Accessed: 17-Jul-2016].
- [56] J. Kanitakis, "Anatomy, histology and immunohistochemistry of normal human skin," *Eur. J. Dermatol.*, vol. 12, no. 4, pp. 390–401, Jul. 2002.
- [57] P. A. J. Kolarsick, M. A. Kolarsick, and C. Goodwin, "Anatomy and Physiology of the Skin;," *J. Dermatol. Nurses Assoc.*, vol. 3, no. 4, pp. 203–213, Jul. 2011.
- [58] E. Proksch, J. M. Brandner, and J.-M. Jensen, "The skin: an indispensable barrier," *Exp. Dermatol.*, vol. 17, no. 12, pp. 1063–1072, Dec. 2008.
- [59] D. Breitkreutz, N. Mirancea, and R. Nischt, "Basement membranes in skin: unique matrix structures with diverse functions?," *Histochem. Cell Biol.*, vol. 132, no. 1, pp. 1–10, Jul. 2009.
- [60] R. E. Burgeson and A. M. Christiano, "The dermal—epidermal junction," *Curr. Opin. Cell Biol.*, vol. 9, no. 5, pp. 651–658, Oct. 1997.
- [61] R. F. Ghohestani, K. Li, P. Rousselle, and J. Uitto, "Molecular organization of the cutaneous basement membrane zone," *Clin. Dermatol.*, vol. 19, no. 5, pp. 551–562, Sep. 2001.
- [62] B. Malissen, S. Tamoutounour, and S. Henri, "The origins and functions of dendritic cells and macrophages in the skin," *Nat. Rev. Immunol.*, vol. 14, no. 6, pp. 417–428, Jun. 2014.
- [63] V. R. Yanofsky, H. Mitsui, D. Felsen, and J. A. Carucci, "Understanding Dendritic Cells and Their Role in Cutaneous Carcinoma and Cancer Immunotherapy," *J. Immunol. Res.*, vol. 2013, p. e624123, Mar. 2013.
- [64] R. A. Clark *et al.*, "The Vast Majority of CLA+ T Cells Are Resident in Normal Skin," *J. Immunol.*, vol. 176, no. 7, pp. 4431–4439, Jan. 2006.
- [65] R. Watanabe *et al.*, "Human skin is protected by four functionally and phenotypically discrete populations of resident and recirculating memory T cells," *Sci. Transl. Med.*, vol. 7, no. 279, p. 279ra39, Mar. 2015.
- [66] C. Park and T. S. Kupper, "THE EMERGING ROLE OF RESIDENT MEMORY T CELLS IN PROTECTIVE IMMUNITY AND INFLAMMATORY DISEASE," *Nat. Med.*, vol. 21, no. 7, pp. 688–697, Jul. 2015.
- [67] K. Hochheiser, S. Bedoui, and T. Gebhardt, "Multilayered T-cell memory in human skin," *Ann. Transl. Med.*, vol. 3, no. 20, Nov. 2015.
- [68] J.-D. Fine and H. Hintner, *Life with Epidermolysis bullosa (EB)*. .
- [69] J.-D. Fine, "Inherited epidermolysis bullosa," *Orphanet J. Rare Dis.*, vol. 5, p. 12, 2010.
- [70] V. L. S. Y. Boeira *et al.*, "Inherited epidermolysis bullosa: clinical and therapeutic aspects," *An. Bras. Dermatol.*, vol. 88, no. 2, pp. 185–198, 2013.
- [71] "Erkrankung." [Online]. Available: <http://www.debra-austria.org/epidermolysis-bullosa/erkrankung.html>. [Accessed: 12-Jul-2016].
- [72] J.-D. Fine *et al.*, "Inherited epidermolysis bullosa: Updated recommendations on diagnosis and classification," *J. Am. Acad. Dermatol.*, vol. 70, no. 6, pp. 1103–1126, Jun. 2014.
- [73] J. Uitto *et al.*, "Progress toward Treatment and Cure of Epidermolysis Bullosa: Summary of the DEBRA International Research Symposium EB2015," *J. Invest. Dermatol.*, vol. 136, no. 2, pp. 352–358, Feb. 2016.
- [74] J.-D. Fine *et al.*, "The classification of inherited epidermolysis bullosa (EB): Report of the Third International Consensus Meeting on Diagnosis and Classification of EB," *J. Am. Acad. Dermatol.*, vol. 58, no. 6, pp. 931–950, Jun. 2008.

- [75] P. A. Coulombe, M. L. Kerns, and E. Fuchs, "Epidermolysis bullosa simplex: a paradigm for disorders of tissue fragility," *J. Clin. Invest.*, vol. 119, no. 7, pp. 1784–1793, Jul. 2009.
- [76] A. Nakano *et al.*, "Laminin 5 mutations in junctional epidermolysis bullosa: molecular basis of Herlitz vs non-Herlitz phenotypes," *Hum. Genet.*, vol. 110, no. 1, pp. 41–51, Nov. 2001.
- [77] L. Bruckner-Tuderman, B. Höpfner, and N. Hammami-Hauasli, "Biology of anchoring fibrils: lessons from dystrophic epidermolysis bullosa," *Matrix Biol.*, vol. 18, no. 1, pp. 43–54, Feb. 1999.
- [78] C. B. Wiebe and H. S. Larjava, "Abnormal deposition of type VII collagen in Kindler syndrome," *Arch. Dermatol. Res.*, vol. 291, no. 1, pp. 6–13, Jan. 1999.
- [79] L. Soro, C. Bartus, and S. Purcell, "Recessive Dystrophic Epidermolysis Bullosa," *J. Clin. Aesthetic Dermatol.*, vol. 8, no. 5, pp. 41–46, May 2015.
- [80] R. Varki, S. Sadowski, J. Uitto, and E. Pfendner, "Epidermolysis bullosa. II. Type VII collagen mutations and phenotype–genotype correlations in the dystrophic subtypes," *J. Med. Genet.*, vol. 44, no. 3, pp. 181–192, Mar. 2007.
- [81] L. R. A. Intong and D. F. Murrell, "Inherited epidermolysis bullosa: New diagnostic criteria and classification," *Clin. Dermatol.*, vol. 30, no. 1, pp. 70–77, Jan. 2012.
- [82] J.-D. Fine, L. B. Johnson, M. Weiner, K.-P. Li, and C. Suchindran, "Epidermolysis bullosa and the risk of life-threatening cancers: The National EB Registry experience, 1986-2006," *J. Am. Acad. Dermatol.*, vol. 60, no. 2, pp. 203–211, Feb. 2009.
- [83] "Squamous Cell Carcinoma (SCC) - SkinCancer.org." [Online]. Available: <http://www.skincancer.org/skin-cancer-information/squamous-cell-carcinoma>. [Accessed: 14-Jul-2016].
- [84] V. Madan, J. T. Lear, and R.-M. Szeimies, "Non-melanoma skin cancer," *Lancet Lond. Engl.*, vol. 375, no. 9715, pp. 673–685, Feb. 2010.
- [85] S. Euvrard *et al.*, "Aggressive squamous cell carcinomas in organ transplant recipients," *Transplant. Proc.*, vol. 27, no. 2, pp. 1767–1768, Apr. 1995.
- [86] S. A. Watt *et al.*, "Integrative mRNA profiling comparing cultured primary cells with clinical samples reveals PLK1 and C20orf20 as therapeutic targets in cutaneous squamous cell carcinoma," *Oncogene*, vol. 30, no. 46, pp. 4666–4677, Nov. 2011.
- [87] Y.-Z. Ng *et al.*, "Fibroblast-Derived Dermal Matrix Drives Development of Aggressive Cutaneous Squamous Cell Carcinoma in Patients with Recessive Dystrophic Epidermolysis Bullosa," *Cancer Res.*, vol. 72, no. 14, pp. 3522–3534, Jul. 2012.
- [88] V. R. Mittapalli *et al.*, "Injury-driven Stiffening of the Dermis Expedites Skin Carcinoma Progression," *Cancer Res.*, p. canres.1348.2015, Dec. 2015.
- [89] V. Küttner *et al.*, "Global remodelling of cellular microenvironment due to loss of collagen VII," *Mol. Syst. Biol.*, vol. 9, p. 657, Apr. 2013.
- [90] I. Martincorena *et al.*, "High burden and pervasive positive selection of somatic mutations in normal human skin," *Science*, vol. 348, no. 6237, pp. 880–886, May 2015.
- [91] J. L. Arbiser *et al.*, "Involvement of p53 and p16 Tumor Suppressor Genes in Recessive Dystrophic Epidermolysis Bullosa-Associated Squamous Cell Carcinoma," *J. Invest. Dermatol.*, vol. 123, no. 4, pp. 788–790, Oct. 2004.
- [92] E. Hoste *et al.*, "Innate sensing of microbial products promotes wound-induced skin cancer," *Nat. Commun.*, vol. 6, p. 5932, Jan. 2015.

- [93] R. Kang, Q. Zhang, H. J. Zeh, M. T. Lotze, and D. Tang, "HMGB1 in Cancer: Good, Bad, or Both?," *Clin. Cancer Res.*, vol. 19, no. 15, pp. 4046–4057, Aug. 2013.
- [94] R. Mallipeddi, "Epidermolysis bullosa and cancer," *Clin. Exp. Dermatol.*, vol. 27, no. 8, pp. 616–623, Nov. 2002.
- [95] J. e. Mellerio *et al.*, "Management of cutaneous squamous cell carcinoma in patients with epidermolysis bullosa: best clinical practice guidelines," *Br. J. Dermatol.*, vol. 174, no. 1, pp. 56–67, Jan. 2016.
- [96] A. W. Arnold, L. Bruckner-Tuderman, C. Zuger, and P. H. Itin, "Cetuximab therapy of metastasizing cutaneous squamous cell carcinoma in a patient with severe recessive dystrophic epidermolysis bullosa," *Dermatol. Basel Switz.*, vol. 219, no. 1, pp. 80–83, 2009.
- [97] N. R. Dean *et al.*, "Wound healing following combined radiation and cetuximab therapy in head and neck cancer patients," *J. Wound Care*, vol. 20, no. 4, pp. 166–170, Apr. 2011.
- [98] "IMMUDEX - Dextramer® Technology." [Online]. Available: [http://www.immudex.com/technology/dextramer-technology.aspx?gclid=CN7myKK52s4CFbgK0wodGCcGcGcG](http://www.immudex.com/technology/dextramer-technology.aspx?gclid=CN7myKK52s4CFbgK0wodGCcGcG). [Accessed: 24-Aug-2016].
- [99] P. Lindinger, S. Mostböck, P. Hammerl, A. Hartl, J. Thalhamer, and S. I. Abrams, "Induction of murine ras oncogene peptide-specific T cell responses by immunization with plasmid DNA-based minigene vectors," *Vaccine*, vol. 21, no. 27–30, pp. 4285–4296, Oct. 2003.
- [100] E. B. Schadeck *et al.*, "CTL epitopes identified with a defective recombinant adenovirus expressing measles virus nucleoprotein and evaluation of their protective capacity in mice," *Virus Res.*, vol. 65, no. 1, pp. 75–86, Dec. 1999.
- [101] C. D. Partidos, A. Delmas, and M. W. Steward, "Structural requirements for synthetic immunogens to induce measles virus specific CTL responses," *Mol. Immunol.*, vol. 33, no. 16, pp. 1223–1229, Nov. 1996.
- [102] C. D. Partidos and M. W. Steward, "Prediction and identification of a T cell epitope in the fusion protein of measles virus immunodominant in mice and humans," *J. Gen. Virol.*, vol. 71 ( Pt 9), pp. 2099–2105, Sep. 1990.
- [103] "pCI Mammalian Expression Vector." [Online]. Available: <https://at.promega.com/products/vectors/mammalian-expression-vectors/pci-mammalian-expression-vector/?activeTab=2>. [Accessed: 31-Oct-2016].
- [104] D. Khurana *et al.*, "Characterization of a spontaneously arising murine squamous cell carcinoma (SCC VII) as a prerequisite for head and neck cancer immunotherapy," *Head Neck*, vol. 23, no. 10, pp. 899–906, Oct. 2001.
- [105] M. Ettinger *et al.*, "Transcutaneous gene gun delivery of hNC16A Induces BPAG2-specific tolerance," *J. Invest. Dermatol.*, vol. 132, no. 6, pp. 1665–1671, Jun. 2012.
- [106] A. Stoecklinger *et al.*, "Epidermal Langerhans Cells Are Dispensable for Humoral and Cell-Mediated Immunity Elicited by Gene Gun Immunization," *J. Immunol.*, vol. 179, no. 2, pp. 886–893, Jul. 2007.
- [107] W. J. Moss and D. E. Griffin, "Measles," *Lancet*, vol. 379, pp. 153–64, 2012.
- [108] R. Weiss, S. Scheiblhofer, J. Freund, F. Ferreira, I. Livey, and J. Thalhamer, "Gene gun bombardment with gold particles displays a particular Th2-promoting signal that over-rules the

- Th1-inducing effect of immunostimulatory CpG motifs in DNA vaccines," *Vaccine*, vol. 20, no. 25–26, pp. 3148–3154, Aug. 2002.
- [109] C. Condon, S. C. Watkins, C. M. Celluzzi, K. Thompson, and L. D. Falo, "DNA-based immunization by in vivo transfection of dendritic cells," *Nat. Med.*, vol. 2, no. 10, pp. 1122–1128, Oct. 1996.
- [110] D. Grčević, S.-K. Lee, A. Marušić, and J. A. Lorenzo, "Depletion of CD4 and CD8 T Lymphocytes in Mice In Vivo Enhances 1,25-Dihydroxyvitamin D<sub>3</sub>-Stimulated Osteoclast-Like Cell Formation In Vitro by a Mechanism That Is Dependent on Prostaglandin Synthesis," *J. Immunol.*, vol. 165, no. 8, pp. 4231–4238, Oct. 2000.
- [111] R. Stripecke, M. del Carmen Villacres, D. Skelton, N. Satake, S. Halene, and D. Kohn, "Immune response to green fluorescent protein: implications for gene therapy," *Publ. Online 02 July 1999 Doi101038sjgt3300951*, vol. 6, no. 7, Jul. 1999.
- [112] A. Nagy, "Cre recombinase: The universal reagent for genome tailoring," *genesis*, vol. 26, no. 2, pp. 99–109, Feb. 2000.
- [113] M. R. Zaidi and G. Merlino, "The Two Faces of Interferon- $\gamma$  in cancer," *Clin. Cancer Res. Off. J. Am. Assoc. Cancer Res.*, vol. 17, no. 19, pp. 6118–6124, Oct. 2011.
- [114] R. de Waal Malefyt, S. Verma, M. T. Bejarano, M. Ranes-Goldberg, M. Hill, and H. Spits, "CD2/LFA-3 or LFA-1/ICAM-1 but not CD28/B7 interactions can augment cytotoxicity by virus-specific CD8+ cytotoxic T lymphocytes," *Eur. J. Immunol.*, vol. 23, no. 2, pp. 418–424, Feb. 1993.
- [115] I. Melero, N. Bach, K. E. Hellström, A. Aruffo, R. S. Mittler, and L. Chen, "Amplification of tumor immunity by gene transfer of the co-stimulatory 4-1BB ligand: synergy with the CD28 co-stimulatory pathway," *Eur. J. Immunol.*, vol. 28, no. 3, pp. 1116–1121, Mar. 1998.
- [116] "WHO | Measles," *WHO*. [Online]. Available: <http://www.who.int/mediacentre/factsheets/fs286/en/>. [Accessed: 26-Oct-2016].
- [117] R. Nanan, A. Rauch, E. Kämpgen, S. Niewiesk, and H. W. Kreth, "A novel sensitive approach for frequency analysis of measles virus-specific memory T-lymphocytes in healthy adults with a childhood history of natural measles," *J. Gen. Virol.*, vol. 81, no. 5, pp. 1313–1319, 2000.
- [118] I. G. Ovsyannikova, N. Dhiman, R. M. Jacobson, R. A. Vierkant, and G. A. Poland, "Frequency of Measles Virus-Specific CD4+ and CD8+ T Cells in Subjects Seronegative or Highly Seropositive for Measles Vaccine," *Clin. Diagn. Lab. Immunol.*, vol. 10, no. 3, pp. 411–416, Jan. 2003.
- [119] A. Stoecklinger *et al.*, "Langerin+ Dermal Dendritic Cells Are Critical for CD8+ T Cell Activation and IgH  $\gamma$ -1 Class Switching in Response to Gene Gun Vaccines," *J. Immunol.*, vol. 186, no. 3, pp. 1377–1383, Jan. 2011.
- [120] D. Nobuoka *et al.*, "Intratumoral peptide injection enhances tumor cell antigenicity recognized by cytotoxic T lymphocytes: a potential option for improvement in antigen-specific cancer immunotherapy," *Cancer Immunol. Immunother.*, vol. 62, no. 4, pp. 639–652, Nov. 2012.
- [121] S. Prijić and G. Sersa, "Magnetic nanoparticles as targeted delivery systems in oncology," *Radiol. Oncol.*, vol. 45, no. 1, pp. 1–16, Jan. 2011.
- [122] T.-Y. Wang, K. E. Wilson, S. Machtaler, and J. K. Willmann, "Ultrasound and Microbubble Guided Drug Delivery: Mechanistic Understanding and Clinical Implications," *Curr. Pharm. Biotechnol.*, vol. 14, no. 8, pp. 743–752, Oct. 2014.
- [123] A. Gershon and S. Krugman, *Measles virus. In Diagnostic Procedures for Viral, Rickettsial, and Chlamydial Infections.*, 5th edition. Washington, DC: American Public Health Association, 1979.

- [124] Z. Ru *et al.*, “Development of a Humanized HLA-A2.1/DP4 Transgenic Mouse Model and the Use of This Model to Map HLA-DP4-Restricted Epitopes of HBV Envelope Protein,” *PLOS ONE*, vol. 7, no. 3, p. e32247, Mar. 2012.
- [125] A. Pajot *et al.*, “A mouse model of human adaptive immune functions: HLA-A2.1-/HLA-DR1-transgenic H-2 class I/class II-knockout mice,” *Eur. J. Immunol.*, vol. 34, no. 11, pp. 3060–3069, Nov. 2004.
- [126] M. O. Ota *et al.*, “Hemagglutinin Protein Is a Primary Target of the Measles Virus—Specific HLA-A2—Restricted CD8+ T Cell Response during Measles and after Vaccination,” *J. Infect. Dis.*, vol. 195, no. 12, pp. 1799–1807, Jun. 2007.

## 7 LIST OF FIGURES

Figure 1 The branches of the human immune system.....	3
Figure 2 Processing of cytoplasmic peptides for presentation on MHC I molecules on the cell surface.....	5
Figure 3 The two pathways of CTL mediated target cell killing.....	7
Figure 4 The three phases of cancer immunoediting.....	9
Figure 5 Histological and schematic depiction of the human skin with its different layers and components. ....	14
Figure 6 A schematic depiction of four subpopulations of memory T cells with different recirculation, proliferation and functional behavior. ....	18
Figure 7 Schematic representation of proteins that are affected in different types of EB. ....	19
Figure 8 Cumulative risk of the development of a first SCC and death from SCC depicted for the major subtypes of RDEB. ....	22
Figure 9 Schematic depiction of pCI_DNA cloning strategy and constructs used for gene gun immunization. ....	28
Figure 10 Immunization protocol for the generation of MV specific immunity in C3H mice.....	34
Figure 11 Formula for the calculation of specific lysis of peptide pulsed target cells in an <i>in vivo</i> CTL assay. ....	39
Figure 12 Antibody titer (IgG) against MV detected in sera from 6 different RDEB patients. ....	43
Figure 13 DNA immunization protocol of C3H/HeNcrI mice for the generation of a MV specific immunity. ....	44
Figure 14 IFN $\gamma$ release by PBMCs upon restimulation with relevant peptides. ....	45
Figure 15 Specific IFN $\gamma$ secretion by LN and SPL cells after restimulation with relevant peptides. ....	46
Figure 16 Identification of functional N81 specific CD8 <sup>+</sup> T cells in vaccinated mice. ....	47
Figure 17 Detection of N81 specific IgG in serum of vaccinated mice by ELISA.....	48
Figure 18 Treatment protocol for <i>in vivo</i> CTL experiment. ....	49
Figure 19 Gene gun vaccination induces generation of MV specific CD8 <sup>+</sup> T cells capable of target cell killing <i>in vivo</i> . ....	50
Figure 20 Blocking of CD8 <sup>+</sup> T cells <i>in vivo</i> leads to reduced killing of MV specific target cells. ....	51
Figure 21 Generation of a MV expressing SCCVII cell line.....	52
Figure 22 Integration PCR of virally transduced SCCVII cells before and after transfection with Cre recombinase.....	53
Figure 23 Immunological phenotyping of SCCVII cell lines.....	54
Figure 24 Experimental design of syngeneic SCCVII tumor challenge in C3H mice.....	55
Figure 25 Gene gun vaccination with MV antigens protects mice against SCCVII_N81 tumor formation. ....	56
Figure 26 CD8 <sup>+</sup> T cells infiltrate tumors of MV vaccinated and empty vector gunned mice. ....	57

## 8 LIST OF TABLES

Table 1 Current classification of inherited EB divided in types and subtypes with affected proteins. .19	
Table 2 Subtypes of recessive dystrophic epidermolysis bullosa (RDEB).....21	
Table 3 Retroviral transduced murine SCC cell lines used for <i>in vivo</i> tumor experiments.....32	
Table 4 Summary of experimental and control cohorts of the tumor challenge study. ....56	
Table 5 List of the primers used in this study.....74	

## 9 LIST OF ABBREVIATIONS

ALL	acute lymphatic leukemia	MDSC	myeloid derived dendritic cell
APC	antigen presenting cell	MHC	major histocompatibility complex
BCC	basal cell carcinoma	MV	measles virus
BMZ	basement membrane zone	N	nucleocapsid protein
bp	base pair	NK	natural killer cell
CD	cluster of differentiation	NMSC	non melanoma skin cancer
CFSE	Carboxyfluorescein succinimidyl ester	PAMP	pathogen-associated molecular patterns
cSCC	cutaneous squamous cell carcinoma	PBMC	peripheral Blood Mononuclear Cell
CTL	cytotoxic T cell	PD	programmed death
CTLA	cytotoxic T lymphocyte associated protein	PT	PBS + 0.1 % Tween
DC	dendritic cell	RDEB	recessive dystrophic Epidermolysis bullosa
DEB	dystrophic Epidermolysis bullosa	RDEB-gen intermed	RDEB generalized intermediate
DEJ	dermal epidermal junction	RDEB-gen severe	RDEB generalized severe
DISC	death-inducing signaling complex	RNA	ribonucleic acid
DNA	deoxyribonucleic acid	SCC	squamous cell carcinoma
EB	Epidermolysis bullosa	SPL	spleen
EBS	Epidermolysis bullosa simplex	TAA	tumor associated antigen
EV	empty vector	TAM	tumor associated macrophage
F	fusion protein	TAP	transporter associated with antigen processing
FACS	fluorescence activated cell sorting	T <sub>CM</sub>	central memory T cells
FADD	FAS-associated protein with Death Domain	TCR	T cell receptor
FCS	fetal calf serum	TEM	transmission electron microscopy
FVD	fixable viability dye	TGF	T cell growth factor
FVD	fixable viability dye	Th	T helper
GFP	green fluorescent protein	TLR	toll like receptor
IDO	indoleamine 2,3-dioxygenase	T <sub>MM</sub>	migratory memory T cells
IFM	immunofluorescence mapping	TNF	tumor necrosis factor
IFN	interferon	Treg	regulatory T cell
IL	interleukin	T <sub>RM</sub>	Tissue resident memory T cells
IL2ss	interleukin 2 signal sequence		
IRES	internal ribosomal entry site		
JEB	junctional Epidermolysis bullosa		
KS	kindler syndrome		
LN	lymph node		

## 10 APPENDIX

### 10.1 PRIMER LIST

Primers that were used for cloning, expression profiling and the confirmation of sequences are depicted in Table 5.

Table 5 List of the primers used in this study.

Name	Sequence 5'-3'
loxP_IRES_fwd	GATCTACGTAATAACTTCGTATAgcatacatTATACGAAGTTATCTAACGTTACTGGCCG
GFP_loxP_rev	GATCGTCGACATAACTTCGTATAatgtatgcTATACGAAGTTATTTACTTGACAGCTCGTC
BamHI_IL2ss_fwd	GATCGGATCCgccaccatgTACAGCATGCAG
MVTh_XhoI_rev	GATCCTCGAGTTTACACGCCCTCCAGCCTG
int_IL2ss_fwd	ATGTACAGCATGCAG CTC GCC
int_MVTh_rev	TTACACGCCCTCCAGCCTG
int_IRES_fwd	CATGAAGCAGCAGACTTCTTC
int_GFP_rev	CATGCCTTGCAAAATGGCGTTAC
mCD137L_fwd	CTCTCCTGTGTTTCGCCAAGC
mCD137L_rev	CCAGCCTTCAGGAGCAACAG
mCD80_fwd	CGACTCGCAACCACACCATTAAG
mCD80_rev	CCCGAAGGTAAGGCTGTTGTTTG
mCD95_fwd	CGCTGTTTTCCCTTGCTGCA
mCD95_rev	ACAGGTTGGTGTACCCCAT
mPDL1_fwd	CGAATCACGCTGAAAGTCAA
mPDL1_rev	GCTGGTCACATTGAGAAGCA
GAPDH_fwd	TGCACCACCAACTGCTTAGC
GAPDH_rev	GGAAGGCCATGCCAGTGA
pMX_seq_fwd	GTGGACCATCCTCTAGACTGCC

### 10.2 SOLUTIONS

#### 1x ACK-buffer

8.29 g (150 mM)      NH<sub>4</sub>Cl (Sigma-Aldrich)

1 g (10 mM)            KHCO<sub>3</sub> (Sigma-Aldrich)

37,2 mg (0.1 mM)     EDTA (Sigma-Aldrich)

Add H<sub>2</sub>O to 1,000 ml, adjust pH to 7.4 and sterile filter.

#### PBS/EDTA

20 % of 0.5 M EDTA (Sigma-Aldrich) in PBS

Dilute 1:5 in PBS for blood collection via the vena saphena.

AEC substrate buffer

9.6 g Citric Acid (Sigma-Aldrich) in 500 ml H<sub>2</sub>O

14.2 g Na<sub>2</sub>HPO<sub>4</sub> (Sigma-Aldrich) in 500 ml H<sub>2</sub>O

Add phosphate solution to citric acid solution until pH = 5.0

AEC substrate stock solution

4 mg/ml AEC substrate in DMF (N,N-Dimethylformamide, Sigma-Aldrich)

AEC substrate

1:15 dilution of AEC substrate stock solution in AEC substrate buffer, filter through a 0.22 µm filter and add 30 % H<sub>2</sub>O<sub>2</sub> at 1:1,500 immediately before use

50x TAE buffer

2M Tris (AppliChem GmbH, Darmstadt, GER)

695 mM NaOAc (Serva Electrophoresis GmbH, Heidelberg, GER)

50 mM EDTA (Sigma-Aldrich)

0.3 % HCl alcohol

4.6 ml 1 M HCl + 45.5 ml ethanol absolute

Cell cultureSolution A

30 mM HEPES (Sigma Aldrich)

9 mM Glucose (Merck KGaA, Grafing, GER)

3 mM KCl (Merck KGaA)

132 mM NaCl (Merck KGaA)

1 mM Na<sub>2</sub>HPO<sub>4</sub> x 7H<sub>2</sub>O (Merck KGaA)

0.3 mM Phenol red (Sigma Aldrich)

1x Trypsin/EDTA

1:10 dilution of Trypsin-EDTA solution 10x (Sigma-Aldrich) in solution A

1x FCS/EDTA

1:10 dilution of FCS (Biochrom) in solution A

Freeze Medium

FCS (Biochrom) adding 10 % DMSO (Sigma-Aldrich)

LB medium

25 g Luria Broth (Sigma Aldrich)

1 L ddH<sub>2</sub>O